1962

The deformation of the electrocapillary curve due to adsorption of organic molecules

Dennis Joseph Kelsh
Iowa State University

THE DEFORMATION OF THE ELECTROCAPILLARY CURVE DUE TO ADSORPTION OF ORGANIC MOLECULES

by

Dennis Joseph Kelsh

A Dissertation Submitted to the
Graduate Faculty in Partial Fulfillment of
The Requirements for the Degree of
DOCTOR OF PHILOSOPHY

Major Subject: Physical Chemistry

Approved:

Signature was redacted for privacy.

In Charge of Major Work

Signature was redacted for privacy.

Head of Major Department

Signature was redacted for privacy.

Dean of Graduate College

Iowa State University
Of Science and Technology
Ames, Iowa

1962

TABLE OF CONTENTS

	Page
INTRODUCTION	1
The Electrical Double Layer	2
Experimental Methods	4
Capillary electrometer	4
Differential impedance bridge	12
OBJECTIVES	18
MATERIALS	19
Mercury	19
Water	19
Perchloric Acid	20
Inert Atmosphere	21
Cleaning Bath	23
Adsorbates	24
Phenol	24
n-Amyl alcohol	24
N-butylacetamide	25
APPARATUS	26
Capillary Electrometer	26
Accuracy and sensitivity	27
Design	29
Method of procedure	34
Differential Capacity Measurements and Impedance Bridge	38

	Page
Electronic apparatus	38
The cell	41
Dropping mercury electrode	43
Procedure	44
EXPERIMENTAL RESULTS	48
Electrocapillary Data	48
Differential Double Layer Capacitance Data	48
DISCUSSION	84
Adsorption Isotherms	89
Dependence of ψ on Γ and V	109
Reorientation of phenol as evidenced by capacity measurements	118
Apparent adsorption from differential capacitance	121
Kinetics of Adsorption	122
N-Butylacetamide	127
SUMMARY	131
SUGGESTED MODIFICATIONS AND EXTENSIONS	133
BIBLIOGRAPHY	135
ACKNOWLEDGEMENTS	139

INTRODUCTION

Electrocapillarity is defined as the study of the surface tension of metals in contact with inert salt solutions, together with all of the effects associated with this phenomenon. The interface between a metal and a salt solution is especially interesting for theoretical reasons, chief of which is the possibility of polarizing the metal surface from some external source and examining the effect of this imposed electric field on the properties of the interface. Such a study is important to electrochemists and others interested in problems involving corrosion, overvoltage, or even the electrical properties of living tissues such as those used in muscular and nervous action, for these phenomena are all directly related to the electrical properties of interphases. Before these and other related subjects can be handled successfully, however, it is important that the electrochemistry of the simplest interphases be well understood. Of these, the mercury-solution interface has been most frequently studied in the past, and although no definitive theory for this system has yet been formulated, the properties of this system are known to a much greater extent than those of any other.

The effect of an electric field at the surface on the extent of adsorption from solution is qualitatively well known. In strong fields, ions and highly polar molecules present in

solution will tend to displace less polar materials from the interface, while at low polarizations the converse is true. In terms of a quantitative picture, however, very little is known about the extent and nature of these displacements.

An electrical double layer consisting of charged particles and oriented dipoles is thought to exist at every interface. For a metal-solution interface, this double layer may consist of a layer of electrons, a layer of adsorbed ions, and a diffuse double layer consisting of an ionic atmosphere in which ions of one sign are in excess of their bulk concentration while those of opposite sign are in defect. The excess charge density in this ionic atmosphere decreases exponentially with distance from the surface; its half thickness is inversely proportional to the square root of concentration, and for aqueous systems with electrolyte concentration greater than 10^{-4} M., is less than 10^{-5} cm. Finally there may exist at the surface neutral molecules which, whether they are preferentially oriented or not, influence the thermodynamic properties of the interface. This thesis is primarily concerned with the effect of such neutral surface active organic materials on the properties of the electrical double layer.

The Electrical Double Layer

Many authors have published extensively on the theory of the electrical double layer existing between a metallic phase

and a solution of electrolyte, but certainly no single theory can be said to be firmly established at this time. A review of the present state of knowledge in this area is beyond the scope of this thesis, but attention will be drawn to several of the more important articles which have appeared. Grahame (1) has published an extensive review article which remains the best introduction to the subject of electrocapillarity known to this writer. More recent reviews include those of Parsons(2, 3) and Damaskin (4), the latter being devoted largely to a review of the Russian literature. Watts-Tobin and co-workers have recently published a series of papers (5, 6, 7) which summarize former results while also forwarding certain new concepts regarding the metal-electrolyte interface.

In an investigation of adsorption at an electrode-solution interface, it is essential that the current flowing across the interface be kept very small, for only then will the effect of concentration changes due to the direct current flow be negligible compared to experimental error. In differential capacity measurements, this current must be negligible in comparison to the capacitative admittance; in electrocapillary work, the current must not generate enough oxidized or reduced material to appreciably change the composition of the interphase, nor must it be large enough to allow the IR drop across the solution to become appreciable in relation to the applied potential. In the absence of substances more

easily oxidized or reduced, the range of potentials over which this current is negligible is largely governed by the rate of evolution from solution of hydrogen at cathodic polarizations, and oxygen at anodic polarizations of the electrode. An activation energy barrier exists for each of these reactions at all metal electrodes, and the size of this barrier is a function of the electrode material chosen. This barrier is especially large in the case of mercury, and hence there exists for this material a wider potential range over which the electrode can be polarized without appreciable current flow. In addition to possessing this high barrier, mercury is relatively easy to purify, forms an electrode free of strains and easily changed, and is relatively inert chemically. Such properties make this material ideally suited for an investigation of this kind.

Experimental Methods

Capillary electrometer

A mercury electrode in contact with any given solution will exhibit its maximum surface tension when the electronic charge density on the surface of the electrode is exactly zero. The truth of this statement can be verified when one considers that charges of like sign tend to repel one another, and for this reason, when a mercury electrode is polarized, charges of like sign existing side by side on the surface will tend to

expand that surface, and hence lower the surface tension. This effect was first experimentally examined by Lippmann (8, 9, 10), who modified the standard capillary-rise technique of measuring surface tension by simply adding an external potential source which could polarize the mercury surface to any desired degree. If a plot of surface tension versus polarizing potential (measured with respect to some non-polarizable reference electrode in solution) is made, a nearly parabolic curve is obtained, and this plot is now commonly referred to as the electrocapillary curve.

The Gibbs adsorption equation, modified to include the electrical work, expresses the thermodynamic relationship between interfacial tension, polarizing potential, and solution composition:

$$- d\gamma = Q\, dV + \sum_i \Gamma_i\, d\mu_i \qquad (1)$$

where γ is the interfacial tension, V is the polarizing potential, Q is the electronic charge density on the electrode side of the double layer, μ_i is the chemical potential of the ith component of the system, and Γ_i is the surface excess of the ith component referred to some arbitrarily defined mathematical surface. If this surface is chosen such that $\Gamma_{Hg} = 0$, then this mathematical surface is chosen in substantial coincidence with the physical surface of the mercury, and for a dilute solution of any adsorbent which tends to form a mono-

layer at the interface, the surface excess is essentially identical to the adsorbate concentration (moles/cm^2) in the compact double layer.

Proper manipulation of Equation 1 will lead to the evaluation of several quantities of thermodynamic interest. Thus, the charge density can be found by graphical differentiation of the electrocapillary curve since

$$Q = - \left(\frac{\partial \gamma}{\partial V}\right)_{\mu_i} \qquad (2)$$

Similarly, the surface excess of any component of interest is given by:

$$\Gamma_i = - \left(\frac{\partial \gamma}{\partial \mu_i}\right)_{V,\ \mu_{j \neq i}} . \qquad (3)$$

Equation 3 implies that adsorption isotherms (plots of surface excess versus bulk concentration) can be obtained by measuring the change in interfacial tension as a function of adsorbate activity at constant polarization.

If a capillary active material is added to an aqueous solution of electrolyte, the electrocapillary curve will become truncated in the region of the electrocapillary maximum (e.c.m.), that is, the region of low charge density on the mercury surface. This is due to the lowering of the interfacial tension caused by the adsorption of the organic material at the interface. This adsorption will occur to a greater extent in regions of low charge density, for in strong fields

the organic material, being less polar in character than the solvent, will be desorbed from the interface in favor of the water and ionic materials. Thus, by studying the interfacial tension as a function of polarization of the mercury surface and bulk concentration of the organic material, information regarding the surface charge density, amount of organic material adsorbed at the interface, variation of amounts of other constituents present in the interphase, orientation of adsorbed species, and heats and entropies of adsorption at any point of the electrocapillary curve can be obtained. Such studies are classical, but only recently have these measurements been exploited to the fullest extent. Reviews of early work have been published elsewhere (11, 12, 13) in addition to the review articles cited previously.

Blomgren et al. (14) have recently published adsorption isotherms based on electrocapillary data for various butyl, phenyl, and napthyl compounds. They find in general that highly soluble compounds show the least tendency to adsorb and hence maintain that strong adsorption is associated with low solubility. Napthyl compounds are found to have an adsorbability 10^3 to 10^4 times higher than corresponding butyl compounds, with phenyl compounds intermediate. For substances with the same hydrocarbon radical, the adsorbability varies with the substituent group by a factor as high as 10^4. These adsorbabilities are calculated on the basis of a Langmuir

model of adsorption, which can be expressed as:

$$\frac{\Gamma_A}{\Gamma_{max} - \Gamma_A} = k\, c_A = \frac{c_A\, e^{-\Delta\bar{F}_A^\circ/RT}}{0.0555} \qquad (4)$$

where c_A is given in moles/cm^3. Such a model assumes that the total number of sites available for water and for the organic adsorbate are the same. For the larger molecules studied by Blomgren *et al.*, this assumption gives rise to a possible error of approximately 15% in the calculated values of $\Delta\bar{F}_A^\circ$. These authors confined their interest to very dilute solutions of adsorbate, and hence did not examine the possibility of a change in orientation of the adsorbed molecules with increased coverage. They concluded that in the concentration range they studied, the butyl compounds were adsorbed perpendicular to the surface with the hydrocarbon tail directed toward the mercury, while phenyl and napthyl compounds lay flat on the mercury. These conclusions were based in part on calculations which compared molecular areas deduced from Fisher-Taylor-Hirschfelder models with areas corresponding to the experimental values of Γ_{max}. Also considered was the shift in the electrocapillary maximum caused by the adsorption of the organic materials: for aliphatic compounds, maximum adsorption was found at potentials negative to the e.c.m. for pure electrolyte, while aromatic materials were adsorbed to a greater extent at positive potentials. These facts would be

consistent with an orientation wherein the aliphatic materials were adsorbed with the positive end of their dipole next to the mercury surface, while the aromatics would prefer to adsorb with the negative end adjacent to the electrode. The authors do not state how they arrive at their experimental values for Γ_{max}, and it is very hard to imagine how they extrapolated their values of Γ_A taken in the neighborhood of 15% saturation concentration and less, especially for those cases where Γ_A was increasing appreciably with increasing bulk concentration at the highest concentration of measurement (see, e.g., phenol).

Frumkin et al. (15) have compared the adsorption properties of several aromatic compounds with their saturated counterparts. In agreement with earlier work of Gerovich (16-19) performed in the same laboratory, these workers found the aromatic compounds to be adsorbed to a greater extent at positive potentials, and to a lesser extent at negative potentials, than the corresponding hydroaromatics. They attribute this difference not only to the flat orientation of the aromatic molecules, but also to a chemical interaction between the π-electrons of the aromatics and the mercury surface, this latter factor becoming very important when the mercury carries a positive charge. The credibility of this conclusion is most striking when one compares the adsorption of a cyclohexylamine cation with its aromatic counterpart, aniline (these basic

amines form cations when dissolved in one molar acid). On a positively charged mercury surface, the cyclohexylamine cation is completely desorbed while the aniline cation is still adsorbed, indicating that the π-electron interaction forces actually prevail over the electrostatic repulsion forces. These results are confirmed by Blomgren *et al.* (14) and also by Conway and Barradas (20), who compared the adsorption of several organic bases (including aniline) with their conjugate acids. These authors calculated adsorption isotherms from their electrocapillary data, and treated them much as Blomgren *et al.* did using a Langmuir isotherm. For a fractional surface coverage of 0.5, they find the bases to be strongly adsorbed at negative polarizations of the mercury surface, with this adsorption energy falling off rapidly at positive potentials even for the aromatic bases studied. This trend is observed for the ionic forms as well as the neutral materials. In general the ions are found to be less strongly adsorbed than neutral bases, with aniline and 2-aminopyridine being notable exceptions. The authors attempt to justify these exceptions by considering special resonance effects as being responsible for the strong adsorption of these cations. They conclude, in disagreement with Blomgren *et al.*, that solubility is not always an important factor in determining the strength of adsorption, for bases and their ions have in most cases quite different solubilities, while the presence or absence of

an ionized center in the molecule makes little difference in the adsorption energy for otherwise similar molecular and electronic structures.

A comment should be made here on the effect of solubility on adsorbability as reflected in the values for $\Delta\overline{F}^{\circ}_{A}$ of Equation 4. This effect is strongly dependent on the standard states chosen, for $\Delta\overline{F}^{\circ}_{A}$ is the free energy change one observes when one mole of organic material in some solution standard state is transformed to one mole of organic material in some adsorbed standard state. If solvent environments of solution and adsorbed standard states are similar, then solubility, that is, solute-solvent interactions, will cancel out; if these environments are not similar, then solubility will not cancel and in such a case, one cannot rightly compare solubilities with adsorbabilities and expect to obtain valid conclusions.

Conway and Barradas also consider the possible effect of a change in orientation of the adsorbed molecules on the strength of the adsorption. They find that their experimental values of adsorption energy decrease linearly with the three-halves power of coverage, but find an abrupt inflection in these linear plots which they attribute to an abrupt change in orientation of the adsorbed species. That such reorientation occurs would be hard to deny, but it seems a bit unreasonable to expect this change to occur all at once as soon as a certain

"critical coverage" is reached. The authors derive an expression for this dependence of $\Delta\overline{F}_A^\circ$ on $\theta^{3/2}$, assuming that the change in adsorption energy is dependent on an electrostatic dipole-dipole interaction, and, at high coverages, an additional van der Waals-London interaction.

In their second paper, Conway and Barradas discuss the interaction of π-electrons with the mercury surface. In agreement with other work cited, they find the most strongly aromatic materials (e.g. aniline) to be adsorbed such that the π-electrons interact to a maximum extent with the electrode surface, but materials having fewer π-electrons have a much smaller tendency to lay flat on the surface. This is reflected in the plots of $\Delta\overline{F}_A^\circ$ vs. $\theta^{3/2}$, which show the less aromatic compounds to be reoriented at much smaller "critical coverages", and strongly aromatic materials are in fact never reoriented (no abrupt change in the linear plot of $\Delta\overline{F}_A^\circ$ vs. $\theta^{3/2}$ occurs).

Differential impedance bridge

In recent years another experimental approach to the study of the electrical double layer has evolved which is much more sensitive to changes in the interfacial region, but which is less well grounded in thermodynamic interpretation. Experimentally one observed that the electrical double layer acts like an electrical condenser, and the capacity of this con-

denser is extremely sensitive to the polarization of the mercury surface and bulk composition of the solution. An alternating current impedance bridge can be used to measure this capacity, and as the quality of available electronic equipment has improved, measurements with such an instrument have become more extensive and refined. Kruger (21) was the first to make any quantitative measurements on the mercury-solution interface with such a bridge, but Grahame must be considered as the one chiefly responsible for the extensive development of the method. His review and others (3, 12, 13, 22) should be consulted for a thorough description of the technique along with typical results obtained by a number of workers.

Hansen et al. (23, 24) have recently inferred adsorption isotherms from differential double layer capacitance measurements for a number of organic compounds. To do this, they used the non-thermodynamic assumption first developed by Frumkin (25) that the compact double layer was composed of two capacities in parallel, one corresponding to the fraction of the surface covered with organic material and the other corresponding to the uncovered fraction. Assuming unimolecular coverage and ignoring the contribution of the diffuse double layer to the measured capacities, they derived an expression for apparent surface coverage as a function of capacity, and applying this expression to their experimental data, were able to infer reasonable coverages for potentials within the

desorption peaks of the capacitance curves.

Breiter and Delahay (26) studied the adsorption of n-amyl alcohol at the mercury solution interface, obtaining electrocapillary data as well as differential capacitance data for this system as a function of potential and concentration of adsorbate. Thus they were able to compare the thermodynamic information inferred from the capacity measurements by means of a model (they also used Frumkin's model) with the information obtained directly with the capillary electrometer. They found that in utilizing differential capacities to obtain such thermodynamic quantities as charge density and surface tension by integration of the expression:

$$C = \left(\frac{\partial Q}{\partial V}\right)_{\mu_i} = -\left(\frac{\partial^2 \gamma}{\partial V^2}\right)_{\mu_i}, \qquad (5)$$

it is important that the capacity extrapolated to zero frequency be used, for the height of the desorption peaks is strongly frequency dependent. Since Hansen *et al.* obtained all of their capacities at 1000 c.p.s., their treatment should be re-examined in light of this. Breiter and Delahay did find, however, that it was not essential to extrapolate to zero frequency in evaluating θ from differential capacities well within the desorption peaks, and in this respect the conclusions of Hansen *et al.* are very likely quite valid. Breiter and Delahay conclude that the Frumkin model gives thermodynamic

results as accurate as those obtained by them from their electrocapillary measurements. This conclusion is limited by their use of the drop-weight-time method of measuring surface tension, which is known to be inherently less accurate than the standard Lippmann electrometer.

Comment should be made at this point concerning a recent paper by Parsons (27) on the relation between capacity and adsorption of surface active material. He bases his treatment on an equation which supposedly represents the Frumkin model of adsorption:

$$C = C_{org}\,\theta + C_w(1 - \theta) \qquad (6)$$

where C is the total capacity, θ the fractional surface coverage, C_{org} the differential capacity when the surface is completely covered with surface active material, and C_w the capacity when surface active material is totally absent from the interface. The mathematical equation describing the model as originally given by Frumkin, however, is:

$$Q = Q_{org}\,\theta + Q_w(1 - \theta) \qquad (7)$$

where the Q's are the charge densities on the electrode for coverages of θ, 1, and 0, respectively. Differentiation of Equation 7 with respect to potential leads to:

$$C = \theta\, C_{org} + (1 - \theta)C_w + (Q_{org} - Q_w)\left(\frac{\partial\theta}{\partial V}\right)_{\mu_i} \qquad (8)$$

Thus the term involving $(\partial\theta/\partial V)_{\mu_i}$ in Equation 8 does not appear in Parsons' expression, and it is just this term which is responsible for the "pseudocapacitance" observed as the surface active material is desorbed from the interface. Thus proper analysis of capacitance data requires that Equation 8 be used rather than Equation 6, and Parsons' paper should be read critically in light of this.

Schapink et al. (28) studied the adsorption of thiourea, aniline, and a mixture of these compounds at a mercury-electrolyte interface by measuring the differential capacitance for a number of concentrations and polarizations. They find that thiourea, unlike most neutral organic compounds, is not desorbed at high positive polarizations of the mercury surface, confirming the earlier measurements of Frumkin (29) with the capillary electrometer. In making their thermodynamic conclusions, however, Schapink et al. failed to extrapolate their capacities to zero frequency before numerically integrating the capacity data by use of Equation 5. Recent analyses of this data by Parsons (30) and by Devanathan (31) have also failed to recognize this fact, and their conclusions are hence subject to the limitations of this procedure.

In addition to obtaining thermodynamic information about the adsorption process, one is able to study the kinetics of adsorption by observing the frequency dependence of differential capacitance at the desorption peaks. As stated previous-

ly, these peaks are strongly frequency dependent, and this is due to the adsorption process proceeding at some finite rate at the interface. The supplementary capacitive current which arises from the desorption process is dependent on the rate at which molecules can be removed from the interface, and the frequency dependence arises if the adsorption process does not occur fast enough to follow the potential changes at high frequencies. Frumkin and Melik-Gaikazyan (32) have proposed a method of choosing between two possible rate controlling mechanisms of adsorption: diffusion control or activation control. They derived equations for capacity in terms of frequency for each mechanism, and hence were able to compare their experimental frequency dependence with that predicted for each mechanism. Melik-Gaikazyan (33) found that for the several aliphatic alcohols he studied, the frequency dependence observed most closely resembled that predicted for the diffusion control mechanism. Lorenz and Möckel (34), using slightly different equations and assuming the adsorption follows a Langmuir model, confirmed this result for butanol, but found measurable adsorption rates for iso-amyl alcohol, cyclohexanol, benzyl alcohol, phenol, methyl-ethyl-ketone, and n-butyric acid.

OBJECTIVES

The objectives of this investigation were fourfold.

1. To design and build a capillary electrometer of sufficient sensitivity to allow precise calculation of adsorption isotherms to be made.

2. To study the adsorption properties of several neutral organic materials at the mercury-solution interface, utilizing both the electrometer and an A.C. impedance bridge.

3. To examine critically the Frumkin model of adsorption purported to generate correct thermodynamic data from differential capacity measurements. These data will be checked with results obtained directly with the capillary electrometer. The effect of frequency on both the capacitance results and the conclusions derived from these results will be examined closely.

4. To investigate the kinetics of adsorption of these materials at the electrode-solution interface in the absence of electrochemical reactions.

MATERIALS

Mercury

Goldsmith Brothers triply distilled mercury was further purified by washing with 5% nitric acid, rinsing with conductivity water, drying and finally by vacuum distillation. The product was stored in Pyrex reagent bottles which had been used as mercury containers for more than a year. These bottles were cleaned prior to use in the acid bath described elsewhere in this thesis. The mercury was added to the electrode reservoir through a pin-hole filter, which removed any dust which might have collected on the surface.

Water

Freshly distilled conductivity water was used in preparing all of the solutions. Tap distilled water was redistilled through an all fused silica continuous double distillation column obtained from Engelhard Industries, Inc. The first stage of this column contained enough sulfuric acid to make its concentration approximately 1 molar when the column was running. Initially the surface tension of the product of the double distillation with no acid added to the first stage was approximately 0.5 dynes/centimeter lower than the literature value. Past experience in this laboratory indicated that long chain amines were the chief source of contamination of the tap

distilled water; hence, the sulfuric acid was used to react with these impurities in the first stage of the column. With this procedure, the surface tension of product as measured with a commercial Cenco-DuNoüy Tensiometer, Cat. No. 70545, was always 71.8 ± 0.2 dynes/centimeter as compared to the literature value of 71.9 d/cm (temp. = 25.5° C.) as quoted from Lange's Handbook (35).

Conductivity of the water was found to be of the order of 10^{-6} mhos/cm; since no efforts were made to exclude carbon dioxide from the product, this relatively high value was considered to be satisfactory.

Perchloric Acid

Perchloric acid was chosen to be the inert electrolyte which fixed the acid concentration of the primitive solutions. The choice was prompted partially by precedent in this laboratory, but chiefly by the fact that the perchlorate ion has little tendency to complex other materials in solution, nor is it oxidized or reduced over a wide range of polarizations. All solutions studied were 0.10 molar in perchloric acid, and were prepared by diluting a measured volume of the concentrated acid with the conductivity water. Baker and Adamson C. P. Reagent Grade perchloric acid was redistilled under partial vacuum, and the product was assumed to be the azeotropic mixture, 72% acid by weight. Using this fact, along with the

listed density of 1.71 for the B-A product, 8.1 ml of the concentrated acid will form 1 liter of 0.10 molar acid when mixed with water. This molarity was selected because previous investigations (1, 23, 24) revealed that increasing the acid concentration had little effect on the capacity of the electrical double layer, indicating that the diffuse layer capacitance was very large, and hence its effect on our measurements was very small.

Pre-electrolysis was carried out for several hours on a number of solutions studied early in this investigation. It was thought that this would insure the removal of any ions which might have interfered in the measurement of the double layer capacity; however, repeating these runs using solutions which had not been subjected to this treatment showed that the pre-electrolysis had no measurable effect on the results obtained, and hence the procedure was discontinued.

Inert Atmosphere

Hydrogen was used to outgas the solutions studied with both the electrometer and the impedance bridge, and also served as the reference electrode for the impedance measurements. Tank hydrogen was purified by passage over copper turnings at 500° C. to remove any oxygen present, through a dry ice-acetone trap, through a commercial De-oxo Catalytic Purifier which consists essentially of finely divided palladium

used to remove the last traces of oxygen, and finally through a trap kept at liquid nitrogen temperature to remove any residual grease from the gas stream. The hydrogen entered the cell through a fritted glass filter stick which dispersed the gas in a stream of small bubbles. The H_2 left the cell through a water bubbler. Provision was made for bypassing the hydrogen stream above the solution during times when experiments were being conducted. Thus the cell was continuously flushed and was under a positive pressure of hydrogen at all times.

Capacitance measurements made when the hydrogen bubbler was left on were normally about 2-5% lower than those taken with it off, probably indicating collection of gas bubbles at the dropping mercury electrode surface. For the 0.615 molar phenol solution, however, capacitance values were 25-40% higher with the bubbler on, and this fact is not completely understood by the writer. At such high concentrations, phenol is probably adsorbed in multilayers, and it could be that these layers, bound by forces much smaller than the initial layer, are disturbed by the agitation of the H_2 bubbles. If this agitation tends to replace phenol molecules with water molecules, the water, having a higher dielectric constant, will give rise to the higher capacitance observed. Since this phenomenon is found to be most pronounced at potentials where one sees a rise in capacitance attributable to desorption of multi-layers, this rationalization is in all probability

partially correct, although it may not be a complete explanation.

When measurements were being made on a solution containing a volatile component, e.g. n-amyl alcohol, phenol, etc., the hydrogen was bubbled through a solution of the same concentration as that being studied prior to its admittance to the cell. The bubbler was used in the cell for only 30-60 minutes in such cases, and the gas pressure was always adjusted to such a level that only enough hydrogen necessary to maintain a positive pressure inside the cell was admitted. To check on any possible change in concentration over the course of a run, the first point taken was always repeated at the end of the run. In every case, the readings were identical within normal experimental error.

Cleaning Bath

All apparatus was cleaned, when size permitted, in a bath consisting of a 3 to 1 mixture of sulfuric and nitric acids, respectively. The bath was kept at a relatively high temperature--100° C.--and was replenished occasionally with nitric acid. Upon removal from the bath, glassware was rinsed with conductivity water and dried in an oven at 80° C.

Adsorbates

Phenol

A. R. grade phenol obtained from Mallinckrodt Chemical Works was fractionally frozen and distilled in a single stage glass still. The corrected boiling point was 181.4 ± 0.1° C. The value reported by Lange (35) is 181.8° C. A saturated aqueous solution of phenol was made up, and from this a relatively strong solution of phenol prepared. This solution was standardized by bromination (36, p. 2253) and was found to be 0.620 ± 0.001 molar. Addition of enough perchloric acid to make the solution 0.10 molar in perchloric acid changed the phenol concentration to 0.615 ± 0.001 molar. All phenol solutions were subsequently made up from this standardized solution. The saturation concentration of phenol is 0.1 molar perchloric acid is assumed to be 0.896 molar (12) at 25° C.

n-Amyl alcohol

Eastman normal amyl alcohol was purified by distilling a sample through a 30 plate Oldershaw column at a reflux ratio of ten to one. The boiling point of the fraction used in these experiments was 137.7 - 137.8° C. at atmospheric pressure. The value reported by Lange (35) is 138.1° C. The saturation concentration of n-amyl alcohol in 0.10 molar perchloric acid is reported to be 0.222 molal at 25° C. (12).

N-butylacetamide

This compound was used as received from Eastman Kodak Company.

APPARATUS

Capillary Electrometer

The principle of the capillary electrometer has been discussed extensively elsewhere (11, 22, 37). Briefly, it can be stated as follows. Consider a tube containing mercury whose lower end dips into a solution to be investigated. This end is drawn out to form a conical capillary so that the interface between the mercury and the solution is formed in this capillary. A varying polarizing potential is now applied between the mercury in the tube and some reference electrode placed in the solution. For such an instrument, the interfacial tension is given approximately by

$$\gamma = \frac{rghd}{2} \qquad (10)$$

where h is the height of mercury in the tube above the meniscus in the capillary

r is the radius of the capillary at the meniscus

d is the density of mercury

g is the acceleration due to gravity.

Now if the meniscus is kept at the same point in the capillary while the interfacial tension is altered by changing the polarizing potential, the height h will have to be adjusted in such a way that

$$\gamma = Ch \qquad (11)$$

where C is a constant.

In order to obtain values of the interfacial tension from readings of the height h, it is necessary either to measure r directly, which is never done in practice, or to standardize the capillary electrometer against a solution for which the interfacial tension at the electrocapillary maximum is known, while always maintaining the meniscus at the same place in the capillary. Such a solution is 0.05 molar sodium sulphate, for which γ_{max} = 426.2 ± 0.2 dynes/cm at a temperature of 25.0 ± 0.3 degrees Centigrade. This is the value obtained from sessile drop measurements by Smolders (38), and was used in preference to the older work of Gouy (39), who found γ_{max} for 0.01 normal sodium sulphate to be 426.7 dynes/cm at 18° C., with a temperature coefficient of

$$\frac{d\gamma_{max}}{dT} = -0.17 \text{ dynes/cm-degree.}$$

Gouy's value is consistent with the newer measurement, however, and either value could be used with confidence.

Accuracy and sensitivity

For a given surface tension, the measured height h is inversely proportional to the radius of the capillary at the meniscus. Thus the smaller r is made, the greater h becomes, and hence h can be measured with a correspondingly greater accuracy. The capillaries normally used had a diameter at the

meniscus of approximately 0.03 mm, which implied that h must be of the order of 45 cm when γ = 425 dynes/cm. Thus, if an accuracy of 0.1 dyne/cm is required for the surface tension, the height h should be measured correctly to 0.1 mm.

A second factor which affects the sensitivity of the method is the amount of taper of the capillary near the null position. For a constant head of mercury, a change in polarization which will increase the surface tension will cause the meniscus to recede up the capillary. The distance of this recession will depend on the slope of the capillary walls; i.e., for a capillary tapering very slowly, the mercury will recede a greater distance than it would for an abrupt taper. This implies that maximum sensitivity will be attained when the capillary tapers very gradually; however, the capillary must never be perfectly cylindrical, for then the position of the meniscus becomes indeterminate.

A third factor to be considered is the effect of temperature. A change of 1° C. of the temperature of the whole column of mercury above the meniscus changes the height (45 cm) by 0.07 mm, and hence causes an error of less than 0.07 dynes/cm in the surface tension. For the same temperature change, the surface tension shifts by 0.17 dynes/cm. All measurements with the electrometer were made at 26.5 $\pm$ 0.9° C., giving rise to a possible fluctuation of 0.2 dynes/cm in the surface tension.

Design

The design of the capillary electrometer incorporates several ideas presented by previous workers (40, 41, 42). The system was made entirely from Pyrex glass, and is shown schematically in Fig. 1. The tapering capillary was formed from precision bore Pyrex capillary tubing of internal diameter 0.0025 ± 0.0005 inches. This tubing was drawn out in a gas flame to the extent that the original outside diameter of 5 mm became approximately 2 mm at the narrowest constriction. The tubing was cut just above this point of minimum diameter, giving the capillary an internal diameter of approximately 0.003 cm at the tip. This was considered to be the optimum size, giving the greatest sensitivity without requiring the use of hazardous positive pressures in the manometer system.

The mercury reservoir directly above the capillary was approximately 27 cm in height. The diameter near the top was relatively large--16 mm--in order to minimize any change in height of the mercury column due to drops expelled during the course of a run. For this reason, the height of the column was measured only before and after each run, with small corrections applied for any change in height which may have occurred. The total change in height was never greater than 0.5 mm, and usually was much smaller than this.

A tungsten wire sealed through the glass near the top of the mercury reservoir served as lead to the polarizing source.

Design

The design of the capillary electrometer incorporates several ideas presented by previous workers (40, 41, 42). The system was made entirely from Pyrex glass, and is shown schematically in Fig. 1. The tapering capillary was formed from precision bore Pyrex capillary tubing of internal diameter 0.0025 ± 0.0005 inches. This tubing was drawn out in a gas flame to the extent that the original outside diameter of 5 mm became approximately 2 mm at the narrowest constriction. The tubing was cut just above this point of minimum diameter, giving the capillary an internal diameter of approximately 0.003 cm at the tip. This was considered to be the optimum size, giving the greatest sensitivity without requiring the use of hazardous positive pressures in the manometer system.

The mercury reservoir directly above the capillary was approximately 27 cm in height. The diameter near the top was relatively large--16 mm--in order to minimize any change in height of the mercury column due to drops expelled during the course of a run. For this reason, the height of the column was measured only before and after each run, with small corrections applied for any change in height which may have occurred. The total change in height was never greater than 0.5 mm, and usually was much smaller than this.

A tungsten wire sealed through the glass near the top of the mercury reservoir served as lead to the polarizing source.

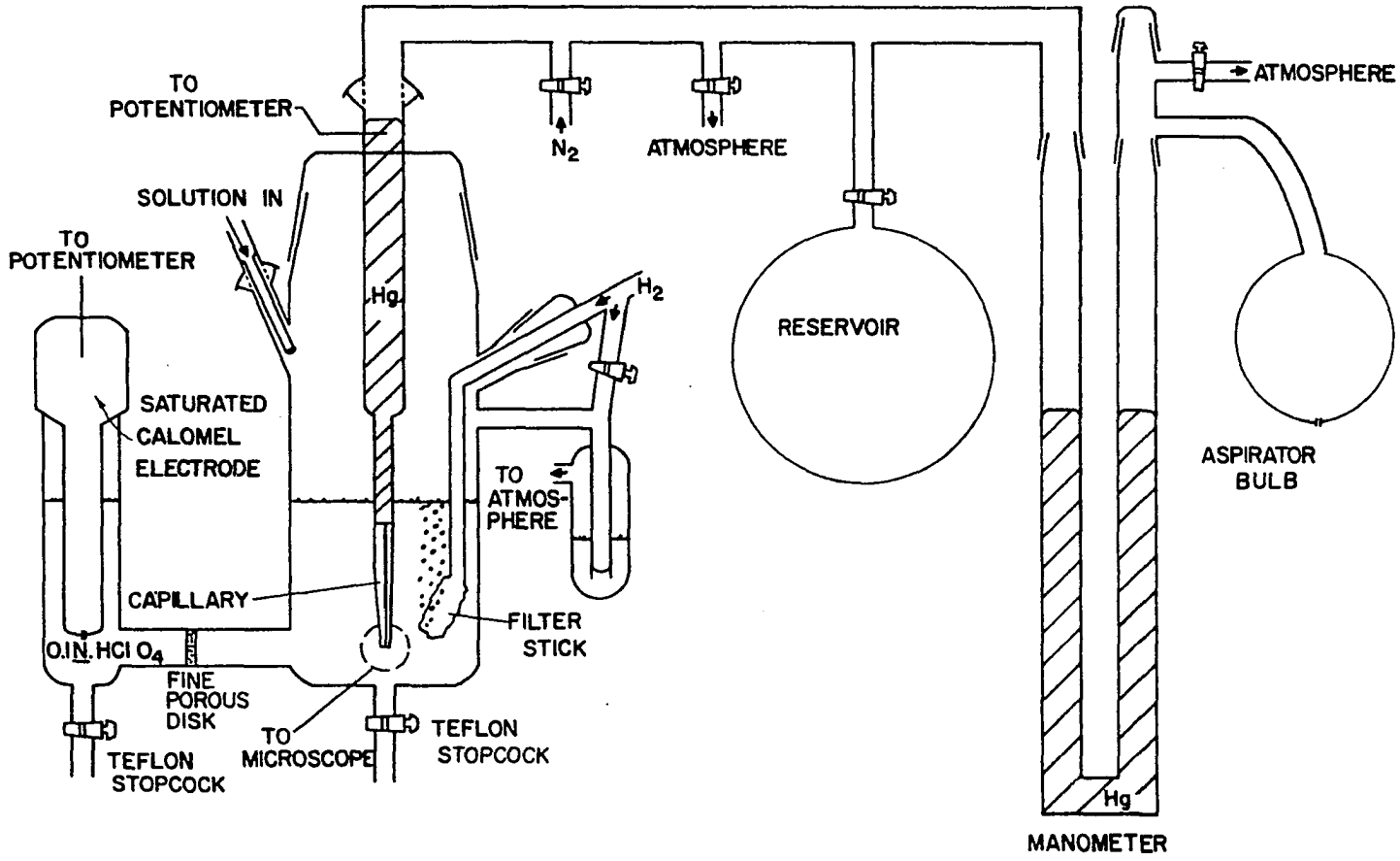

Figure 1. Capillary electrometer schematic

A saturated calomel electrode served as the reference electrode. The porous plug separating the cell proper from the compartment containing the reference electrode minimized the transfer of chloride ion to the solution. A Leeds and Northrup K-2 Potentiometer monitored the voltage supplied by three two-volt cells of a wet-cell storage battery. These cells, wired in parallel, provided a potential source which drifted very little with time.

All ball joints and standard tapers attached or leading to the cell proper were greaseless. The large ball joint connecting the mercury reservoir to the manometer system was lubricated lightly with Apiezon N stopcock grease, which was used also on the three stopcocks attached to the manometer system.

The enclosure connecting the mercury reservoir to the manometer had a total volume of approximately two liters. The one liter reservoir was added to give greater sensitivity to the pressure monitoring which was done with a standard nitrogen regulator valve mounted directly on the nitrogen tank. Polyethylene tubing was used to connect the nitrogen supply to the manometer system.

The outlet to the atmosphere ended as a tapering 1 mm inside diameter capillary which gave good control of pressure release. The system was designed in such a way as to allow the operator to add gas (and so increase pressure) via the

nitrogen tank or release it to the atmosphere while at the same time observing the level of the mercury in the capillary through a microscope.

The manometer itself was constructed of large bore (20 mm) tubing to eliminate the need for any correction for capillary depression effect (43). An opaque white background was provided, and each meniscus was illuminated from the side by a small flashlight. Movable brass cylinders around each arm of the manometer served to eliminate interfering glare from above. A Gaertner cathetometer was used to measure pressures with a precision of 0.05 mm.

The aspirator bulb attached to the atmosphere side of the manometer was used to insure complete wetting of the capillary walls, i.e., no doubt was left as to whether the mercury was sticking in the capillary or not. The bulb was used to oscillate the mercury in the capillary just prior to each measurement, and also after each measurement to make sure no change had taken place.

The meniscus in the capillary was observed through a microscope having an eyepiece scale and a magnification of 23 diameters. Specifically, a Gaertner scale micrometer microscope, M105A, with objective of 48 mm effective focal length, was used. The focal distance was large enough to permit both the mercury column and the tip of the capillary to be simultaneously sharply in focus. In this way, the mercury could be

brought to exactly the same distance from the tip of the capillary (about 0.20 mm) as seen through the eyepiece scale. The tip of the capillary was defined as that point at which separation of a drop of mercury from the column occurred. This eliminated any errors which might be caused by any change of illumination of the capillary tip with respect to the microscope. It also eliminated any errors which may have been introduced by moving the microscope with respect to the capillary. This feature is essential for the cleaning of the cell and the calibration of the capillary.

In order to obtain good definition, the capillary was illuminated from behind by a small electric bulb which was placed behind a white translucent background. A flat piece of glass was fused to the front side of the electrometer cell, thus allowing the capillary to be viewed through optically plane glass.

The entire apparatus, exclusive of the hydrogen purification train and potentiometer system, was attached to a Dexangle frame which was securely braced and mounted on a large and very heavy soap-stone. This eliminated most of the vibration problems, but even more effective in this regard was the use of a relatively thick, and therefore rigid, capillary. The greatest difficulty with vibration occurred in reading the manometer, not in observing the level of the mercury in the capillary.

Method of procedure

All parts of the cell proper were cleaned periodically in the hot acid bath, rinsed with conductivity water, and dried. Mercury was added to the reservoir, and the cell was then assembled.

Solutions were added to both the electrometer and impedance bridge cells through Pyrex funnels bent in such a way as to allow easy pouring and handling. Each funnel ended in a feed-through ball joint which allowed the solutions to be added to the cells without coming in contact with the ball joints themselves. After a solution had been added to the cell, the funnel was replaced by a ball joint having a sealed end.

When the cell was assembled after cleaning, the capillary was always allowed to stand in conductivity water for a day or two before any interfacial tension measurements were made. We found, as had Craxford previously (40), that the capillary radius tends to increase significantly in size with soaking until it finally reaches a constant value. This may be due to the glass being leached by the water, wet by the solution, or forming a gel-like substance; whatever the cause, it was easily compensated for once it was known to be occurring. The capillary was never allowed to dry out unless the cell was cleaned in the acid bath; then it had to be resoaked for at least 24 hours before it could be used.

When a new capillary was constructed and attached to the apparatus, the mercury was made to oscillate up and down in the capillary by use of the aspirator bulb; this hastened the wetting of the capillary by the solution. The capillary was then tested for sensitivity, and also for reproducibility of the position of the meniscus for a given polarization. To work satisfactorily, the capillary must be nearly but not quite cylindrical, and its inner surface must be smooth. By using the precision bore capillary tubing as starting material, it was quite easy to create a tapering capillary having these desired characteristics.

If, after prolonged use, a capillary became dirty as evidenced by a sticking meniscus, it became necessary to either replace it with another or find some suitable way of cleaning it. One method of cleaning which worked satisfactorily was the use of a 1 to 2 per cent solution of hydrofluoric acid. Such a solution would clean the capillary in less than ten minutes; making the mercury oscillate up and down in the capillary several times was all that was required. After such cleaning, the capillary again had to be standardized, for the smallest change in radius would make an appreciable difference in the surface tensions observed. This method of cleaning could not be utilized more than once on a given capillary, for repeated use would roughen the interior to such an extent that solution would not wet the walls thoroughly.

Satisfactory data could be obtained with the electrometer at all potentials between those at which hydrogen and oxygen are formed by electrolysis; this was a range of about 1.5 volts. It was very obvious when either gas began forming, for the meniscus could not be controlled at all, much less brought back to the point of reference. Occasionally bubbles of gas would appear some distance up the capillary; in such case, the bubble had to be removed by forcing mercury out the capillary tip.

When changing from one solution to another, the following procedure was used. After the old solution was removed, the cell was rinsed with conductivity water. Then the cell was filled with conductivity water, and the mercury caused to flow out the end and then retreat back up the capillary a distance of two or three centimeters. It was allowed to stand like this for several minutes, and then the operation was repeated. This was done three or four times, and the conductivity water was then replaced by the new solution. Again the mercury was forced out the end and back up the capillary in the same fashion three or four times before measurements commenced.

Each measurement consisted of applying a measured potential between the mercury meniscus and the calomel electrode, and then adjusting the pressure in the manometer system until the equilibrium position of the meniscus was on the chosen cross mark in the microscope eyepiece scale. The manometer

pressure was then recorded, along with the hydrogen pressure above the solution as measured by the water bubbler. Measurements of the height of mercury in the reservoir above the meniscus, the height of solution above the capillary tip, and the temperature were made only at the beginning and end of a run, with corrections applied for any changes which occurred in these values. A few drops of mercury were expelled between each polarization to assure the formation of a new surface. When this was not done, low values of surface tension were observed, as evidenced by data for the 0.010 molar phenol solution at potentials of -0.55, -0.65, -0.75, and -0.85 volts relative to the saturated calomel electrode. To eliminate as much operator prejudice as possible from the results, data were taken at increments of 0.100 volts, and since values were recorded for each 0.025 volts, the entire potential range was scanned four times during the course of a run.

Since the depolarization current I and the solution resistance R are so small (I is of the order of 10^{-9} amps, and R approximately 60 ohms for 0.1 N. $HClO_4$), the IR correction to polarizing potential was neglected. Also neglected was the liquid junction potential between the 0.10 normal $HClO_4$ and saturated KCl; since this potential is essentially the same for all solutions studied, it will not affect the comparison of results for these solutions. It was first thought advisable to minimize this junction potential as much as possible,

and for this reason a 0.1 N. KCl solution was used in the sidearm of the cell containing the calomel electrode. This was used in taking the n-amyl alcohol data; for the phenol and N-butylacetamide, 0.1 N. $HClO_4$ was used in the sidearm. This caused a change in junction potential of 0.020 volts as measured by the shift of the e.c.m. for 0.1 N. $HClO_4$.

Differential Capacity Measurements and Impedance Bridge

Differential double layer capacities were measured by a modification of the method described by Grantham (44) using, except for minor modifications, instrumentation constructed by him. For clarity, description of apparatus and techniques will be repeated here; single spaced sections are quoted from Grantham, double spaced sections describe modifications introduced by the present author.

Electronic apparatus

A schematic diagram of the bridge is shown in Figure 2. A Leeds and Northrup shielded ratio box, catalog number 1553, served as the central connecting terminal. A shielded step-down transformer is incorporated in this box. Shielded binding posts made connection to the various external pieces of equipment. All electrical connections were made with high quality shielded cables.

The input signal to the transformer in the ratio box was supplied by a Hewlett-Packard Model 200 CD wide range oscillator. The signal from the oscillator was attenuated by use of a simple potential divider constructed from precision resistors. This permitted operation of the oscillator at a high output level where best frequency stability was observed while allowing use of a low level signal for the operation of the

bridge.

The measuring arm of the bridge consisted of a Freed Transformer Co. Model 1350 decade capacitor and a non-inductively wound Leeds and Northrup decade resistance, Catalog No. 4764, in series connection. The lowest capacity range was covered by a continuously variable air capacitor with a maximum value of 1000 micro-microfarads. Four decades in units of 0.001 microfarad, 0.01 microfarad, 0.1 microfarad, and 1 microfarad extended the range of the decade capacitor to 11 microfarads. The decade resistance had six units variable in increments of 0.01, 0.1, 1, 10, 100, and 1000 ohms, respectively, and covered the range from 0.01 ohm to 11,000 ohms. Contact resistances were negligible in both of these circuit elements and the reproducibility in settings were consequently limited only by other factors in the measurement.

A second pair of elements like the above were used in the substitution procedure to be described later. The connections to this cell analog were made as nearly identical with those to the cell proper as could be achieved.

The null detector for the bridge was based on a DuMont Type 304-H cathode ray oscilloscope with both X and Y input terminals. The output signal from the bridge was of such low level that amplification was necessary prior to display on the oscilloscope screen. The bridge output was first amplified by a Hewlett-Packard wide band amplifier, Model 450 A, operating at a gain of 100 to 1. This signal was in turn amplified by a twin-tee narrow band amplifier designed and constructed in this laboratory. Pairs of tees used in the measurement were constructed for use at nominal frequencies of 100, 500, 5000, and 10,000 cycles per second. The filtered, amplified signal from the twin tee produced the Y displacement on the cathode ray oscilloscope screen.

To gain some additional sensitivity in the measurements, a phase sensitive technique was used. A second Hewlett-Packard Model 450 A wide band amplifier was connected to the bridge so that the input signal to the bridge could be amplified and used to produce the X deflection on the oscilloscope screen. Thus, a series of Lissajou's figures showed the amplitude of the output signal from the bridge and the phase of this signal with respect to the input. A horizontal straight line indicated a balance condition. The X axis of the cathode ray oscilloscope was calibrated and used to measure the input signal to the bridge.

The mercury electrode was polarized by means of a Leeds and Northrup Student Potentiometer. To eliminate effectively the path available for the alternating current flow parallel

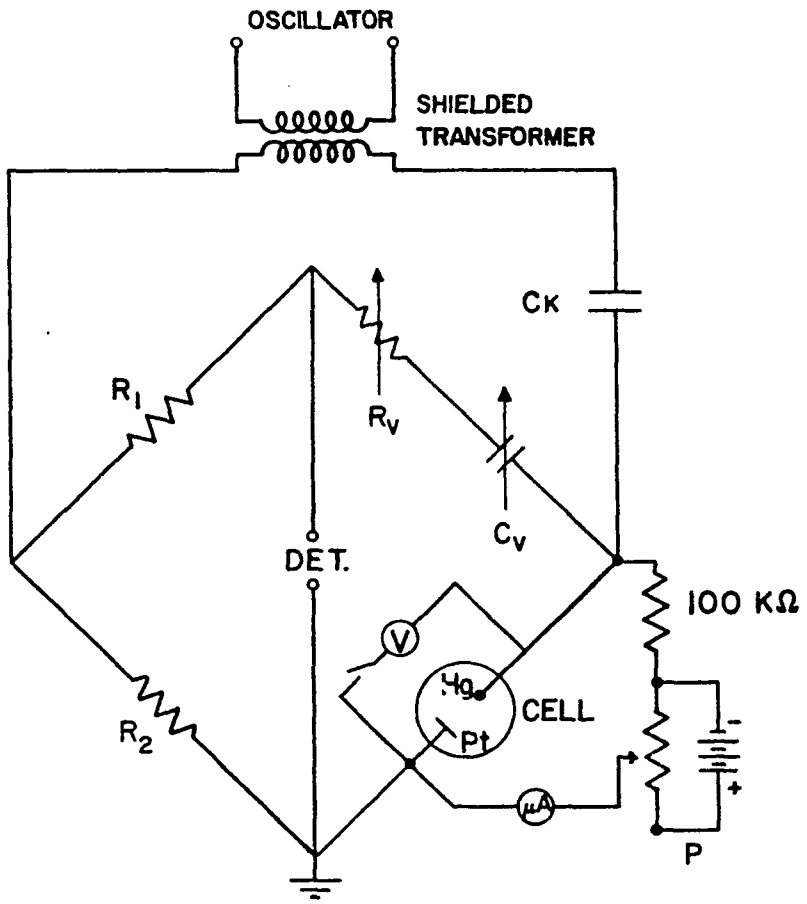

SCHEMATIC DIAGRAM OF A.C.
IMPEDANCE BRIDGE

Figure 2. Impedance bridge schematic

to the path through the double layer and solution, a 100,000 ohm resistor was placed in series with this polarizing source. A Rubicon, Type B, high precision potentiometer was used to measure the polarization of the mercury surface in reference to the standard hydrogen electrode. The Rubicon potentiometer was switched out of the circuit during capacity measurements, thus removing any alternate path for the A.C. current flow. C_K was a 60 microfarad condenser which essentially eliminated the direct current path from the electrodes through the oscillator transformer.

Six volt storage batteries supplied current to the potentiometers. The Rubicon potentiometer slide wire was calibrated against an Eppley Laboratories standard cell Catalog number 100. A Rubicon galvanometer, catalog number 3411, with a sensitivity of 1.5 microvolts per millimeter was used in the calibration. The potentiometer was completely enclosed in a grounded metal box for shielding.

A Simpson microammeter with a full scale deflection of $\pm$ 25 x 10^{-6} amperes was connected in series with the cell and potentiometer to detect and measure any direct current in the system. Capacity measurements were not made whenever this current exceeded 0.5 micro-amps.

The cell

A schematic diagram of the cell used in the capacitance measurements is shown in Figure 3. The container for the solution was formed from a 55/60 Pyrex double walled standard taper, outer. The ring seal at the bottom completed a thermostatting jacket through which water from a constant temperature source could be circulated. The temperature of a solution in the cell could be maintained constant within limits of ± 0.15 degrees near 25° C.

A 55/60 Pyrex standard taper, inner, closed the cell against the atmosphere and served as a support for the various components of the cell. A gas dispersing tube was connected to this support by a ring seal, and a Teflon-plug stopcock directed the incoming gas through this tube when closed, or, when open, forced the gas to bypass the tube while maintaining an atmosphere of hydrogen above the solution. The platinum gauze reference electrode was also connected to the support by a firm platinum wire sealed through a glass sheath, which in turn was ring-sealed to the support.

The dropping mercury electrode was inserted through a Teflon plug, the outside of which had been machined to fit tightly the 12/30 Pyrex standard taper, outer, which was attached to the top of the cell support. The electrode could just as well have been ring sealed through a 12/30 Pyrex standard taper, inner, but the Teflon plug had been used

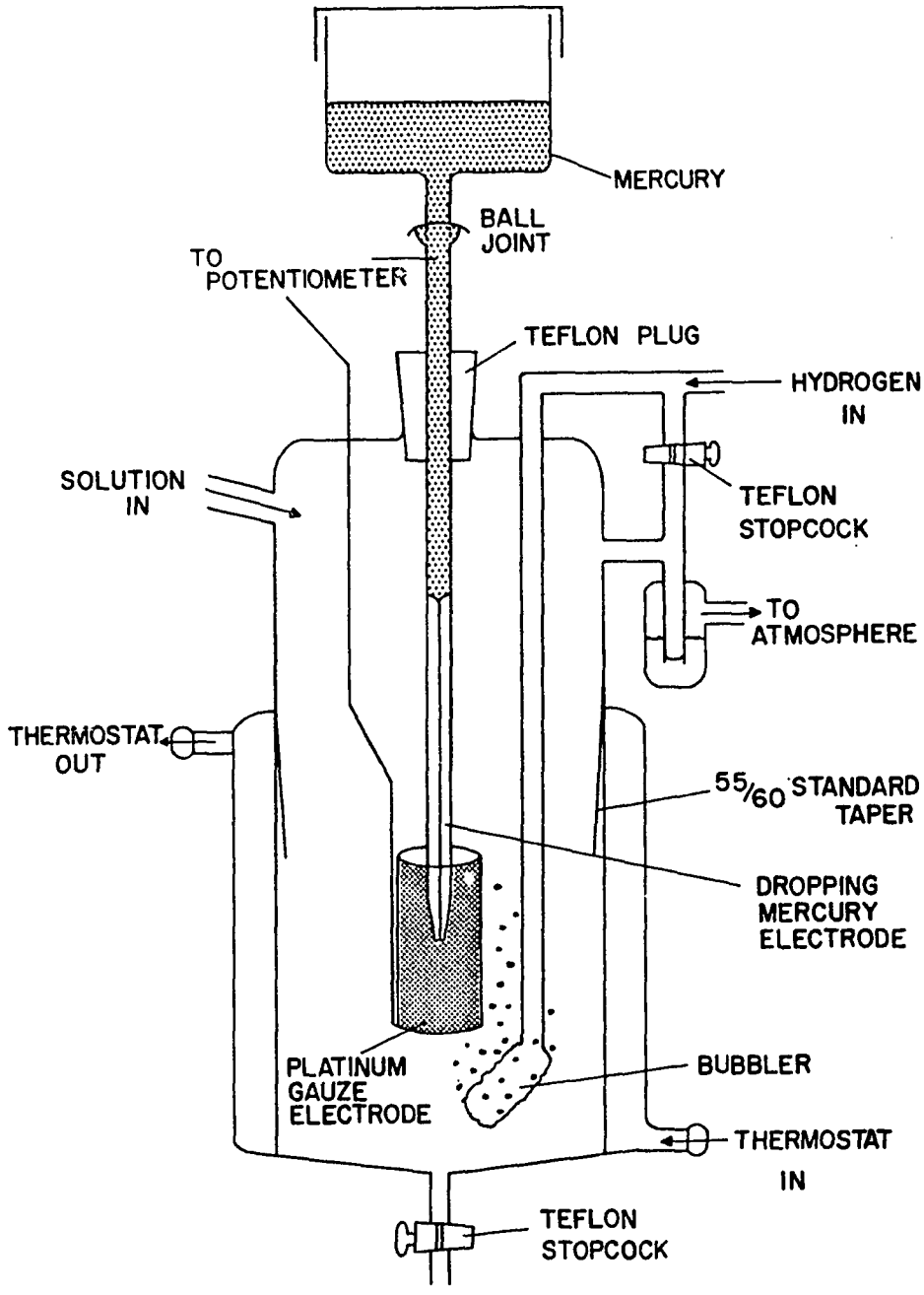

Figure 3. Impedance bridge cell schematic

successfully by Grantham and was easily changed whenever the electrode had to be changed.

The dropping mercury electrode was fed by a reservoir of large cylindrical cross-section in order that flow of mercury through the capillary during the course of a day would not significantly change the height of mercury above the electrode tip, and hence cause no change in the volume flow rate of the mercury. A greaseless ball joint connected this reservoir to the electrode in order to facilitate removal of the electrode from the cell when that became necessary.

Dropping mercury electrode

The dropping mercury electrode was formed from the same precision bore capillary tubing used in the construction of the capillary electrometer. A central segment of this tubing about two inches in length was heated over a wide gas flame and, when soft, was pulled to give an extension about two inches in length. The diameter of the capillary, both inner and outer, decreased as a result. A head of about 40 centimeters of mercury applied to the capillary was necessary to produce a flow rate of approximately 10^{-4} grams per second. A drop of mercury was formed and fell from the tip in sixty to one hundred seconds. Desicote, a Beckman product which forms a hydrophobic surface layer when applied to clean air-dry glass, was drawn into the tube by capillary action and,

after rising some three or four centimeters up the tube, was forced out with nitrogen. After rinsing the capillary interior with acetone, Desicote was again applied in the same manner, and after rinsing again with acetone the capillary was dried by forcing nitrogen through the tubing for several hours. This procedure produced an electrode which showed very little anomalous frequency dispersion caused by solution creeping between the mercury and the glass walls of the capillary (44).

Procedure

The procedure for measurement involved setting a capacity value on the variable arm of the bridge and observing the variation of the Lissajou figure depicting the state of bridge balance. If the resistance of the variable arm of the bridge is adjusted properly, the Lissajou figure passes through a horizontal straight line configuration. At this instant, the size of the droplet is such that its double layer capacity and its resistance are just the proper values necessary to balance the bridge. If the surface area of the drop at this instant is known, then one can easily calculate the capacitance per unit area of electrode surface. By determining the volume flow rate of the mercury through the capillary, and assuming a spherical shape for the mercury droplet at the instant of balance, the age of the drop can be used as a measure of the surface area.

To calculate the surface area, A, of a droplet at any time, t, we assume that the volume flow rate is constant with time, and the droplet is perfectly spherical at the balance point. Under these stipulations, the volume of a droplet is given by

$$\frac{4}{3}\pi r^3 = V,$$

and the surface area is

$$4\pi r^2 = A.$$

If $\rho = 13.56$ g./cm^3 is the density of mercury, then it is true that

$$\frac{\chi}{\rho} = \frac{4/3\ \pi\ r^3}{t}$$

where χ is the flow rate of the mercury and

t is the age of the droplet.

Manipulation of this equation gives

$$A = 4\pi r^2 = 3^{2/3}\ (4\pi)^{1/3}\ \left(\frac{\chi t}{\rho}\right)^{2/3}$$

or

$$\log A = 2/3 \log \left[0.78427\ \chi t\right].$$

Thus, to determine the surface area, the age of the droplet t was measured with a stopwatch, and the flow rate χ measured by weighing the mercury expended from the electrode over a period of several hours. This mercury was washed well with conductivity water and acetone, and then dried thoroughly prior to weighing. All times were measured with a reproducibility of

± 0.2 seconds in 70 seconds.

The cell impedance was measured as a function of applied potential and frequency at a temperature of 24.9° C. The Rubicon potentiometer was calibrated with the standard cell and then set to the potential difference desired between the mercury and hydrogen electrodes. The Student potentiometer was adjusted to the point where the desired potential was attained, and the Rubicon potentiometer was then switched out of the circuit. The output of the oscillator was adjusted to correspond to the proper frequency of the tees in the high gain amplifier, and the impedance of the mercury electrode was then measured at this particular frequency and polarization by proper adjustment of the decade capacitors and resistors in the balancing arm of the bridge. After completing a potential scan at a given frequency, the twin tees were replaced by those corresponding to some other frequency, and the procedure was repeated. The frequency of the signal was periodically checked with a counter, and the frequencies measured during use of a particular pair of tees could be adjusted to the same value within limits of ± 0.3 cycles per second at 100.0 cycles per second, and within limits of ± 5 cycles per second at 9050 cycles per second.

A substitution technique was used to eliminate effects due to asymmetries in the bridge network and in the electrical leads. The cell was replaced by a series combination of a decade resistance with a decade capacitance. This cell analogue combination became the adjustable arm of the bridge in the calibration procedure. The resistance and the capacitance

which initially balanced the cell impedance were in turn balanced by adjusting the resistance and capacitance in the analogue. By using identical shielded electrical leads for connecting both the cell and the analogue to the bridge terminals, the identity of the impedance of the analogue with that of the cell was insured.

EXPERIMENTAL RESULTS

Electrocapillary Data

In Tables 1-3 are listed the values of interfacial tension for solutions of n-amyl alcohol, phenol and N-butylacetamide, respectively, at various concentrations and polarizations of the mercury surface. All solutions are 0.10 normal in perchloric acid. The mercury electrode potential is expressed in volts relative to the electrocapillary maximum for 0.10 normal perchloric acid with no adsorbate present. Adsorbate activities, which were unavailable, were approximated by the reduced concentration, C/Co, which is simply the adsorbate concentration divided by the saturation concentration at the temperature of measurement. Values of Co were taken from earlier work (24) and were, for n-amyl alcohol, 0.222, and for phenol, 0.896, moles per liter. The electrocapillary behavior of N-butylacetamide was only qualitatively examined and therefore the concentration is expressed simply in moles per liter. The electrocapillary curves drawn from the data of Tables 1-3 are shown in Figures 4-6, respectively.

Differential Double Layer Capacitance Data

Tables 4-13 list values of the differential capacity of the mercury-aqueous solution interface for the three adsorbates studied as functions of polarizing potential and frequency

Table 1. Dependence of surface tension at mercury-aqueous solution interface on polarizing potential and concentration of n-amyl alcohol in 0.10 N. $HClO_4$. Interfacial tension in dynes/cm. Electrode potential of Hg surface in volts relative to the electrocapillary maximum for 0.10 N. $HClO_4$

Electrode potential	C/Co 0.014	0.028	0.042	0.084	0.139	0.333	0.694	1.000
- .757	365.5	367.7	367.1	367.4	367.4	365.9	363.4	359.2
- .707	371.7	373.9	373.6	373.5	372.7	371.3	366.3	360.7
- .657	377.8	380.3	380.5	379.6	379.4	375.3	369.0	363.2
- .607	383.9	385.8	384.9	385.0	383.8	378.8	371.6	365.9
- .557	389.8	391.5	391.5	389.6	388.9	381.5	373.8	368.4
- .507	395.1	396.0	395.7	394.5	392.3	384.0	376.0	370.5
- .482		398.7	397.6		393.5	384.9		371.8
- .457	399.7	401.1	400.4	398.3	395.4	386.4	377.6	372.7
- .432	402.0	403.0	401.6	400.4	396.7	387.2		372.8
- .407	404.0	404.8	403.7	401.3	397.7	388.2	379.8	374.3
- .382	406.6	407.0	405.4	403.5	398.6	389.7		375.3
- .357	408.5	408.9	408.1	403.8	399.8	390.0	381.2	376.0
- .332	410.4	410.3	408.4	405.4	401.0	390.9		376.5
- .307	411.3	412.1	409.7	406.0	401.8	391.4	383.2	377.8
- .282	413.7	413.3	411.2	407.7	402.1	392.0		378.1
- .257	415.1	414.8	413.7	407.5	403.0	393.1	384.3	379.1
- .232	416.4	416.2	413.5	408.8	403.7	393.7		379.6
- .207	417.4	417.1	414.3	409.2	404.6	394.2	386.0	380.7
- .182	419.5	417.9	415.4	410.6	405.1	394.8		380.8
- .157	420.1	419.0	417.1	410.7	405.7	395.5	386.7	381.4

Table 1 (Continued).

Electrode potential	C/Co 0.014	0.028	0.042	0.084	0.139	0.333	0.694	1.000
- .132	421.0	419.9	416.5	411.6	406.2	396.3		381.9
- .107	421.4	420.6	417.3	411.4	406.4	396.8	388.3	382.5
- .082	422.5	421.2	418.3	413.2	407.3	396.9		383.0
- .057	423.1	421.5	419.3	412.3	407.6	397.3	388.6	383.3
- .032	423.5	422.1	419.1	413.3	408.5	397.7		383.8
- .007	423.2	422.5	419.3	413.2	408.6	398.1	389.7	384.2
+ .018	423.8	422.4	419.8	414.5	409.0	398.5		383.8
+ .043	423.8	422.5	420.6	413.5	409.3	398.5	389.8	384.8
+ .068	423.4	422.2	420.1	414.2	409.6	399.4		385.3
+ .093	422.2	421.9	419.8	414.3	409.7	399.5	391.0	385.4
+ .118	421.9	421.0	420.1	415.1	409.9	399.3		385.3
+ .143	421.5	420.3	419.7	413.9	409.7	399.7	390.4	385.5
+ .168	420.8	419.1	418.8	414.8	410.1	399.5	391.2	386.0
+ .193	419.1	418.4	417.2	413.8	410.1	400.1	391.4	386.1
+ .218	418.4	416.8	417.1	414.7	410.0	399.7		385.8
+ .243	416.4	414.8	415.8	412.8	409.5	399.7	390.8	386.0
+ .268	415.1	412.1	413.9	412.3	409.2	399.4	391.6	386.3
+ .293	412.2	412.0	412.0	410.6	408.8	399.9	391.5	385.9
+ .318	411.2	409.8	411.0	409.5	407.5	398.8		385.4
+ .343	408.5	407.0	408.2	406.4	405.4	398.3	390.1	384.7
+ .368	407.0	405.1	406.3	405.0	389.5	398.0	390.8	385.1
+ .393	403.2	403.4	403.0	402.6	401.9	396.8	390.3	384.2
+ .418		399.7	401.7		399.9	395.5		383.0
+ .443	398.8	396.4	398.5	396.9	396.3	393.8	388.9	382.3
+ .468		394.3	396.1		394.2		388.0	381.1

Table 1 (Continued).

Electrode potential	C/Co 0.014	0.028	0.042	0.084	0.139	0.333	0.694	1.000
+ .493	391.7	392.3	392.5	391.7	390.9	388.9	385.8	379.6
+ .518		387.9	389.9				384.6	
+ .543	385.1	383.9	385.9	384.1	384.3	383.1	382.1	376.2
+ .593		378.2	378.8	378.1	377.3		375.6	
+ .643	367.4	368.6	370.6	369.5	369.0	368.0	369.4	365.8
+ .693			362.7	362.0	360.4		360.2	
+ .743				351.7	350.5	350.0	352.3	351.0

Table 2. Dependence of surface tension at mercury-aqueous solution interface on polarizing potential and concentration of phenol in 0.10 N. $HClO_4$. Interfacial tension in dynes/cm; electrode potential of Hg surface in volts relative to ECM for 0.1 N. $HClO_4$; concentration in moles per liter

Electrode potential	Phenol concentration 0	0.001	0.005	0.010	0.030	0.060	0.100
- .777	365.0	364.4	364.8	364.8	364.6	363.9	363.6
- .727	371.4	371.3	371.3	371.3	370.9	370.4	369.5
- .677	377.9	377.5	377.6	377.7	377.2	376.2	374.9
- .627	383.8	383.6	383.8	383.6	382.5	381.3	379.4
- .602	387.0	386.8	386.7	386.3	385.4	383.4	381.3
- .577	389.7	389.3	389.2	388.8	387.7	385.6	382.9
- .552	392.4	392.1	392.0	391.6	390.0	387.5	384.5
- .527	394.9	394.8	394.5	394.1	392.0	389.1	385.8
- .502	397.5	397.3	397.0	396.2	394.0	390.6	387.0
- .477	399.9	399.6	399.0	398.5	395.6	392.1	387.9
- .452	402.3	401.8	401.1	400.5	397.1	393.2	389.0
- .427	404.4	404.2	403.3	402.2	398.6	394.4	390.0
- .402	406.7	405.9	405.4	404.0	399.9	395.3	390.8
- .377	408.5	408.3	406.9	404.4	401.1	396.2	391.3
- .352	410.7	410.1	408.6	407.0	402.1	396.8	391.8
- .327	412.2	411.8	410.2	408.4	402.7	397.3	392.6
- .302	414.1	413.3	411.6	409.2	403.9	398.0	393.1
- .277	415.7	414.7	412.4	408.9	403.9	398.4	393.3
- .252	417.4	416.1	413.7	411.3	405.0	398.8	394.9
- .227	418.4	417.7	414.4	412.2	405.1	399.1	394.0
- .202	419.8	418.6	415.7	412.6	405.7	399.5	394.5
- .177	420.9	419.6	415.9	411.7	405.8	399.8	394.5
- .152	422.0	420.3	416.5	413.5	406.2	399.8	394.7
- .127	422.7	420.7	416.7	413.8	406.0	399.7	394.6
- .102	423.6	421.6	417.1	413.8	406.3	400.1	394.6
- .077	424.1	422.1	417.3	412.8	406.1	399.6	394.5
- .052	424.6	422.3	417.5	414.0	406.1	399.6	394.6
- .027	424.9	422.4	416.8	413.6	405.7	399.4	394.2
- .002	425.1	422.1	416.9	413.2	405.4	399.1	394.0
+ .023	424.9	422.1	416.4	412.8	404.9	398.6	393.6

Table 2 (Continued).

Electrode potential	Phenol concentration 0	0.001	0.005	0.010	0.030	0.060	0.100
+ .048	424.9	421.9	416.1	412.3	404.5	398.1	393.2
+ .073	424.2	421.1	415.0	411.5	403.5	397.8	392.6
+ .098	423.6	420.4	414.5	410.7	402.9	397.2	391.9
+ .123	422.8	419.8	413.3	409.8	402.0	396.2	391.2
+ .148	422.0	418.9	412.7	408.8	401.3	395.3	390.5
+ .173	420.6	417.1	411.3	407.7	400.0	394.6	389.5
+ .198	419.2	416.1	410.2	406.1	398.9	393.4	388.9
+ .223	418.0	414.6	408.2	404.9	397.5	392.1	387.6
+ .248	416.6	413.4	407.3	403.5	396.3	390.9	386.6
+ .273	414.5	411.3	405.2	402.0	394.7	389.7	385.2
+ .298	412.6	409.4	403.9	400.0	393.0	388.0	383.9
+ .323	410.5	407.3	401.4	398.3	391.2	386.4	381.9
+ .348	408.6	405.6	399.9	396.4	389.8	384.6	380.6
+ .373	406.1	402.8	397.5	394.2	387.3	382.9	378.7
+ .398	403.6	400.4	395.3	392.1	385.7	380.7	376.7
+ .423	400.9	397.6	392.4	389.7	383.2	378.7	374.8
+ .448	398.2	395.5	390.4	387.4	381.2	376.3	372.7
+ .473	395.1	392.5	387.8	384.7	378.6	374.2	370.2
+ .498	392.2	389.6	385.0	382.2	376.1	371.5	367.9
+ .523	388.9	386.3	381.9	379.4	373.3	368.8	365.4
+ .548	385.4	382.9	379.0	376.3	370.7	366.0	362.7
+ .573	381.7	379.1	375.7	373.2	367.4	362.8	359.8
+ .623	374.1	371.5	368.9	366.6	361.3	356.5	353.6
+ .673	365.9	362.6	361.6	359.4	354.7	349.6	346.5
+ .723	356.8		353.3	351.2	347.3	340.9	338.3

Table 3. Dependence of surface tension at mercury-aqueous solution interface on polarizing potential for 0.10 molar N-butylacetamide in 0.10 normal perchloric acid. Interfacial tension in dynes/cm. Electrode potential of mercury surface in volts relative to electrocapillary maximum for 0.10 normal $HClO_4$

Electrode potential	γ	Electrode potential	γ	Electrode potential	γ
- .677	358.8	- .177	396.0	+ .323	400.9
- .627	363.8	- .127	398.8	+ .373	398.6
- .577	367.8	- .077	400.3	+ .423	394.9
- .527	372.6	- .027	402.2	+ .473	390.9
- .477	376.4	+ .023	403.3	+ .523	385.6
- .427	380.4	+ .073	404.4	+ .573	379.6
- .377	384.0	+ .123	404.8	+ .623	372.5
- .327	387.7	+ .173	404.9	+ .673	364.6
- .277	390.5	+ .223	403.9	+ .723	355.2
- .227	393.2	+ .273	403.1		

of the A.C. signal imposed on the electrode. The polarizing potential is given in volts relative to a saturated hydrogen electrode in 0.10 normal perchloric acid; the electrocapillary maximum for 0.10 normal perchloric acid lies at a potential of -0.167 volts relative to this electrode. This potential was determined by direct measurement of the potential between the hydrogen electrode and a saturated calomel electrode immersed in 0.10 normal perchloric acid; the potential was found to be -0.306 volts. Electrocapillary data indicated the e.c.m. for 0.10 normal perchloric acid lay at -0.473 volts relative to the saturated calomel electrode.

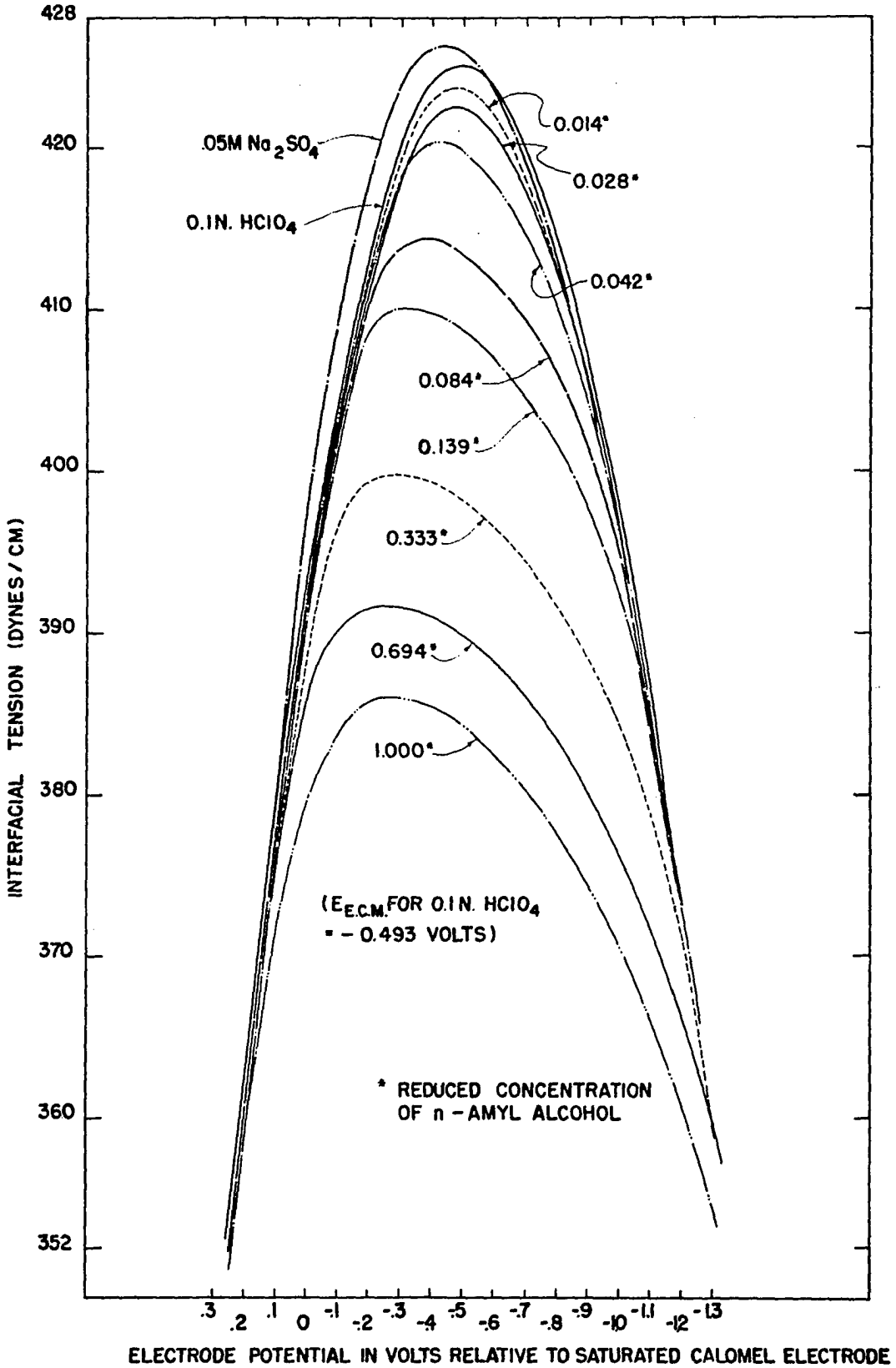

Figure 4. Electrocapillary curves for n-amyl alcohol

Figure 5. Electrocapillary curves for phenol

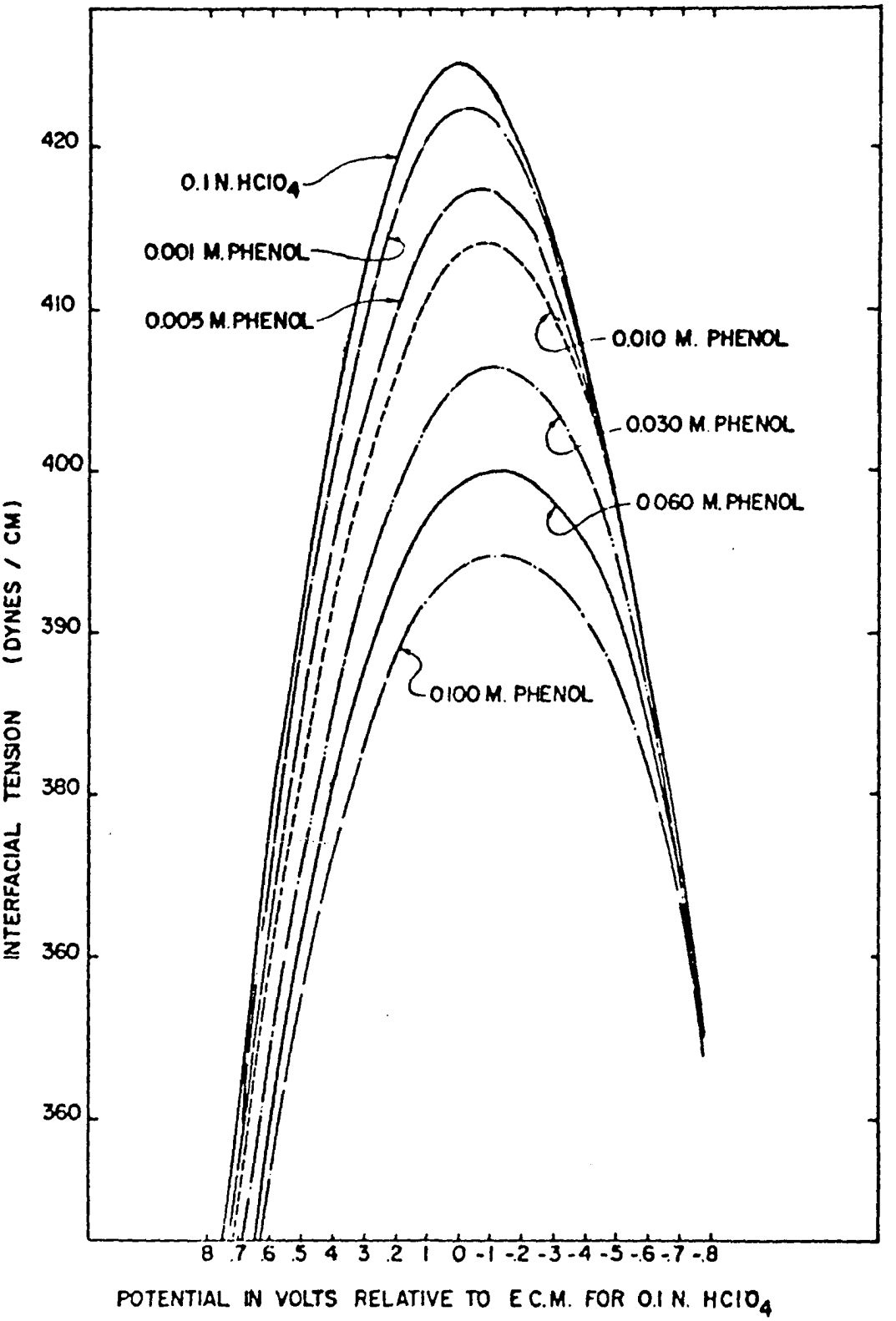
420
410
400
390
380
360
360
INTERFACIAL TENSION (DYNES / CM)
0.1 N. HClO4
0.001 M. PHENOL
0.005 M. PHENOL
0.010 M. PHENOL
0.030 M. PHENOL
0.060 M. PHENOL
0100 M. PHENOL
8 .7 .6 .5 4 3 .2 1 0 -1 -2 -3 -4 -5 -6 -7 -8
POTENTIAL IN VOLTS RELATIVE TO E.C.M. FOR 0.1 N. HClO4

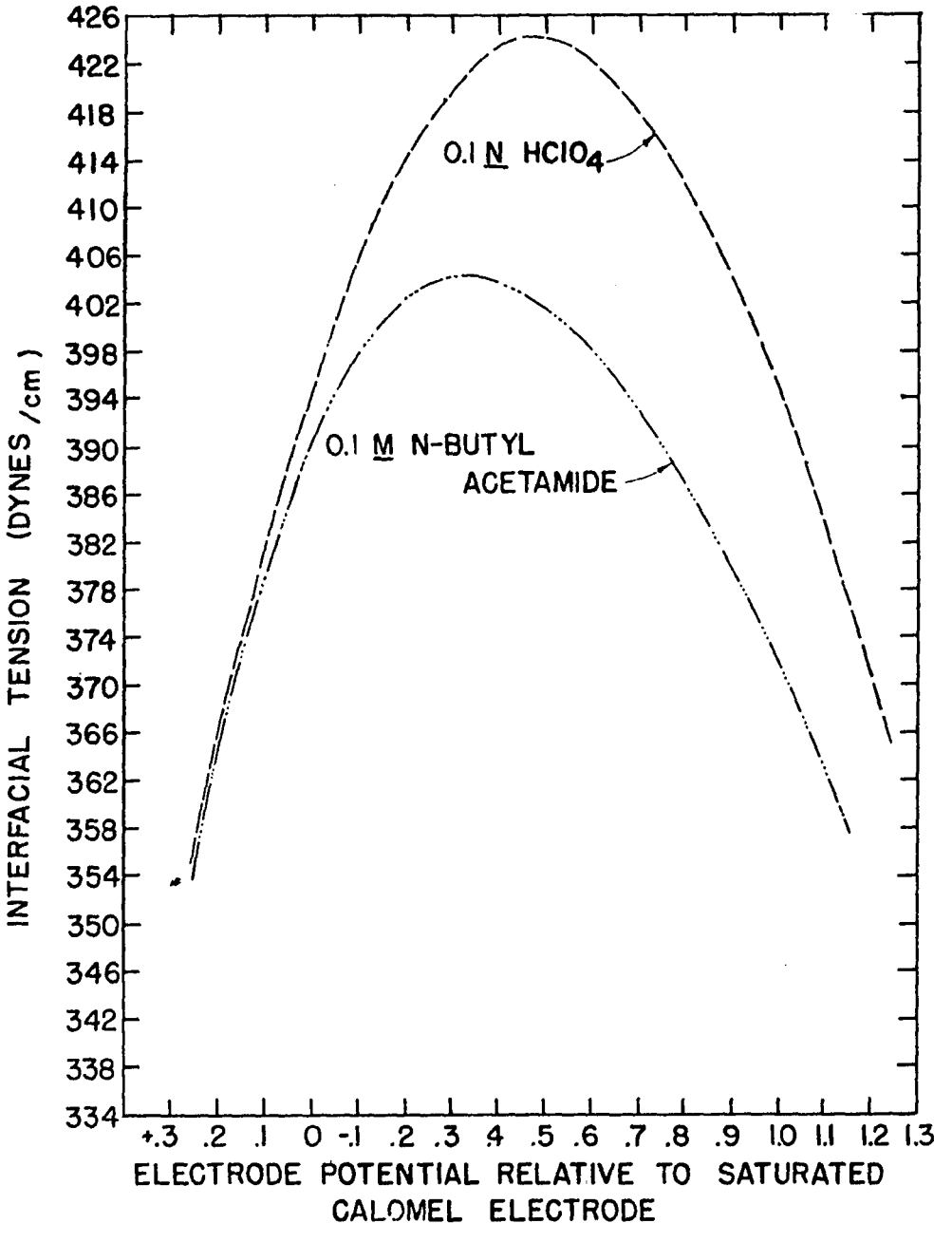

Figure 6. Electrocapillary curves for N-butylacetamide

The capacity at zero frequency was obtained by means of a straight line extrapolation of a plot of square root of frequency versus capacity at constant potential and solution concentration. This zero frequency capacity was integrated twice with respect to polarizing potential, the first integral being the charge density, Q, and the second being the interfacial tension, Υ, for that particular solution and potential. These integrations were performed with the aid of the Cyclone Computer, using a program based on Simpson's rule of numerical integration, that is:

$$\int_{a}^{a-2h} F\,dx = -\int_{a-2h}^{a} F\,dx$$

$$= -\frac{h}{3}\left[F(a-2h) + 4F(a-h) + F(a)\right]$$

where 2h is the difference in potential between two consecutive points of evaluation. The error generated by use of this formula is always less than or equal to

$$\left[\frac{-h^5}{90} F^{(4)}(\delta)\right], \quad (a - 2h < \delta < a)$$

where $F^{(4)}(\delta)$ represents the fourth derivative of F with respect to potential evaluated at δ. Our choice of h = 0.025 volts was small enough to insure that this possible error would be insignificant in relation to the precision of the experimental data.

The charge density, Q, and interfacial tension, Υ, ob-

tained by the integration of the zero frequency capacity are also tabulated in Tables 4, 6-11, for the phenol solutions. The two constants of integration needed for these evaluations were chosen with the aid of the experimental electrocapillary curves: the potential at which $Q = 0$, that is, the e.c.m., and the value of the interfacial tension at the e.c.m. The calculated values of interfacial tension are seen to be in excellent agreement with the experimental electrocapillary curves of Figure 5.

This integration procedure emphasizes the importance of using the zero frequency capacity to obtain the thermodynamic quantities Q and γ. Use of capacity taken at some arbitrary frequency would make no difference at the e.c.m., since the integration constants taken from electrocapillary data determine the values of Q and γ at this point, but the difference becomes great when one determines values for these quantities at potentials strongly anodic or cathodic relative to the e.c.m.

Another way one can visualize the importance of using the zero frequency capacity is to examine the capacity curves at various frequencies for a surfactant having both anodic and cathodic desorption peaks. If a potential V is chosen large enough to insure that all organic material is desorbed from the interface at potentials of +V and -V, then the capacity curve at these potentials will substantially coincide with the

capacity curve obtained with no adsorbate present in solution. Hence, it should be possible to integrate each of these capacity curves from -V to +V and obtain the same answer. In other words, the area enclosed by the capacity curves for C = 0 and C = C' which lies beneath the curve for C = 0 should equal the sum of the areas lying above the curve for C = 0. Examination of Figure 8 for n-amyl alcohol will show that this is true if the zero-frequency capacity is examined, but at high frequencies, the area beneath the C = 0 curve is seen to be much greater than the sum of the areas enclosed by the desorption peaks.

Grantham (44) and others have shown conclusively that with no adsorbate present in solution, the capacity is independent of frequency over the entire potential range. Data of Table 4 which are plotted in Figure 7 show that a fairly uniform frequency dependence was observed by us for 0.10 normal perchloric acid. This is probably due to a slight amount of solution creep between the capillary walls and the mercury in our electrode in spite of the use of the hydrophobic Desicote to prevent this occurrence. This frequency dependence is very small when compared to that observed at the desorption peaks for n-amyl alcohol (compare Figures 7 and 8), but becomes appreciable when considering the nature of the anodic desorption peak for phenol which is less dependent on frequency (see Figure 9).

Figure 10 shows the capacity curves at zero frequency for

the various solutions of phenol studied. Figure 11 is a plot of charge density versus potential for these solutions.

Table 4. Dependence of differential capacity of mercury-aqueous solution interface on frequency, ω, and polarizing potential, V, for 0.10 normal perchloric acid. Charge density, Q, and interfacial tension, γ, computed by integration of zero frequency capacitance curves. Capacity in μfds/cm^2; Q in μ coul/cm^2; γ in dynes/cm; V in volts relative to hydrogen electrode ($V_{e.c.m.}$ = -0.167 volts for 0.10 normal perchloric acid); ω in cycles per second. $C_{\omega=0}$ obtained by straight line extrapolation of a graph of $\sqrt{\omega}$ versus capacity at constant potential

V	$C_{\omega=9,050}$	$C_{\omega=4,910}$	$C_{\omega=500}$	$C_{\omega=100}$	$C_{\omega=0}$	Q	γ
- .800	14.66	15.03	15.37	15.33	15.43	-11.8820	
- .750	14.66	15.14	15.42	15.40	15.50	-11.1086	388.0
- .700	14.80	15.20	12.53	15.52	15.56	-10.3314	
- .650	15.02	15.49	15.72	15.76	15.80	-9.5467	399.1
- .600	15.37	15.73	16.10	16.08	16.16	-8.7487	
- .550	15.85	16.30	16.43	16.54	16.58	-7.9342	408.6
- .500	16.36	16.84	17.05	17.10	17.14	-7.0932	
- .450	17.20	17.73	17.88	17.85	17.92	-6.2161	415.7
- .400	17.81	18.46	18.80	18.77	18.92	-5.2941	
- .350	19.16	19.72	20.00	20.17	20.21	-4.3163	421.0
- .300	20.90	21.34	21.43	21.69	21.68	-3.2723	
- .250	22.72	23.21	23.55	23.82	23.88	-2.1393	424.3
- .200	24.70	25.34	25.86	26.06	26.17	-0.8905	
- .150	26.36	27.40	27.75	27.98	28.10	+0.4734	425.1
- .100	26.89	27.90	28.53	28.64	28.82	1.8994	
- .050	26.77	27.27	28.53	28.50	28.75	3.3408	423.2
0.000	25.75	26.33	27.62	27.48	27.90	4.7595	
+ .050	24.60	25.13	26.31	26.28	26.54	6.1215	418.4
+ .100	23.45	24.04	25.00	24.99	25.28	7.4150	
.150	22.93	23.39	24.02	24.10	24.25	8.6528	411.0

Table 4 (Continued).

V	$C_{\omega=9,050}$	$C_{\omega=4,910}$	$C_{\omega=500}$	$C_{\omega=100}$	$C_{\omega=0}$	Q	Y
.200	22.32	22.48	23.46	23.53	23.75	9.8528	
.250	22.12	22.48	23.19	23.26	23.44	11.0327	401.2
.300	22.12	22.48	23.30	23.35	23.50	12.2055	
.350	22.52	23.21	23.63	23.81	23.90	13.3905	389.0
.400	23.03	23.42	24.31	24.28	24.55	14.6009	
.450	23.78	24.32	25.29	25.19	25.55	15.8501	374.3
.500	24.60	25.17	26.08	26.06	26.38	17.1462	
.550	25.72	26.77	27.37	27.47	27.67	18.4966	357.2
.600	27.01	28.16	28.80	28.90	29.05	19.9159	
.650	28.54	30.72	31.29	32.22	32.28	21.4370	337.3
.700	30.85	34.49			~35	23.1143	

Table 5. Dependence of differential capacity of mercury-aqueous solution interface on frequency, ω, and polarizing potential, V, for C/Co = 0.139 n-amyl alcohol. Capacity in μfds/cm^2; V in volts relative to hydrogen electrode ($V_{e.c.m.}$ = -0.167 for 0.10 normal $HClO_4$); ω in cycles per second. $C_{\omega=0}$ obtained by straight line extrapolation of a graph of $\sqrt{\omega}$ versus capacity at constant potential

V	$C_{\omega=9,050}$	$C_{\omega=4,910}$	$C_{\omega=500}$	$C_{\omega=100}$	$C_{\omega=0}$
-.800	22.09	23.30			
-.750		25.13	28.64	29.33	30.1
-.700	21.70	23.85	27.87	28.71	29.65
-.650	18.21	18.98	22.16	22.63	23.25
-.600	13.85	14.56	16.15	16.54	16.85
-.550	11.14	11.39	12.21	12.38	12.52
-.500	9.13	9.30	9.70	9.84	9.90
-.450	7.88	8.04	8.23	8.29	8.35
-.400	7.07	7.17	7.30	7.34	7.38
-.350	6.55	6.63	6.68	6.74	6.78
-.300	6.20	6.32	6.35		6.40
-.250	6.13	6.16	6.19	6.23	6.26
-.200	6.24	6.32	6.27		6.32
-.150	6.56	6.52	6.57	6.65	6.65
-.100	7.25	7.36	7.37		7.41
-.050	8.85	8.85	9.13	9.10	9.14
0.000	11.84	12.12	12.42	12.92	12.94
+.050	19.83	18.91	19.92	20.78	20.82
+.100	30.61	32.43	38.54	41.22	41.90
+.150	40.72	45.73	56.85	59.43	62.5
+.200	34.38	37.33	41.92	41.89	43.3
.250	28.98	30.14	32.03	31.89	32.5
.300	26.34	27.22	28.00	28.24	28.4
.350	25.32	26.10	27.00	27.59	27.7
.400	25.00	25.74	26.54	26.74	26.9
.450	25.42	26.10	27.00	27.10	27.35
.500	25.85	26.64	27.62	27.84	28.05
.550	26.76	27.64	28.78	29.45	29.55
.600	28.87	29.35	31.18	32.06	32.27
.650	31.32	32.43	34.32	36.71	35.5
.700	35.56	35.08	41.67	58.38	43.8

Table 6. Dependence of differential capacity of mercury-aqueous solution interface on frequency, ω, and polarizing potential, V, for 0.001 molar phenol. Charge density, Q, and interfacial tension, γ, computed by integration of zero frequency capacitance curves. Capacity in μfds/cm^2; Q in μ coul/cm^2; γ in dynes/cm; V in volts relative to hydrogen electrode ($V_{e.c.m.}$ = -0.167 for 0.10 normal $HClO_4$); ω in cycles per second. $C_{\omega=0}$ obtained by straight line extrapolation of a graph of $\sqrt{\omega}$ versus capacity at constant potential

V	$C_{\omega=9,050}$	$C_{\omega=4,910}$	$C_{\omega=500}$	$C_{\omega=100}$	$C_{\omega=0}$	Q	γ
- .800	14.95	15.43	15.54	15.60	15.65	-11.506	384.9
- .750	15.37	15.55	15.72	15.77	15.81	-10.7193	
- .700	15.37	15.98	16.04	16.32	16.42	-9.91	395.6
- .650	15.98	16.17	16.56	16.66	16.74	-9.08	
- .600	15.92	16.84	17.21	17.45	17.60	-8.23	405.2
- .550	16.71	17.13	17.80	18.30	18.40	-7.33	
- .500	16.99	17.65	18.60	19.06	19.25	-6.385	412.5
- .450	17.63	17.96	19.31	19.80	20.02	-5.402	
- .400	17.81	18.63	19.84	20.44	20.60	-4.387	417.9
- .350	18.81	19.07	20.49	21.21	21.36	-3.339	
- .300	19.54	20.21	21.44	22.14	22.32	-2.250	421.2
- .250	21.17	21.50	22.79	23.37	23.50	-1.106	
- .200	22.29	22.84	23.98	24.51	24.67	+0.099	422.3
- .150	23.21	23.78	24.80	25.12	25.32	1.351	
- .100	23.21	23.85	24.56	25.00	25.10	2.613	421.0
- .050	22.39	23.10	23.76	24.05	24.15	3.850	
0.000	21.72	22.09	22.74	22.86	23.02	5.029	417.1
+ .050	20.82	21.27	21.81	21.97	22.10	6.155	
+ .100	20.00	20.31	20.91	21.14	21.26	7.237	411.0
+ .150	19.54	20.01	20.56	20.88	21.05	8.293	

Table 6 (Continued).

V	$C_{\omega=9,050}$	$C_{\omega=4,910}$	$C_{\omega=500}$	$C_{\omega=100}$	$C_{\omega=0}$	Q	Υ
+ .200	19.61	19.81	20.49	20.79	20.88	9.339	402.7
+ .250	19.61	20.01	20.82	21.22	21.35	10.392	
+ .300	20.00	20.52	21.44	21.96	22.12	11.474	392.3
+ .350	20.65	21.27	22.39	22.85	23.05	12.600	
+ .400	21.62	22.21	23.43	24.28	24.36	13.782	379.7
+ .450	22.85	23.48	25.05	25.60	25.90	15.033	
+ .500	24.12	24.80	26.53	27.43	27.55	16.365	364.6
+ .550	25.54	26.44	28.26	28.89	29.20	17.785	
+ .600	27.26	28.16	30.13	30.93	31.25	19.298	346.8
+ .650	29.37	30.56	32.90	33.83	34.18	20.929	
+ .700	32.00	33.79	40.24	60.40	-	-	

Table 7. Dependence of differential capacity of mercury-aqueous solution interface on frequency, ω, and polarizing potential, V, for 0.005 molar phenol. Charge density, Q, and interfacial tension, γ, computed by integration of zero frequency capacitance curves. Capacity in μfds/cm^2; Q in μ coul/cm^2; γ in dynes/cm; V in volts relative to hydrogen electrode ($V_{e.c.m.}$ = -0.167 for 0.10 normal perchloric acid); ω in cycles per second. $C_{\omega=0}$ obtained by straight line extrapolation of a graph of $\sqrt{\omega}$ versus capacity at constant potential

V	$C_{\omega=9,050}$	$C_{\omega=4,910}$	$C_{\omega=500}$	$C_{\omega=100}$	$C_{\omega=0}$	Q	γ
- .800	16.18	16.72	16.95	16.87	17.00	-11.795	382.9
- .750	16.64	17.29	17.78	17.76	17.97	-10.922	
- .700	17.51	18.10	18.70	18.84	18.95	-10.001	393.8
- .650	17.97	18.84	19.79	20.05	20.27	-9.023	
- .600	18.47	19.49	20.77	21.10	21.43	-7.982	402.9
- .550	18.64	19.64	21.47	21.90	22.28	-6.887	
- .500	18.47	19.49	21.47	22.01	22.40	-5.769	409.7
- .450	18.13	19.12	21.11	21.66	22.05	-4.657	
- .400	17.66	18.70	20.51	21.08	21.45	-3.569	414.4
- .350	17.66	18.49	20.03	20.46	20.77	-2.518	
- .300	17.97	18.84	20.11	20.56	20.77	-1.482	417.0
- .250	18.72	19.49	20.43	20.68	20.90	-0.441	
- .200	19.44	20.03	20.77	20.89	21.08	+0.609	417.3
- .150	19.54	20.19	20.77	20.78	20.95	1.660	
- .100	19.44	20.03	20.51	20.47	20.75	2.703	415.7
- .050	18.99	19.56	19.95	19.97	20.15	3.727	
0.000	18.42	19.02	19.49	19.48	19.68	4.719	412.0
+ .050	17.89	18.63	18.98	19.03	19.17	5.688	
+ .100	17.65	18.23	18.70	18.76	18.90	6.638	406.3
+ .150	17.51	18.10	18.63	18.76	18.93	7.583	

Table 7 (Continued).

V	$C_{\omega=9,050}$	$C_{\omega=4,910}$	$C_{\omega=500}$	$C_{\omega=100}$	$C_{\omega=0}$	Q	Y
+ .200	17.66	18.23	18.84	18.94	19.11	8.533	398.7
+ .250	17.97	18.70	19.34	19.39	19.60	9.501	
+ .300	18.64	19.27	20.11	20.27	20.42	10.499	389.2
+ .350	19.44	20.27	21.11	21.22	21.45	11.541	
+ .400	20.63	21.38	22.52	22.77	22.92	12.648	377.6
+ .450	21.84	22.93	24.20	24.64	24.90	13.839	
+ .500	23.79	24.48	26.25	26.59	26.95	15.129	363.8
+ .550	25.34	26.67	28.39	28.93	29.30	16.533	
+ .600	27.54	28.55	31.15	31.93	32.35	18.071	347.2
+ .650	29.70	31.35	33.89	34.87	35.40	19.762	
+ .700	33.67	35.55	43.69	59.77	-	-	

Table 8. Dependence of differential capacity of mercury-aqueous solution interface on frequency, ω, and polarizing potential, V, for 0.010 molar phenol. Charge density, Q, and interfacial tension, γ, computed by integration of zero frequency capacitance curves. Capacity in μfds/cm^2; Q in μ coul/cm^2; γ in dynes/cm; V in volts relative to hydrogen electrode ($V_{e.c.m.}$ = -0.167 for 0.10 normal perchloric acid); ω in cycles per second. $C_{\omega=0}$ obtained by straight line extrapolation of a graph $\sqrt{\omega}$ versus capacity at constant potential

V	$C_{\omega=9,050}$	$C_{\omega=4,910}$	$C_{\omega=500}$	$C_{\omega=100}$	$C_{\omega=0}$	Q	γ
- .800	17.50	18.10	18.45	18.51	18.63	-11.561	
- .750	18.38	19.12	19.71	19.97	20.08	-10.593	388.6
- .700	19.34	20.19	21.04	21.41	21.55	-9.555	
- .650	20.03	21.11	22.42	22.76	23.02	-8.442	398.1
- .600	20.11	21.27	23.03	23.50	23.85	-7.266	
- .550	19.82	21.05	22.82	23.39	23.73	-6.075	405.4
- .500	18.80	20.01	21.71	22.35	22.60	-4.912	
- .450	17.81	18.80	20.30	20.88	21.15	-3.814	410.3
- .400	16.99	17.81	18.96	19.58	19.68	-2.794	
- .350	16.57	17.27	18.04	18.51	18.61	-1.845	413.1
- .300	16.57	17.27	17.80	18.04	18.17	-0.929	
- .250	16.99	17.65	17.96	18.18	18.27	-0.018	414.0
- .200	17.43	17.96	18.20	18.44	18.53	+0.901	
- .150	17.73	18.21	18.45	18.65	18.73	1.832	413.1
- .100	17.81	18.29	18.53	18.65	18.75	2.769	
- .050	17.58	18.21	18.36	18.65	18.72	3.705	410.4
0.000	17.43	17.88	18.28	18.44	18.52	4.636	
+ .050	17.20	17.81	18.04	18.24	18.30	5.556	405.7
+ .100	17.06	17.65	18.04	18.18	18.26	6.470	
+ .150	17.13	17.65	18.04	18.24	18.31	7.384	399.3

Table 8 (Continued).

V	$C_{\omega=9,050}$	$C_{\omega=4,910}$	$C_{\omega=500}$	$C_{\omega=100}$	$C_{\omega=0}$	Q	Y
+ .200	17.35	17.88	18.28	18.51	18.60	8.306	
+ .250	17.66	18.29	18.70	18.92	19.04	9.246	391.0
+ .300	18.29	18.89	19.33	19.59	19.65	10.213	
+ .350	18.98	19.81	20.41	20.71	20.81	11.223	380.7
+ .400	20.11	20.84	21.60	21.78	21.97	12.293	
+ .450	21.75	22.33	23.35	23.72	23.90	13.439	368.4
+ .500	23.35	24.01	25.34	25.62	25.91	14.679	
+ .550	25.21	26.39	27.69	28.36	28.58	16.033	353.7
+ .600	27.54	28.82	30.59	31.02	31.38	17.529	
+ .650	30.52	31.84	34.32	35.16	35.61	19.174	336.2
+ .700	34.53	36.50	44.17	61.04	-	-	

Table 9. Dependence of differential capacity of mercury-aqueous solution interface on frequency, ω, and polarizing potential, V, for 0.030 molar phenol. Charge density, Q, and interfacial tension, γ, computed by integration of zero frequency capacitance curves. Capacity in μfds/cm^2; Q in μ coul/cm^2; γ in dynes/cm; V in volts relative to hydrogen electrode ($V_{e.c.m.}$ = -0.167 for 0.10 normal perchloric acid); ω in cycles per second. $C_{\omega=0}$ obtained by straight line extrapolation of a graph of $\sqrt{\omega}$ versus capacity at constant potential

V	$C_{\omega=9,050}$	$C_{\omega=4,910}$	$C_{\omega=500}$	$C_{\omega=100}$	$C_{\omega=0}$	Q	γ
- .800	22.18	23.04	23.53	23.72	23.84	-10.727	
- .750	23.65	24.36	26.08	26.18	26.62	-9.453	387.5
- .700	23.93	25.24	27.20	27.31	27.92	-8.086	
- .650	22.93	24.36	26.49	26.87	27.35	-6.698	395.6
- .600	21.29	22.03	24.21	24.17	24.65	-5.391	
- .550	18.29	19.16	20.82	20.99	21.45	-4.235	401.0
- .500	16.24	16.57	18.04	17.84	18.15	-3.247	
- .450	14.44	14.81	15.66	15.60	15.90	-2.402	404.3
- .400	13.30	13.66	14.24	14.00	14.38	-1.651	
- .350	12.74	13.08	13.42	13.38	13.54	-0.956	406.0
- .300	12.69	13.00	13.30	13.26	13.40	-0.283	
- .250	13.13	13.43	13.66	13.56	13.64	+0.392	406.2
- .200	13.80	14.28	14.38	14.33	14.43	1.090	
- .150	14.59	15.03	15.36	15.34	15.48	1.838	405.2
- .100	15.49	15.85	16.16	16.18	16.28	2.634	
- .050	15.98	16.50	16.97	16.95	17.10	3.471	402.5
0.000	16.44	16.98	17.42	17.46	17.58	4.337	
+ .050	16.71	17.13	17.72	17.77	17.91	5.225	398.2
+ .100	16.85	17.35	17.88	17.92	18.07	6.124	
+ .150	16.99	17.50	17.96	18.01	18.14	7.030	392.0

Table 9 (Continued).

V	$C_{\omega=9,050}$	$C_{\omega=4,910}$	$C_{\omega=500}$	$C_{\omega=100}$	$C_{\omega=0}$	Q	Y
+ .200	17.21	17.65	18.28	18.25	18.50	7.946	
+ .250	17.58	18.04	18.53	18.59	18.72	8.875	384.1
+ .300	17.97	18.46	19.06	19.20	19.32	9.826	
+ .350	18.72	19.25	19.90	19.87	20.08	10.809	373.8
+ .400	19.73	20.21	20.93	20.89	21.09	11.839	
+ .450	20.74	21.47	22.20	22.26	22.48	12.927	362.4
+ .500	22.42	23.14	24.02	24.17	24.41	14.094	
+ .550	24.36	25.08	26.19	26.16	26.57	15.362	348.3
+ .600	26.55	27.65	28.53	29.31	29.47	16.759	
+ .650	29.51	30.56	32.31	32.89	33.25	18.325	331.5
+ .700	34.52	37.00	46.96	-	-	-	

Table 10. Dependence of differential capacity of mercury-aqueous solution interface on frequency, ω, and polarizing potential, V, for 0.060 molar phenol. Charge density, Q, and interfacial tension, γ, computed by integration of zero frequency capacitance curves. Capacity in μfds/cm^2; Q in μ coul/cm^2; γ in dynes/cm; V in volts relative to hydrogen electrode ($V_{e.c.m.}$ = -0.167 for 0.10 normal perchloric acid); ω in cycles per second. $C_{\omega=0}$ obtained by straight line extrapolation of a graph of $\sqrt{\omega}$ versus capacity at constant potential

V	$C_{\omega=9,050}$	$C_{\omega=4,910}$	$C_{\omega=500}$	$C_{\omega=100}$	$C_{\omega=0}$	Q	γ
- .800	27.68	28.82	30.68	30.64	31.40	-9.528	381.3
- .750	27.53	28.82	31.15	31.44	32.08	-7.926	
- .700	24.96	25.88	27.99	28.85	29.10	-6.389	389.3
- .650	20.76	21.47	23.00	23.37	23.70	-5.071	
- .600	17.20	17.90	18.67	19.10	19.25	-4.003	394.4
- .550	14.17	14.80	15.42	15.63	15.77	-3.128	
- .500	12.68	12.96	13.23	13.43	13.49	-2.397	397.5
- .450	11.26	11.66	11.88	11.99	12.02	-1.765	
- .400	10.78	10.94	11.09	11.11	11.15	-1.187	399.3
- .350	10.44	10.52	10.70	10.75	10.80	-0.639	
- .300	10.60	10.70	10.82	10.79	10.85	-0.098	400.0
- .250	11.06	11.18	11.26	11.31	11.35	+0.455	
- .200	11.84	12.08	12.12	12.09	12.15	1.038	399.5
- .150	13.01	13.13	13.24	13.38	13.40	1.675	
- .100	13.98	14.51	14.50	14.51	14.52	2.371	397.8
- .050	15.37	15.60	15.80	16.01	16.02	3.136	
0.000	16.50	16.57	16.88	17.10	17.10	3.965	394.7
+ .050	16.91	17.34	17.64	17.76	17.84	4.840	
+ .100	17.27	17.65	18.11	18.24	18.33	5.744	389.8
+ .150	17.57	17.96	18.36	18.50	18.57	6.665	

Table 10 (Continued).

V	$C_{\omega=9,050}$	$C_{\omega=4,910}$	$C_{\omega=500}$	$C_{\omega=100}$	$C_{\omega=0}$	Q	Y
+ .200	17.73	18.37	18.61	18.67	18.72	7.597	383.2
+ .250	17.88	18.37	18.79	18.93	18.98	8.538	
+ .300	18.29	18.71	19.14	19.20	19.33	9.494	374.6
+ .350	18.89	19.33	19.80	19.86	20.01	10.473	
+ .400	19.53	20.10	20.50	20.67	20.71	11.489	364.1
+ .450	20.63	21.05	21.60	21.79	21.90	12.548	
+ .500	22.03	22.62	23.19	23.16	23.44	13.679	351.6
+ .550	23.56	24.32	25.00	25.12	25.35	14.899	
+ .600	25.59	26.52	27.24	27.55	27.90	16.274	336.7
+ .650	28.53	29.24	30.58	31.09	31.34	17.717	
+ .700	32.98	34.93	43.46	53.07	-	-	

Table 11. Dependence of differential capacity of mercury-aqueous solution interface on frequency, ω, and polarizing potential, V, for 0.100 molar phenol. Charge density, Q, and interfacial tension, γ, computed by integration of zero frequency capacitance curves. Capacity in μfds/cm^2; Q in μ coul/cm^2; γ in dynes/cm; V in volts relative to hydrogen electrode ($V_{e.c.m.}$ = -0.167 for 0.10 normal perchloric acid); ω in cycles per second. $C_{\omega=0}$ obtained by straight line extrapolation of a graph of $\sqrt{\omega}$ versus capacity at constant potential

V	$C_{\omega=9,050}$	$C_{\omega=4,910}$	$C_{\omega=500}$	$C_{\omega=100}$	$C_{\omega=0}$	Q	γ
- .850	30.87	32.35	35.60	36.12	36.85	-9.607	
- .830	31.51			36.12	36.70		
- .800	30.72	32.01	34.18	34.88	35.35	-7.787	380.1
- .750	26.09	27.03	28.39	28.10	28.80	-6.179	
- .700	20.50	21.50	21.47	21.91	21.90	-4.922	386.4
- .650	16.64	16.91	17.14	16.95	17.19	-3.948	
- .600	13.54	13.98	13.97	14.11	14.17	-3.166	390.3
- .550	11.84	11.94	12.18	12.15	12.19	-2.515	
- .500	10.58	10.79	10.80	10.86	10.90	-1.942	392.9
- .450	9.80	10.00	10.05	10.10	10.13	-1.418	
- .400	9.31	9.44	9.66	9.66	9.70	-0.922	394.3
- .350	9.14	9.44	9.48	9.52	9.55	-0.442	
- .300	9.26	9.35	9.66	9.66	9.70	+0.039	394.7
- .250	9.62	10.00	10.10	10.25	10.30	0.536	
- .200	10.31	10.47	10.92	10.98	11.05	1.067	394.2
- .150	11.35	11.98	12.12	12.34	12.36	1.649	
- .100	12.74	12.96	13.66	13.69	13.90	2.305	392.5
- .050	14.09	14.80	15.09	15.27	15.33	3.037	
0.000	15.38	16.23	16.66	16.74	16.90	3.849	389.5
+ .050	16.57	17.42	17.72	18.00	18.08	4.725	

Table 11 (Continued).

V	$C_{\omega=9,050}$	$C_{\omega=4,910}$	$C_{\omega=500}$	$C_{\omega=100}$	$C_{\omega=0}$	Q	Y
+ .100	17.36	18.13	18.62	18.76	18.88	5.650	384.7
+ .150	17.81	18.63	19.06	19.30	19.39	6.606	
+ .200	18.13	18.89	19.42	19.48	19.63	7.582	378.1
+ .250	18.38	19.07	19.61	19.77	19.90	8.572	
+ .300	18.55	19.34	19.80	19.97	20.11	9.570	369.6
+ .350	18.90	19.81	20.30	20.58	20.68	10.585	
+ .400	19.44	20.41	20.93	21.23	21.32	11.630	359.0
+ .450	20.22	21.27	21.84	22.28	22.39	12.720	
+ .500	21.28	22.58	23.41	23.60	23.91	13.874	346.2
+ .550	22.94	24.21	24.91	25.51	25.67	15.107	
+ .600	24.91	26.22	27.49	27.59	28.00	16.445	331.1
+ .650	27.26	29.38	30.36	32.73	32.85	17.949	
+ .700	31.82	35.55	47.49	-	-		

Table 12. Dependence of differential capacity of mercury-aqueous solution interface on frequency, ω, and polarizing potential, V, for 0.615 molar phenol. Capacity in μfds/cm^2; V in volts relative to hydrogen electrode ($V_{e.c.m.}$ = -0.167 for 0.10 normal perchloric acid); ω in cycles per second. $C_{\omega=0}$ obtained by straight line extrapolation of a graph of $\sqrt{\omega}$ versus capacity at constant potential

V	$C_{\omega=9,050}$	$C_{\omega=4,910}$	$C_{\omega=500}$	$C_{\omega=100}$	$C_{\omega=0}$
- .850	14.25	14.73	15.09	16.42	16.13
- .800	11.94	12.03	12.84	12.38	12.52
- .750	10.47	10.69	10.82	10.75	10.83
- .700	9.44	9.57	9.85	9.80	9.87
- .650	8.74	8.85	8.93	8.92	8.97
- .600	8.14	8.27	8.51	8.40	8.50
- .550	7.76	7.92	8.00	7.93	7.99
- .500	7.49	7.56	7.83	7.69	7.80
- .450	7.31	7.41	7.45	7.49	7.52
- .400	7.14	7.24	7.45	7.27	7.44
- .350	7.07	7.10	7.23	7.20	7.24
- .300	7.00	7.07	7.23	7.11	7.20
- .250	7.07	7.17	7.30	7.19	7.28
- .200	7.35	7.41	7.55	7.40	7.47
- .150	7.79	7.85	8.13	8.00	8.12
- .100	8.74	8.85	9.13	8.88	9.04
- .050	10.10	10.26	10.62	10.28	10.53
0.000	11.89	12.10	12.45	12.24	12.48
+ .050	13.79	14.11	14.51	14.47	14.70
+ .100	15.49	15.81	16.36	16.20	16.47
+ .150	16.85	17.27	17.88	17.77	18.08
+ .200	17.81	18.37	18.88	18.85	19.00
+ .250	18.64	19.16	19.90	19.76	19.97
+ .300	19.26	19.81	20.51	20.36	20.65
+ .350	19.73	20.31	21.14	21.00	21.25
+ .400	20.22	20.84	21.70	21.68	22.07
+ .450	20.76	21.35	22.28	22.15	22.60
+ .500	21.38	22.00	22.88	22.95	23.21
+ .550	22.03	22.69	23.74	23.92	24.20
+ .600	23.03	23.75	25.10	25.27	25.54
+ .650	24.47	25.55	27.61	28.63	29.00
+ .700	26.21	27.40	33.43		~33.5

Table 13. Dependence of differential capacity of mercury-aqueous solution interface on polarizing potential for 0.10 molar N-butylacetamide (NBA). Potential in volts relative to hydrogen electrode ($V_{e.c.m.}$ = -0.167 for 0.10 N. $HClO_4$). Capacity in $\mu fds/cm^2$. A.C. frequency = 100 cycles/sec.

Potential	$C_{\omega=100}$	Potential	$C_{\omega=100}$	Potential	$C_{\omega=100}$
- .850	8.06	- .300	12.82	+ .200	31.40
- .800	7.95	- .250	13.69	+ .250	33.59
- .750	7.99	- .200	14.57	+ .300	34.45
- .700	8.09	- .150	15.52	+ .350	34.45
- .650	8.33	- .100	16.46	+ .400	34.16
- .600	8.68	- .050	17.93	+ .450	33.88
- .550	9.09	0.000	19.59	+ .500	33.59
- .500	9.62	+ .050	21.97	+ .550	33.30
- .450	10.30	+ .100	24.98	+ .600	35.00
- .400	11.03	+ .150	28.50	+ .650	38.81
- .350	11.91				

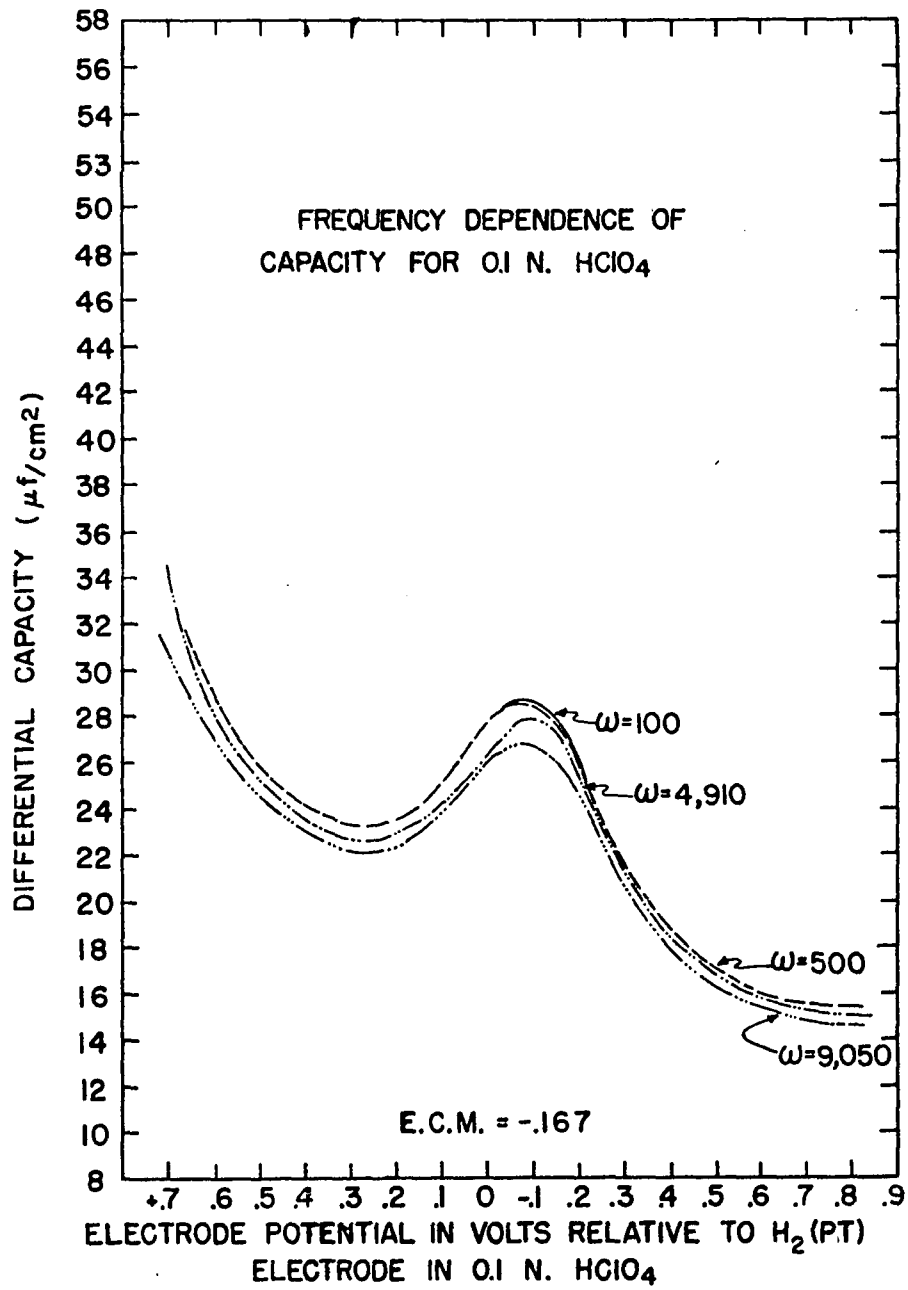

Figure 7. Capacity for 0.1 N. $HClO_4$

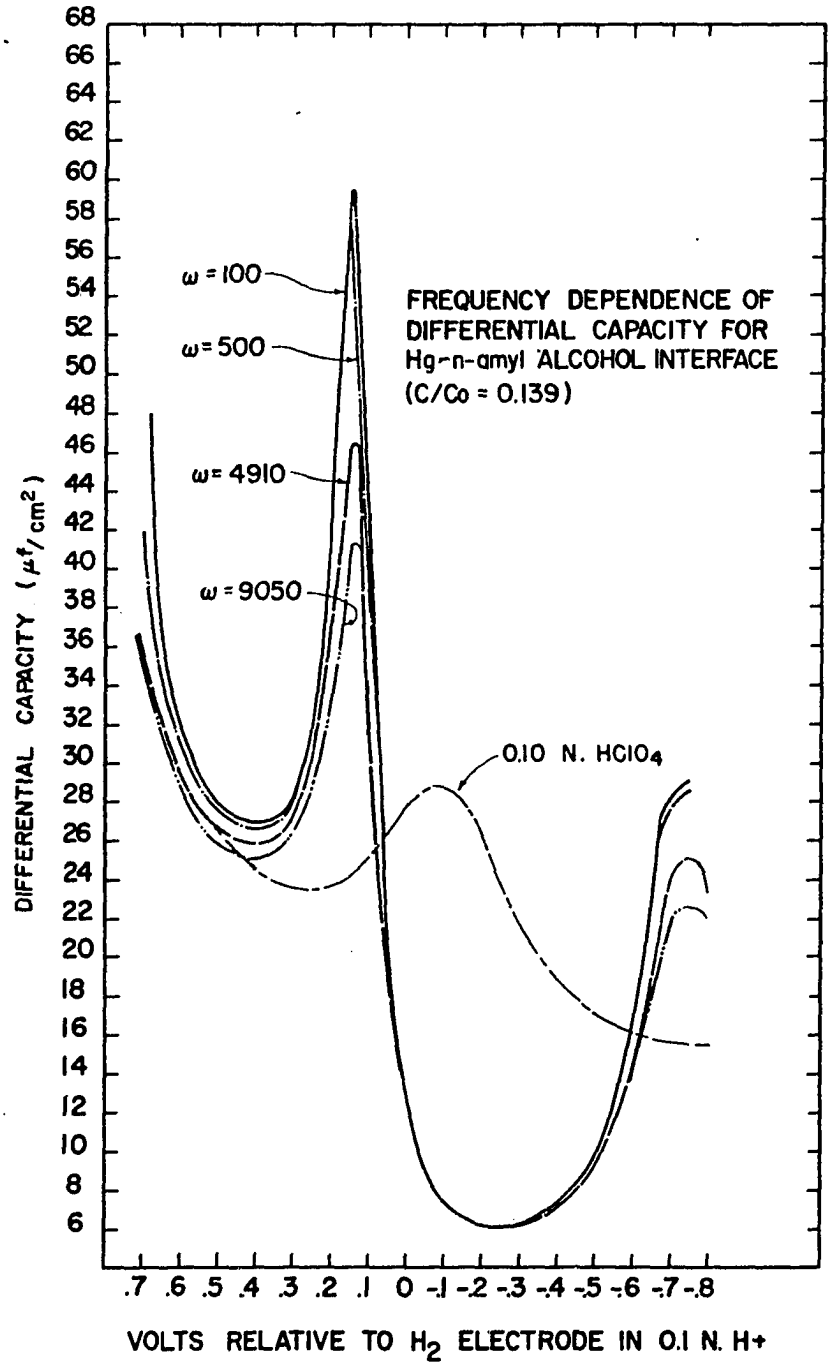

Figure 8. Capacity for C/Co = 0.139 n-amyl alcohol

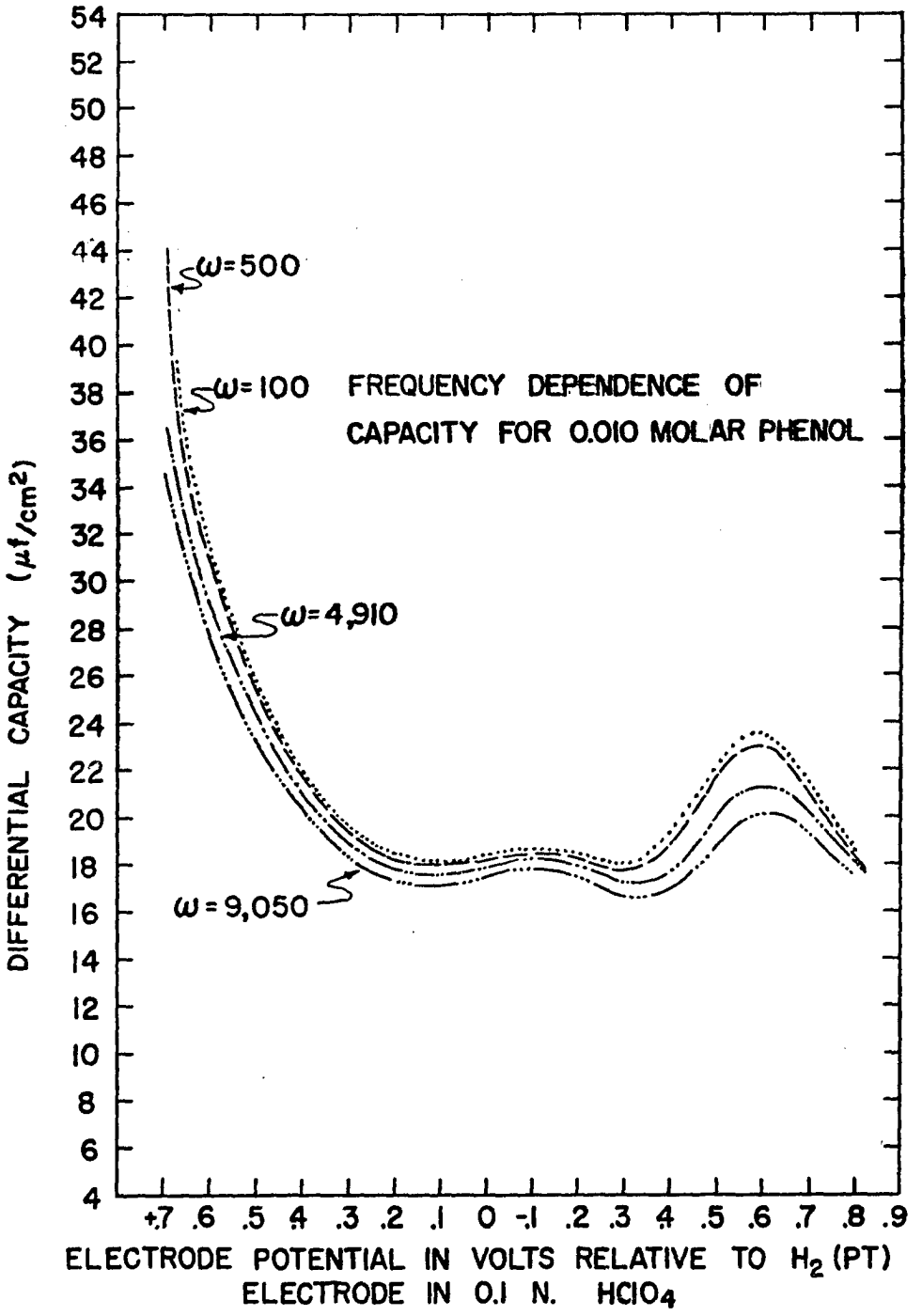

Figure 9. Capacity for C = 0.010 molar phenol

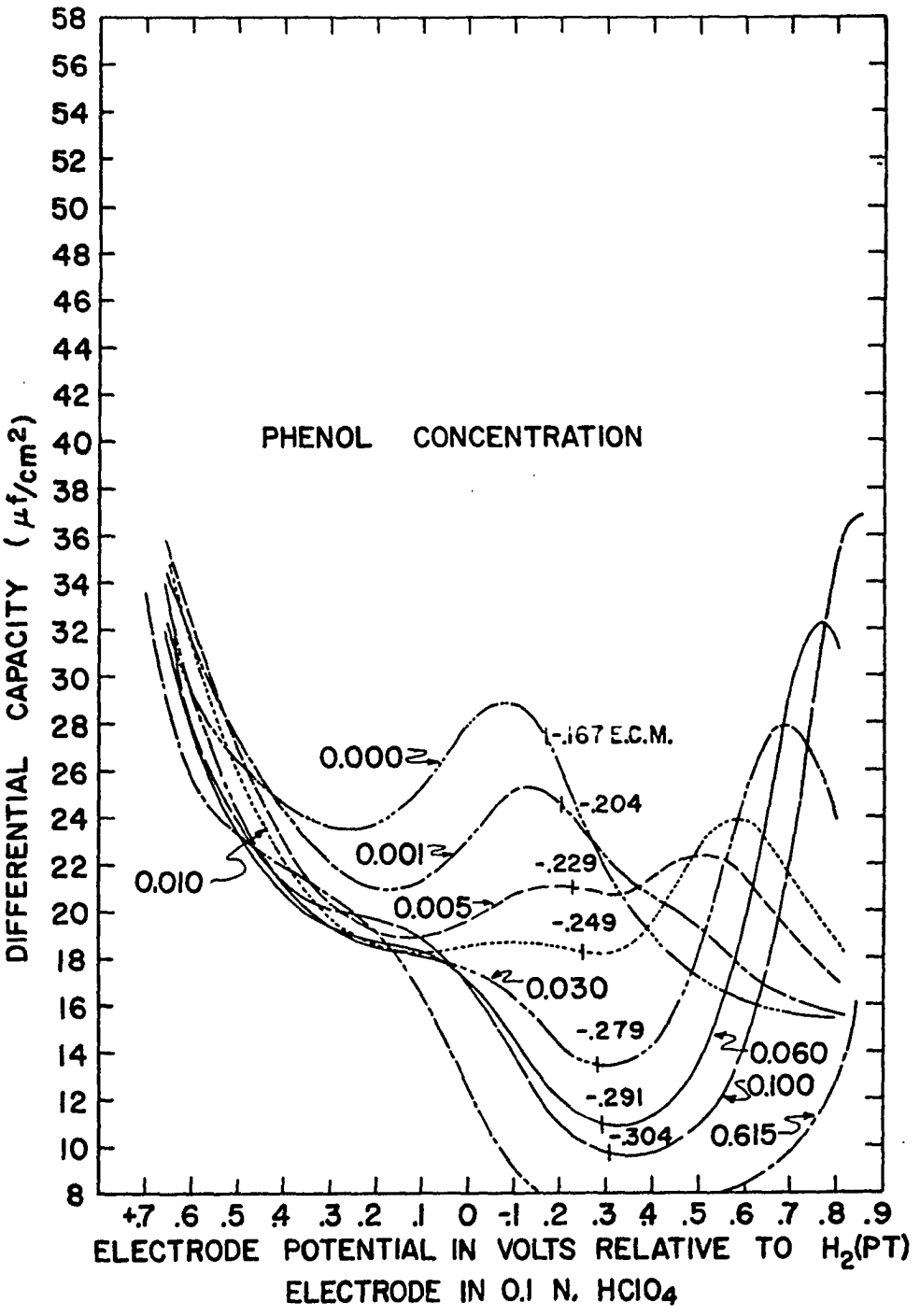

Figure 10. Capacity for phenol solutions (w = 0)

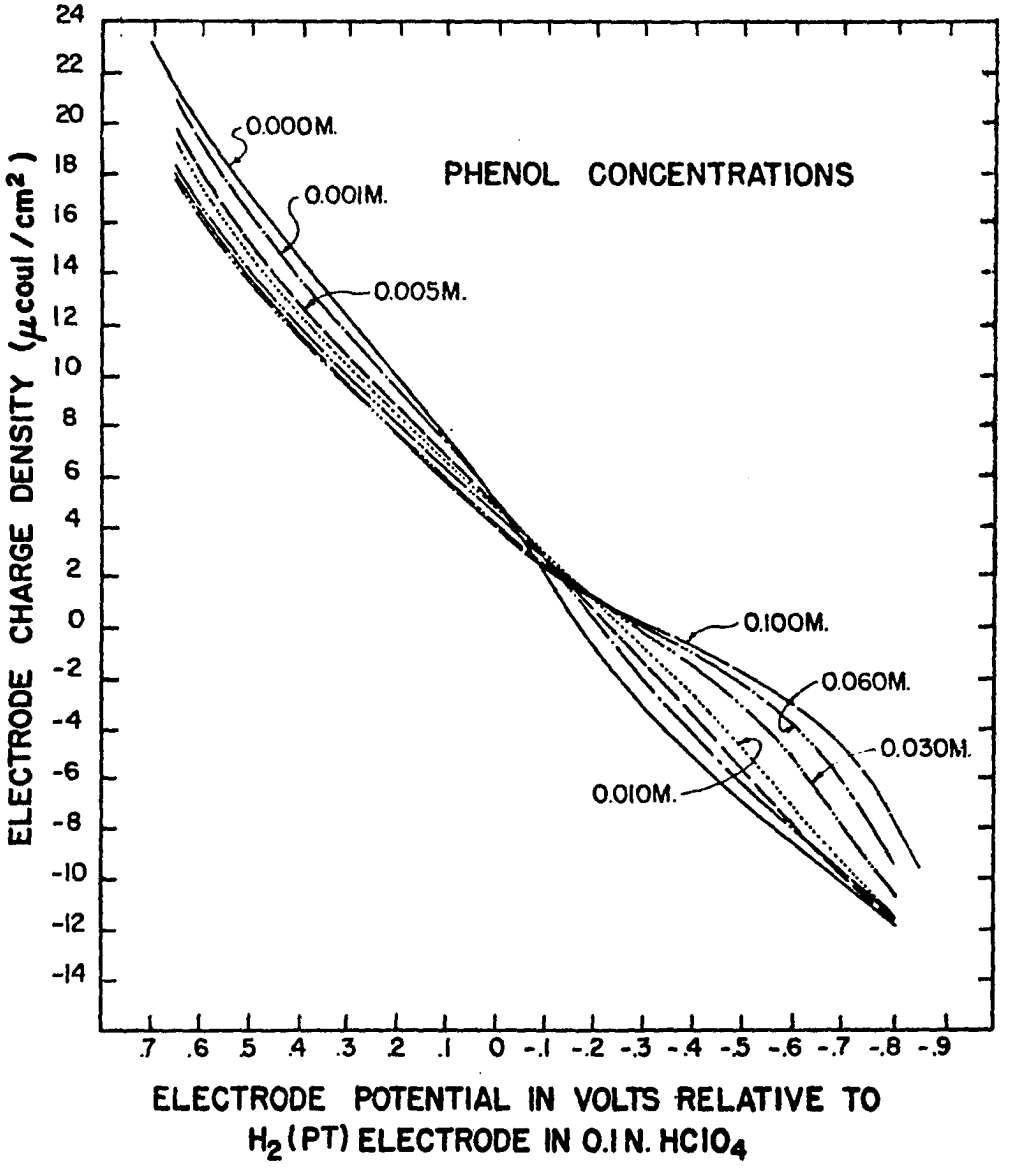

Figure 11. Charge density vs. potential for phenol solutions

DISCUSSION

When the concentration of only one component of a solution is varied, Equation 1 becomes

$$- d\gamma = Q\, dV + \Gamma\, d\mu \tag{12}$$

where Γ and μ are respectively the surface excess and chemical potential of that component. From this basic equation of electrocapillarity, one can derive other thermodynamic expressions which may be useful in checking the conclusions drawn from any model of adsorption one might propose. With this in mind, we consider the charge density as a function of chemical potential and polarization of the electrode, which implies

$$dQ = \left(\frac{\partial Q}{\partial \mu}\right)_V d\mu + \left(\frac{\partial Q}{\partial V}\right)_\mu dV \tag{13}$$

and

$$\left(\frac{\partial Q}{\partial \Gamma}\right)_V = \left(\frac{\partial Q}{\partial \mu}\right)_V \left(\frac{\partial \mu}{\partial \Gamma}\right)_V = \left(\frac{\partial \Gamma}{\partial V}\right)_\mu \left(\frac{\partial \mu}{\partial \Gamma}\right)_V \tag{14}$$

Equation 14 follows from Equation 12, since, if $d\gamma$ is an exact differential, it must be true that

$$\left(\frac{\partial Q}{\partial \mu}\right)_V = \left(\frac{\partial \Gamma}{\partial V}\right)_\mu \tag{15}$$

Considering μ as a function of Γ and V and following similar reasoning, one finds

$$d\mu = \left(\frac{\partial \mu}{\partial \Gamma}\right)_V d\Gamma + \left(\frac{\partial \mu}{\partial V}\right)_\Gamma dV \qquad (16)$$

which implies

$$\left(\frac{\partial \mu}{\partial V}\right)_\mu = 0 = \left(\frac{\partial \mu}{\partial \Gamma}\right)_V \left(\frac{\partial \Gamma}{\partial V}\right)_\mu + \left(\frac{\partial \mu}{\partial V}\right)_\Gamma \qquad (17)$$

Combining Equation 17 with Equation 14 yields

$$\left(\frac{\partial Q}{\partial \Gamma}\right)_V = -\left(\frac{\partial \mu}{\partial V}\right)_\Gamma \qquad (18)$$

which can also be written

$$\left(\frac{\partial \ln a}{\partial V}\right)_\Gamma = -\frac{1}{RT}\left(\frac{\partial Q}{\partial \Gamma}\right)_V \qquad (18')$$

since $d\mu = RT\, d \ln a$, where a is the activity of the component of interest.

At constant Γ, Equation 18' can be integrated as

$$\int_{a_1}^{a_2} d \ln a = \int_{V_1}^{V_2} \frac{-1}{RT}\left(\frac{\partial Q}{\partial \Gamma}\right)_V dV \quad . \qquad (19)$$

If $V_1 = 0$ and V_2 = some arbitrary V, integration of Equation 19 gives

$$(\ln a)_V = (\ln a)_{V=0} - \frac{1}{RT}\int_0^V \left(\frac{\partial Q}{\partial \Gamma}\right)_V dV \quad . \qquad (20)$$

Suppose that for $V = 0$, $\Gamma = F(a)$, and suppose $\Gamma = \Gamma_1$ when $a = a_1$. To obtain the same adsorption Γ_1 at some arbitrary V as occurred at activity a when $V = 0$, we must have an activity a_2 such that

$$a_1 = a_2 \, e^{+\frac{1}{RT}\int_0^V (\partial Q/\partial \Gamma)_V \, dV} \tag{21}$$

Thus in general, if $\Gamma = F(a)$ when $V = 0$, then

$$\Gamma = F\left(ae^{+\frac{1}{RT}\int_0^V (\partial Q/\partial \Gamma)_V \, dV}\right) \quad \text{when } V \neq 0. \tag{22}$$

$$= F\left(ae^{-\frac{S\phi}{RT}}\right)$$

where

$$\phi = -\int_0^V \frac{1}{S}\left(\frac{\partial Q}{\partial \Gamma}\right)_V dV = -\int_0^V \left(\frac{\partial Q}{\partial \theta}\right)_V dV \tag{23}$$

and where $\theta = \Gamma S$.

We now introduce the surface pressure, π, defined as

$$\pi(a,V) = \gamma(0,V) - \gamma(a,V) \quad . \tag{24}$$

Thus

$$d\pi = d\gamma(0,V) - d\gamma(a,V) \quad ,$$

and from Equation 12

$$d\pi = -Q_w \, dV - \left[-Q \, dV - \Gamma \, d\mu\right]$$

$$= (Q - Q_w)dV + \Gamma \, RT \, d \ln a \tag{25}$$

Therefore

$$\left(\frac{\partial \ln a}{\partial V}\right)_\pi = -\left(\frac{Q - Q_w}{\Gamma RT}\right) = \frac{Q_w - Q}{\Gamma RT} \tag{26}$$

Integrating gives

$$\int_{a_1}^{a_2} d \ln a = \frac{1}{RT} \int_{V_1=0}^{V_2=V} \frac{Q_w - Q}{\Gamma} dV \qquad (27)$$

Therefore

$$a_2 = a_1 e^{+\frac{1}{RT}\int_0^V \frac{Q_w - Q}{\Gamma} dV} \qquad (28)$$

If $\pi = F(a)$ when $V = 0$, then

$$\pi = F\left(a e^{-\frac{1}{RT}\int_0^V \frac{Q_w - Q}{\Gamma} dV}\right) \qquad \text{at arbitrary } V,$$

$$= F\left(a e^{-\frac{S\psi}{RT}}\right) \qquad (29)$$

where

$$\psi = + \int_0^V \frac{1}{S} \frac{Q_w - Q}{\Gamma} dV = + \int_0^V \frac{Q_w - Q}{\theta} dV \quad . \qquad (30)$$

Up to this point we have assumed nothing; Equation 22 holds whether ϕ and $(\partial Q/\partial\theta)_V$ depend on θ or not, and Equation 29 holds whether ψ and $(Q_w - Q)/\theta$ depend on θ or not. We now use these derived relations to examine the Frumkin model of adsorption (25), which was presented in our Equation 7 as

$$Q = \theta Q_{org} + (1 - \theta) Q_w \qquad (7)$$

where the Q's are the charge densities at surface coverages of θ, 1, and 0, respectively. Equation 7 generates the

relationships

$$\left(\frac{\partial Q}{\partial \theta}\right)_V = Q_{org} - Q_w \qquad (31)$$

and

$$\frac{Q_w - Q}{\theta} = Q_w - Q_{org} \quad . \qquad (32)$$

Examination of Equations 31 and 32 in conjunction with Equations 23 and 30 leads one to the conclusion that $\psi = \emptyset$ as long as Q varies linearly with θ as expressed by Equation 7.

For a given π, let $a = a_o$ when $V = 0$ (and so $\psi = 0$), and let $a = a'$ when $V = V'$ ($\psi = \psi'$). Then by Equation 29

$$\ln a' - S\psi'/RT = \ln a_o \qquad (33)$$

or

$$\ln a' - \ln a_o = \Delta \ln a = \frac{S\psi'}{RT} \quad . \qquad (34)$$

Equation 34 thus shows us a way of evaluating ψ from electrocapillary data, for from these data we can plot π vs. ln a, where a is approximated by the reduced concentration, at constant potential V. At a given π, for each V, we subtract from the value of ln a the value of ln a required to give the same value of π when $V = 0$. The difference is $S\psi/RT$ for that π and V. Repeating this procedure for several values of π and V, one can find the dependence of $S\psi/RT$ on π and V. The plots of π vs. ln C/Co are shown for n-amyl alcohol and phenol in Figures 12 and 13, respectively. These plots are drawn from

the data of Tables 14 and 15, respectively. Tables 16 and 17 give $S\psi/RT$ as a function of π and V, and Figures 14 and 15 are plots based on these data. Comparison of Figures 14 and 15 reveals the different electrocapillary behaviors of n-amyl alcohol and phenol. For the alcohol, the data can be approximated within experimental error by a horizontal straight line, indicating that ψ is a function of V alone, independent of π (and hence independent of Γ). For phenol, however, ψ is dependent on π as well as V, as evidenced by the non-horizontal lines approximating the data. More on this dependence on π will be said later when this dependence will be expressed as a function of the surface excess, Γ.

Adsorption Isotherms

Calculation of adsorption isotherms from electrocapillary data is most often done by a graphical differentiation of plots such as those of Figures 12 and 13, using the fact that

$$-\frac{d\gamma}{d\mu} = \Gamma = +\frac{d\pi}{d\mu} \qquad (35)$$

at constant V. Thus, plots of Γ vs. bulk concentration of adsorbate can be made for various polarizations of the mercury surface, and such graphs summarize the effects of polarization and concentration on adsorption most succinctly. Graphical differentiation of experimental data is a procedure subject to considerable error, however, even when the data are extensive

Table 14. Dependence of surface pressure on polarizing potential, V, and reduced concentration, C/Co, of n-amyl alcohol in 0.10 N. $HClO_4$. Surface pressure in dynes/cm; electrode potential in volts relative to e.c.m. for C/Co = 0

V	C/Co							
	0.014	0.028	0.042	0.084	0.139	0.333	0.694	1.000
- .607	2.4	0.4	1.4	1.4	2.2	7.6	14.7	20.3
- .507	2.5	0.7	1.5	2.8	5.1	13.1	21.1	26.8
- .407	2.1	1.4	2.6	5.5	9.0	18.4	26.7	32.5
- .307	2.0	2.0	4.1	8.2	12.5	22.6	30.9	36.6
- .207	1.9	2.7	5.3	10.6	15.3	25.5	33.8	39.6
- .107	1.8	3.0	6.0	12.1	16.8	27.2	35.3	41.2
0.000	1.4	2.7	5.4	11.8	16.5	26.9	35.1	40.9
+ .093	1.1	2.1	3.7	9.7	14.3	24.7	33.0	38.6
+ .193	0.7	2.0	1.8	6.2	10.0	20.2	28.5	34.1
+ .293	0.8	2.2	1.5	2.9	4.8	14.1	21.9	27.8
+ .393	0.9	1.9	1.3	2.5	2.8	8.0	14.5	20.9

and follow a smooth curve with very little scatter. A more satisfactory method would consist of finding some analytical expression which would represent the data as precisely as possible. This expression could be differentiated exactly, and any deviations of the data from this expression, hopefully a small part of the total, could be graphically differentiated

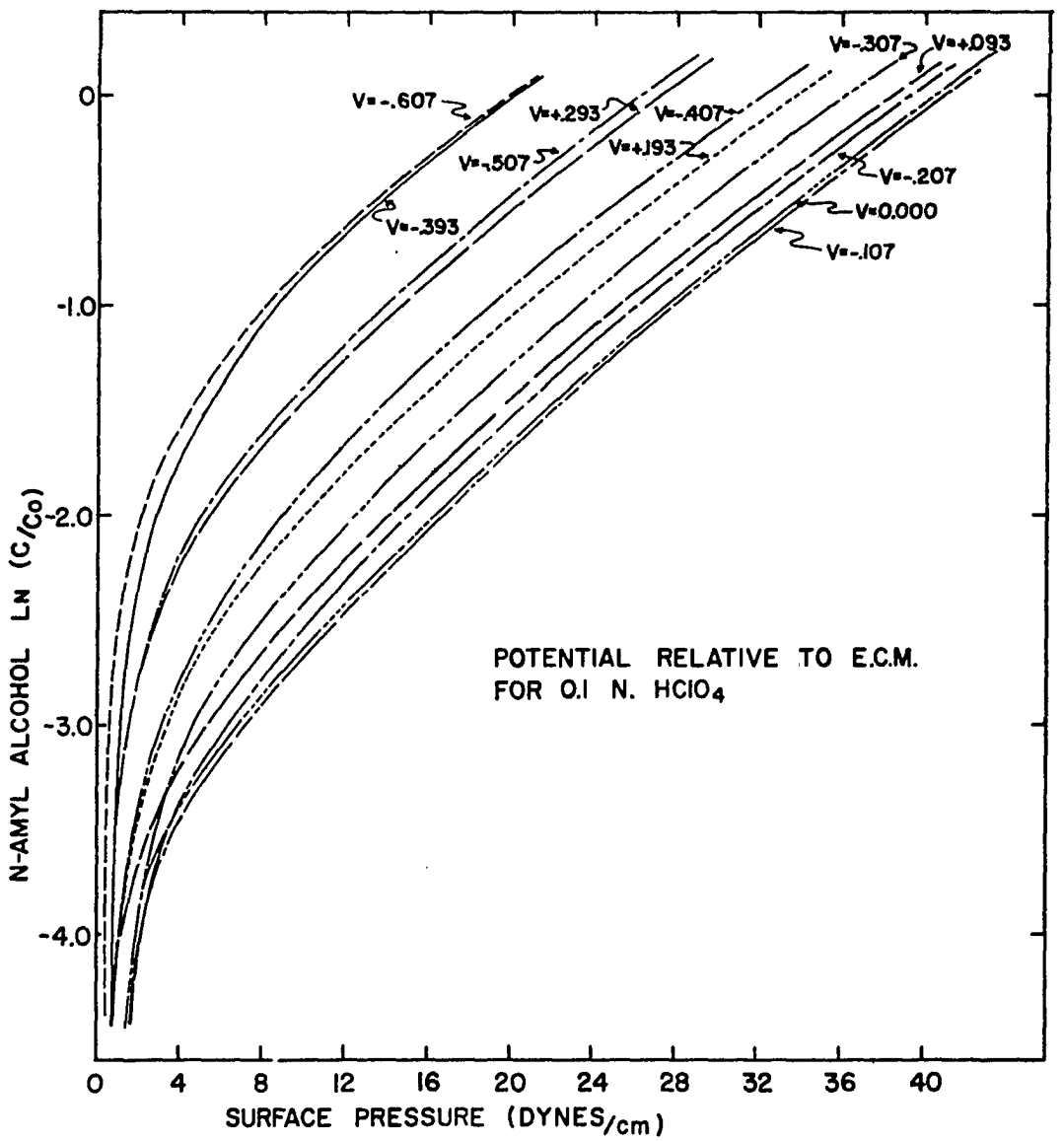

Figure 12. π vs. ln C/Co for n-amyl alcohol

Table 15. Dependence of surface pressure on polarizing potential, V, and concentration C of phenol in 0.10 N. $HClO_4$. Surface pressure in dynes/cm; electrode potential in volts relative to e.c.m. for C = 0; concentrations expressed in moles/liter

V	C=.001	C=.005	C=.010	C=.030	C=.060	C=.100
- .625	0.0	0.1	0.1	1.1	2.5	4.5
- .525	0.0	0.5	0.9	3.0	5.8	9.2
- .425	0.3	1.1	2.1	5.9	10.0	14.6
- .325	0.6	2.3	3.9	9.4	14.9	19.8
- .225	0.7	3.8	6.2	13.0	19.2	24.3
- .125	1.6	5.9	8.9	15.4	21.8	27.0
- .025	2.7	7.8	11.4	19.3	25.6	30.6
0.000	2.8	8.1	11.8	19.7	26.0	31.0
+ .075	3.0	8.9	12.7	20.7	26.5	31.6
+ .175	3.2	9.4	12.9	20.6	26.0	30.9
+ .275	3.3	9.3	12.6	19.9	25.0	29.3
+ .375	3.3	8.6	11.8	18.6	23.2	27.5
+ .475	2.6	7.3	10.5	16.5	20.9	24.9
+ .575	2.7	6.0	8.6	14.2	18.3	22.0
+ .675	3.3	4.3	6.4	11.2	16	-

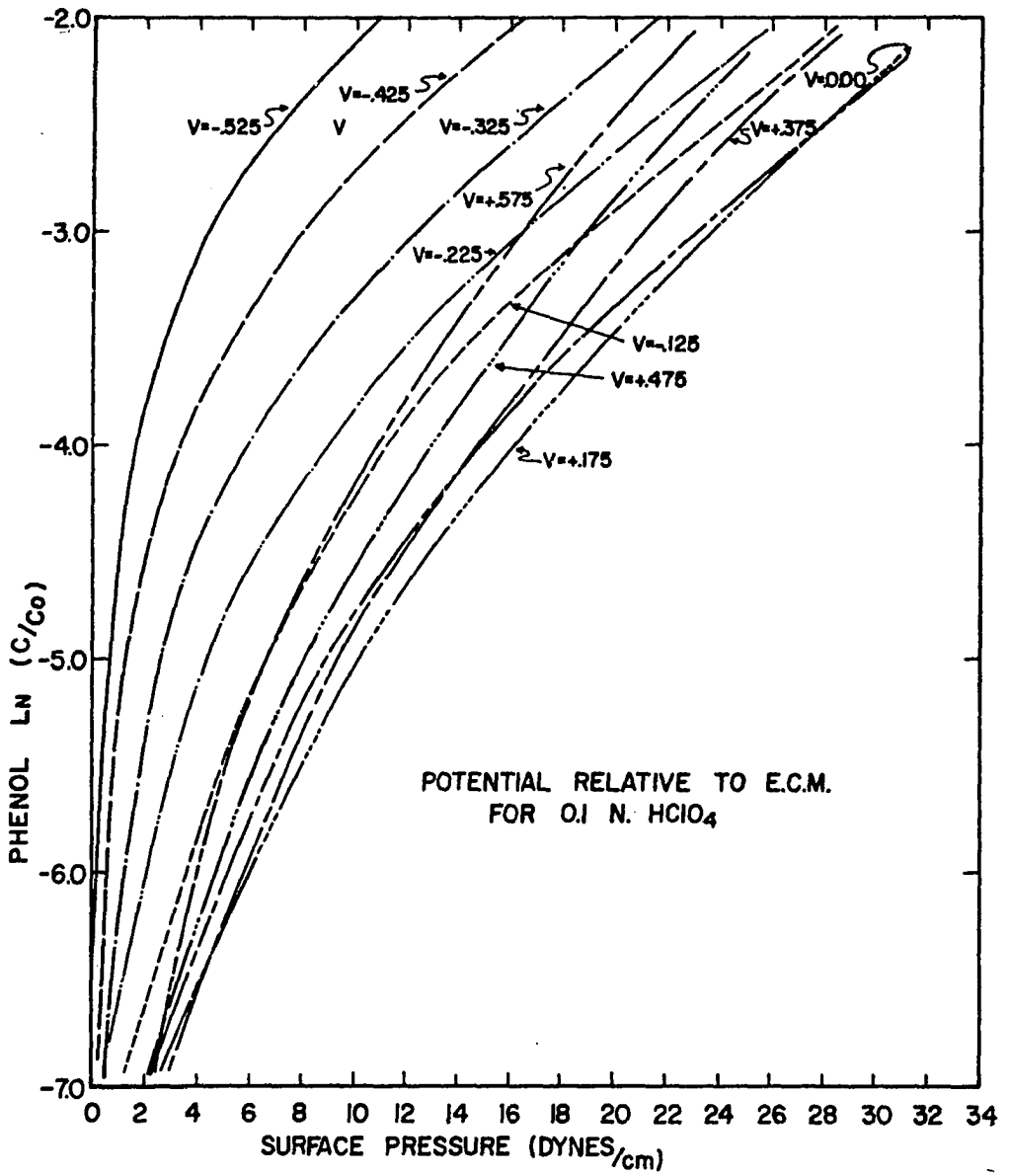

Figure 13. π vs. ln C/Co for phenol

Table 16. Dependence of $S\psi/RT$ on surface pressure π and polarizing potential V for aqueous solutions of n-amyl alcohol. Surface pressure in dynes/cm; potential in volts relative to e.c.m. for 0.1 N. $HClO_4$

V	π=3	π=6	π=9	π=12	π=18	π=24	π=30
- .607	+1.79	1.83	1.84	1.81	1.70	-	-
- .507	+1.15	+1.25	1.26	1.25	1.20	1.14	-
- .407	+ .53	+ .70	+ .75	+ .78	+ .76	+ .71	+ .65
- .307	+ .13	+ .33	+ .36	+ .37	+ .38	+ .36	+ .34
- .207	- .08	+ .06	+ .08	+ .10	+ .12	+ .12	+ .11
- .107	- .11	- .05	- .04	- .04	- .03	- .03	- .03
+ .093	+ .18	+ .19	+ .21	+ .21	+ .22	+ .20	+ .18
+ .193	+ .46	+ .61	+ .63	+ .63	+ .62	+ .58	+ .53
+ .293	+1.11	1.19	1.19	1.18	1.13	1.06	-
+ .393	+1.61	1.73	1.79	1.77	1.68	-	-

and this correction added to the differential obtained analytically. The success of such a procedure depends to a great extent on keeping the deviation between data and their analytical representation small, otherwise the unavoidable error in differentiating graphically will become nearly as large as it would have been had the data been attacked in that manner directly. Thus, it is imperative that if this method is to be used, a reasonably accurate representation of the data must be

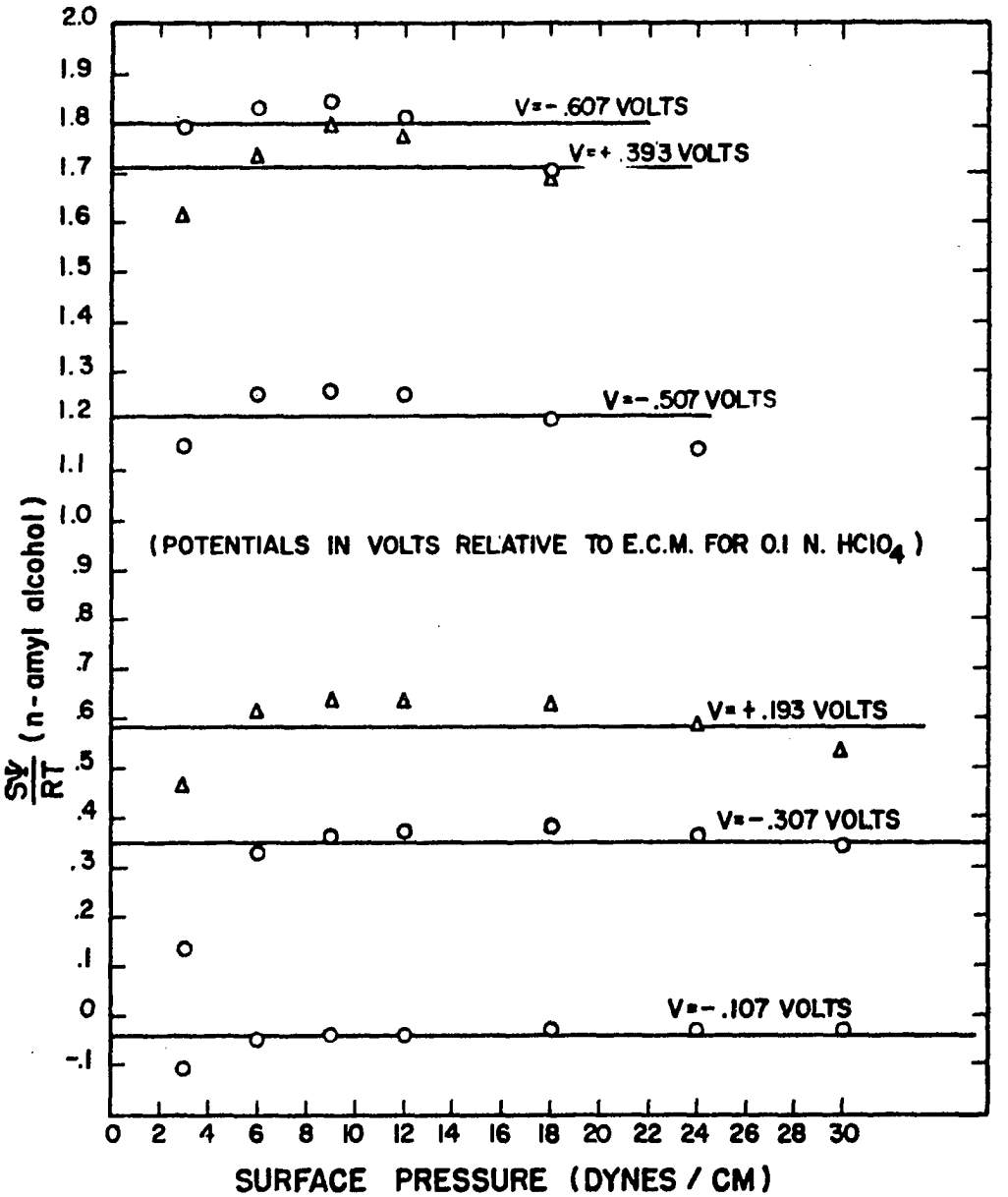

Figure 14. $S\psi/RT$ vs. π for n-amyl alcohol

Table 17. Dependence of $S\psi/RT$ on surface pressure π and polarizing potential V for aqueous solutions of phenol surface pressure in dynes/cm; potential in volts relative to e.c.m. for C = 0.0

V	π=3	π=5	π=6	π=8	π=10	π=15	π=20	π=25
- .525	3.30	+3.20	3.09	2.84	2.70	-	-	-
- .425	2.62	+2.50	2.40	2.23	2.10	1.85	-	-
- .325	1.92	+1.88	1.81	1.62	1.50	1.17	1.18	-
- .225	1.15	+1.28	1.23	1.05	0.96	.84	.72	.68
- .125	.50	+ .51	.62	.55	.51	.51	.45	.42
- .025	.05	+ .05	.08	.07	.05	.05	.04	.04
+ .075	-.08	- .13	-.17	-.21	-.17	-.15	-.12	-.08
+ .175	-.13	- .22	-.24	-.31	-.25	-.22	-.13	-.03
+ .275	-.15	- .20	-.25	-.27	-.20	-.11	-.03	+.09
+ .375	-.20	- .20	-.18	-.15	-.07	+.03	+.17	+.33
+ .475	+.08	+ .15	+.18	+.21	+.20	+.38	+.50	+.67
+ .575	+.12	+ .49	+.60	+.59	+.59	+.75	+.93	-

made by the analytical expression chosen.

An expression which was thought to have the best chance of fitting the data was a form of the Volmer isotherm modified by an additional correction term which, it was hoped, would be small:

$$\ln \frac{C}{\pi} = \alpha + \beta\pi + \Delta \ln \frac{C}{\pi} \qquad (36)$$

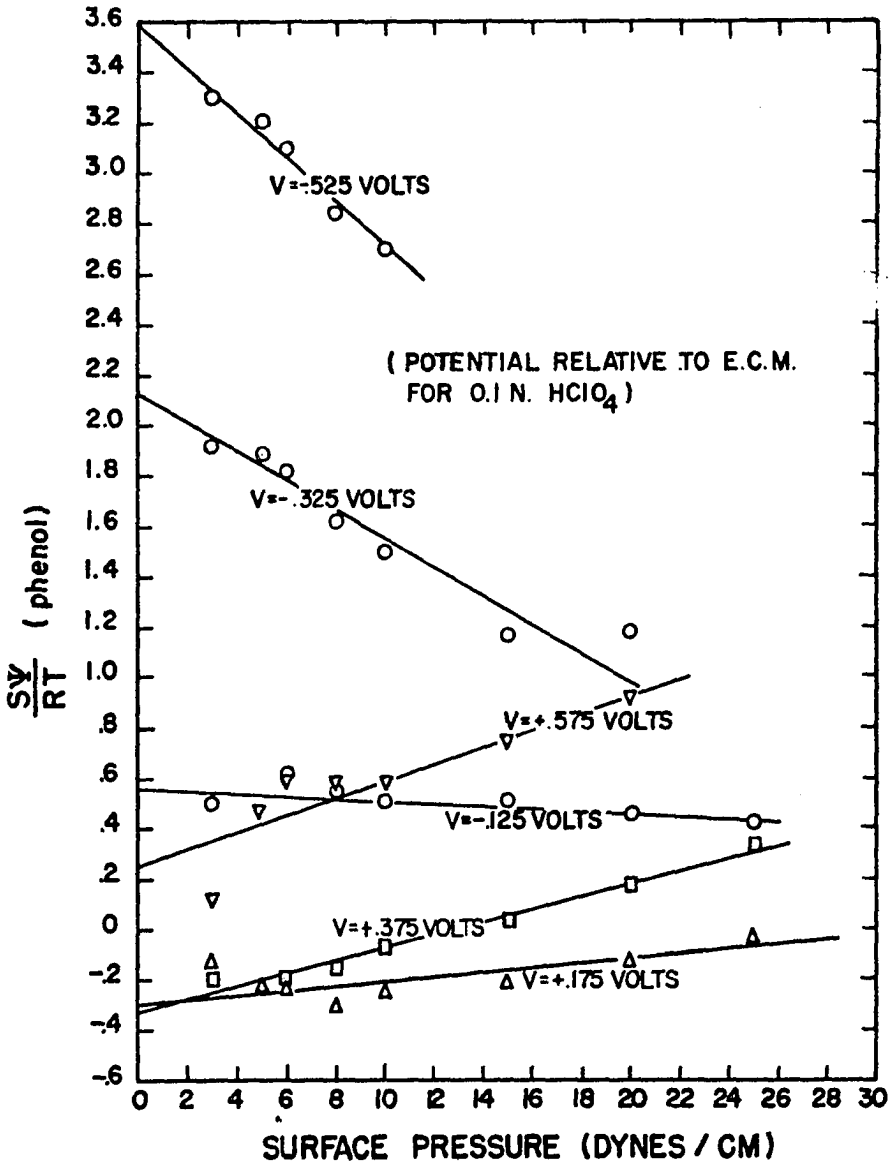

Figure 15. Sψ/RT vs. π for phenol

where C is the bulk concentration of adsorbate, π the surface pressure, α and β are constants, and $\Delta \ln C/\pi$ the correction term. Assuming that the activity of the adsorbate is given by the bulk concentration, Equation 35 may be written as

$$\frac{d\ RT\ \ln\ C}{d\pi} = \frac{1}{\bar{\Gamma}} = \frac{2.303\ d\ RT\ \log\ C}{d\pi} \qquad (37)$$

Rearrangement and differentiation of Equation 36 gives

$$\frac{d\ \ln\ C}{d\pi} = \frac{1}{\pi} + \beta + \frac{d\ \Delta\ \ln\ C/\pi}{d\pi} = \frac{1}{RT\bar{\Gamma}} \qquad (38)$$

when combined with Equation 37. Thus, $\bar{\Gamma}$ can be determined from Equation 38 as

$$\frac{1}{\bar{\Gamma}} = \frac{RT}{\pi} + \beta RT + RT\ \frac{d\ \Delta\ \ln\ C/\pi}{d\pi} \qquad (39)$$

To check the ability of the Volmer isotherm expression to fit our data, a plot of log C/π versus π was made for several potentials. The data are tabulated in Tables 18 and 19, and some typical graphs for phenol are shown in Figure 16. For large values of π the data are remarkably linear, with deviations from a straight line fit occurring only as π approaches zero. Such deviations would be expected, since at small π, log C/π is extremely sensitive to any variation in π, and hence the experimental error becomes an appreciable factor. These deviations from linearity can be taken care of through the correction factor, Δ log C/π, and as long as this quantity

Table 18. Dependence of log C/π on polarization and bulk concentration of n-amyl alcohol. Concentration expressed as reduced concentration C/Co, polarizing potential of electrode in volts relative to e.c.m. for 0.1 N. $HClO_4$

V	C/Co								
	0.014	0.028	0.042	0.084	0.139	0.333	0.694	1.000	β
- .507	-2.234	-1.456	-1.581	-1.523	-1.565	-1.598	-1.485	-1.430	.0710
- .307	-2.133	-1.832	-1.979	-1.984	-1.954	-1.828	-1.673	-1.562	.1088
- .107	-2.109	-2.030	-2.155	-2.159	-2.082	-1.912	-1.706	-1.615	
- .007	-2.000	-1.984	-2.109	-2.148	-2.074	-1.907	-1.705	-1.612	.1094
+ .093	-1.895	-1.895	-1.933	-2.062	-2.012	-1.870	-1.677	-1.587	
+ .293	-1.757	-1.875	-1.553	-1.553	-1.538	-1.627	-1.501	-1.444	.0773
+ .493	-1.968	-1.895	-1.331	-1.437	-1.199	-1.226	-1.022	-1.134	.0676

Table 19. Dependence of log C/π on polarization and bulk concentration of phenol. Concentration expressed in moles/liter; polarizing potential, V, of electrode in volts relative to e.c.m. for 0.1 N. $HClO_4$

V	C=.001	C=.005	C=.010	C=.030	C=.060	C=.100	$\frac{\beta}{2.303}$
- .625	$+\infty$	-1.301	-1.000	-1.564	-1.620	-1.653	
- .525	$+\infty$	-2.000	-1.954	-2.000	-1.985	-1.964	.0060
- .425	-2.477	-2.342	-2.322	-2.294	-2.222	-2.164	.0146
- .325	-2.778	-2.663	-2.591	-2.496	-2.395	-2.297	.0186
- .225	-2.845	-2.881	-2.792	-2.637	-2.505	-2.386	.0223
- .125	-3.204	-3.072	-2.949	-2.710	-2.560	-2.431	.0240
0.000	-3.447	-3.210	-3.072	-2.817	-2.637	-2.491	.0286
+ .075	-3.477	-3.250	-3.104	-2.839	-2.645	-2.500	.0297
+ .175	-3.505	-3.274	-3.111	-2.837	-2.637	-2.490	.0321
+ .275	-3.519	-3.270	-3.100	-2.822	-2.620	-2.467	.0363
+ .375	-3.519	-3.236	-3.072	-2.792	-2.587	-2.439	.0402
+ .475	-3.415	-3.164	-3.021	-2.740	-2.542	-2.396	.0414
+ .575	-3.431	-3.079	-2.935	-2.675	-2.484	-2.342	.0422
+ .675	-3.519	-2.935	-2.806	-2.572	-2.426	-	

is not too large in relation to log C/π, the graphical differentiation of Δ log C/π vs. π plots will not introduce large errors in the determination of Γ by Equation 39.

From the linear plots of log C/π vs. π, one can determine β, since the slope of each of these plots is $\beta/2.303$. The

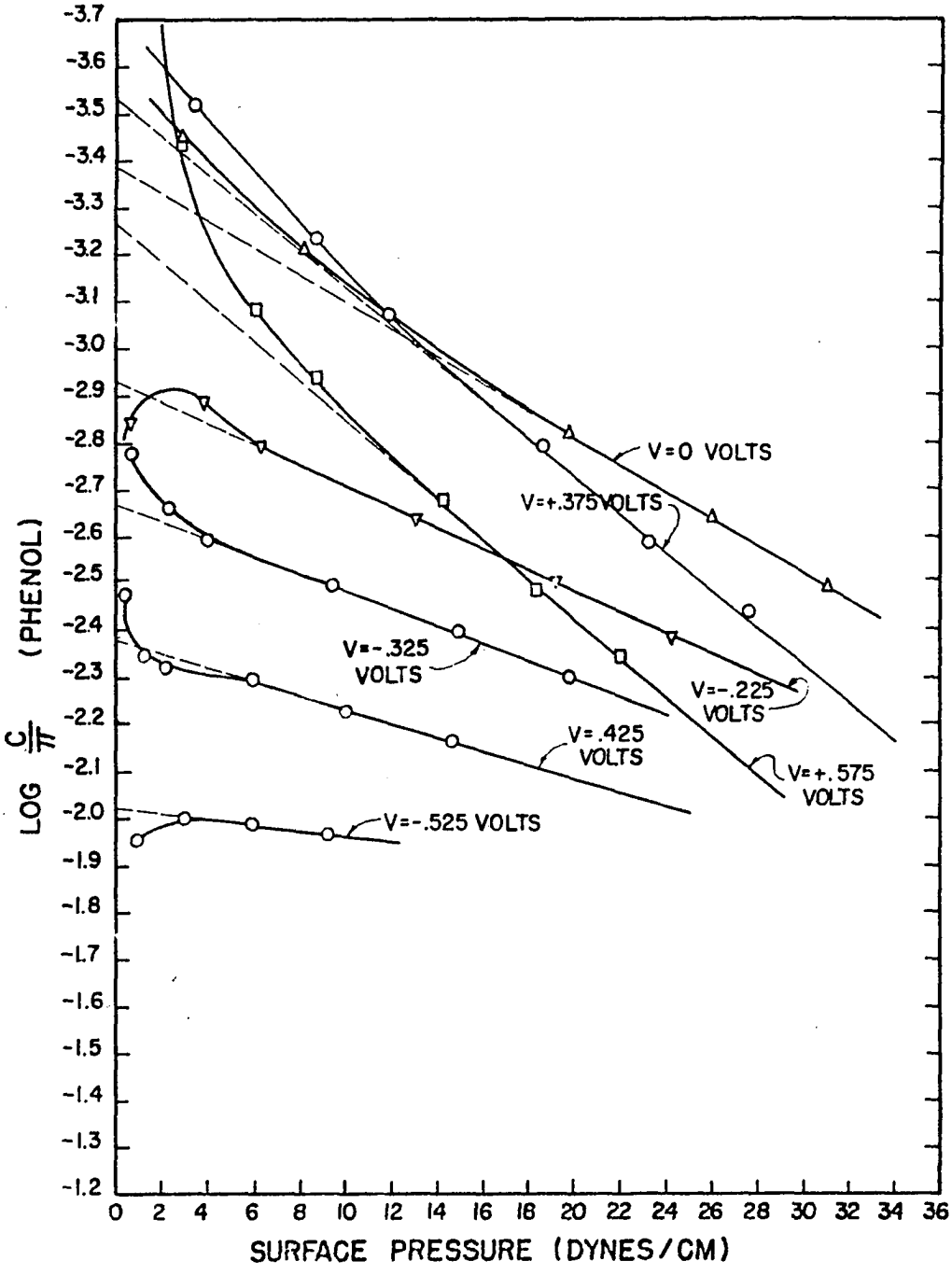

Figure 16. Log C/π vs. π for phenol

values of β for each potential studied are also tabulated in Tables 18 and 19.

Since each term in Equation 39 can now be evaluated, Γ can be determined as a function of π, and hence of the bulk concentration C, at any potential V. The results of such evaluations are tabulated in Tables 20 and 21. These data allow one to plot the adsorption isotherms for n-amyl alcohol and phenol, and this is done for some selected potentials in Figures 17 and 18, respectively.

To be sure these isotherms are not just ghosts of the method used to calculate them, a second expression was sought which would also fit the data reasonably well and could also be differentiated in a manner analogous to that used for the Volmer isotherm. Such an expression is

$$\pi = \Gamma_m RT \ln (1 + ac) + \Delta\pi \qquad (40)$$

where π is the surface pressure, C the bulk concentration, Γ_m and a are constants, and $\Delta\pi$ the correction term which again is hopefully small. Representative phenol data for V = +0.175 volts were tabulated, and a plot of π vs. (1 + ac) made on semi-log paper for various values of the parameter a. The data followed a linear trend at low values of π when a = 700; the straight line drawn through the data also passed through the point (1 + ac) = 1 when π = 0, further justifying our choice of a. Γ_m can now be determined by substituting values

Table 20. Dependence of surface excess, Γ, on polarization and bulk concentration on n-amyl alcohol. Concentration expressed as reduced concentration, C/Co; electrode potential in volts relative to e.c.m. for 0.1 N. $HClO_4$; Γ in moles/cm^2 x 10^{10}

V = - .507		V = - .307		V = - .007		V = + .293		V = + .493	
C/Co	Γ	C/Co	Γ	C/Co	Γ	C/Co	Γ	C/Co	Γ
.045	.91	.021	.82	.021	.93	.050	.87	.05	.71
.109	1.89	.042	1.65	.035	2.16	.116	1.52	.300	1.37
.153	2.83	.060	2.43	.047	2.91	.159	2.65	.470	2.01
.202	3.62	.083	3.08	.060	3.50	.198	3.45	.640	2.61
.255	4.01	.106	3.63	.075	3.94	.241	4.04	.790	3.16
.310	4.21	.131	3.96	.090	4.07	.289	4.30	.930	3.64
.374	4.21	.159	4.24	.107	4.00	.346	4.31		
.444	4.42	.191	4.51	.128	3.94	.410	4.30		
.525	4.72	.229	4.66	.154	4.00	.485	4.59		
.615	5.12	.272	4.77	.185	4.28	.572	4.96		
.712	5.43	.320	4.85	.221	4.49	.670	5.25		
.822	5.72	.377	4.98	.264	4.69	.782	5.52		
.943	6.00	.440	5.02	.314	4.88	.908	5.78		
1.07	6.26	.515	5.06	.374	5.05	1.05	6.02		
		.602	5.22	.442	5.20				
		.875	5.56	.672	5.54				
				.995	5.83				

Table 21. Dependence of surface excess, Γ, on polarization and bulk concentration of phenol. Concentration expressed in moles/liter; electrode potential in volts relative to e.c.m. for 0.1 N. $HClO_4$; Γ in moles/cm^2 x 10^{10}

V = -.425		V = -.025		V = +.175		V = +.375		V = +.575		V = -.225	
C	Γ	C	Γ	C	Γ	C	Γ	C	Γ	C	Γ
.0097	.78	.0008	.66	.0007	.68	.0007	.64	.0007	.40	.0022	.78
.0196	1.48	.0016	1.12	.0013	1.18	.0013	1.07	.0021	.88	.0054	1.33
.0313	2.05	.0031	1.50	.0021	1.56	.0024	1.38	.0049	1.30	.0095	1.73
.0452	2.53	.0052	1.84	.0036	1.86	.0043	1.65	.0088	1.63	.0142	2.23
.0600	3.01	.0079	2.12	.0057	2.12	.0071	1.88	.0137	1.87	.0198	2.66
.0765	3.44	.0112	2.47	.0085	2.33	.0103	2.09	.0201	2.16	.0265	2.99
.0940	3.83	.0153	2.76	.0118	2.53	.0144	2.37	.0288	2.32	.0343	3.28
		.0200	3.07	.0158	2.70	.0200	2.58	.0398	2.51	.0435	3.53
		.0258	3.28	.0209	2.83	.0275	2.70	.0543	2.61	.0540	3.72
		.0328	3.46	.0272	3.01	.0377	2.82	.0735	2.73	.0660	3.97
		.0408	3.60	.0360	3.15	.0507	2.91	.0984	2.82	.0800	4.15
		.0507	3.73	.0472	3.31	.0706	2.99			.0965	4.32
		.0627	3.84	.0603	3.48	.0848	3.07				
		.0770	3.95	.0760	3.67						
		.0940	4.05	.0925	3.75						

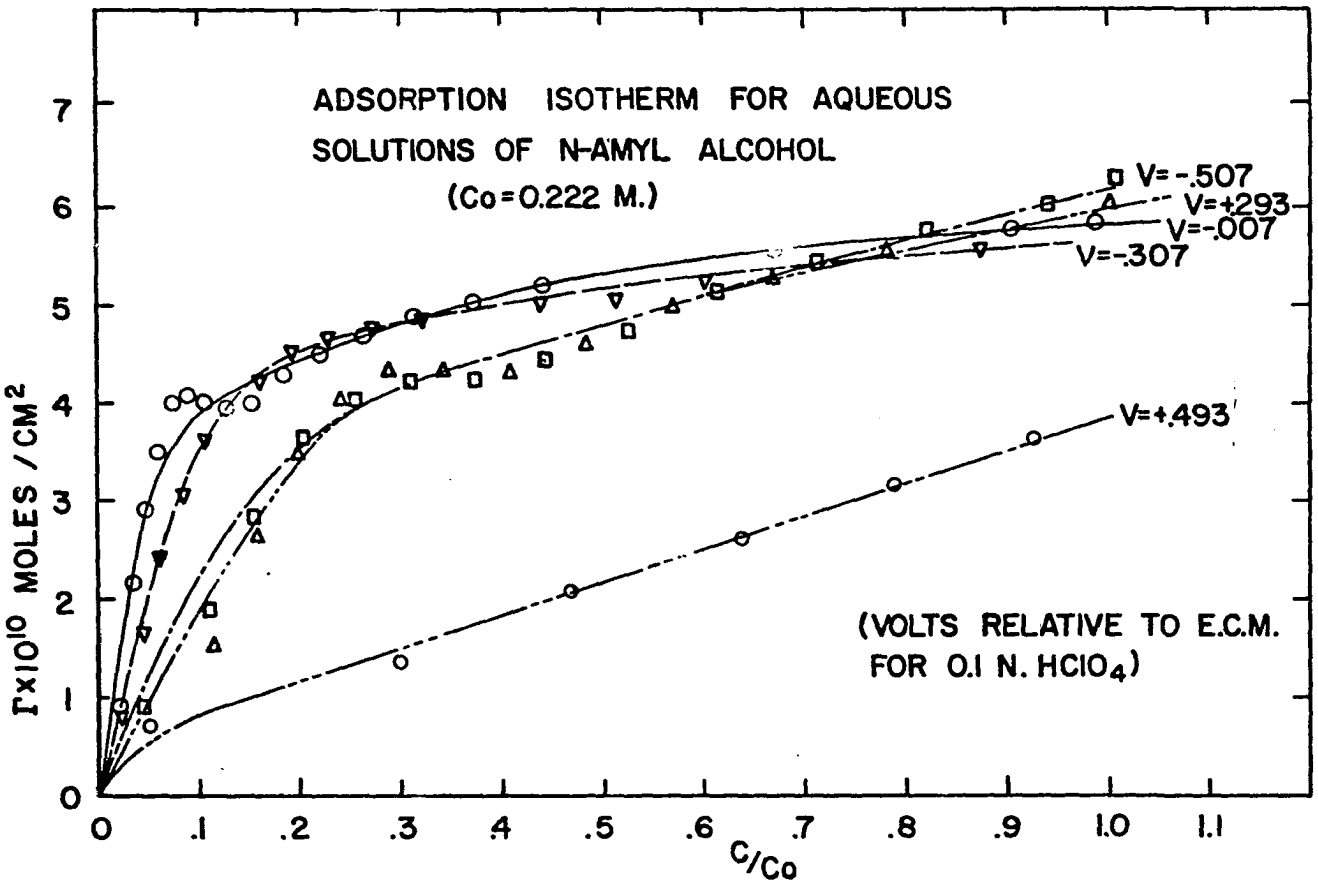

Figure 17. Adsorption isotherms for n-amyl alcohol

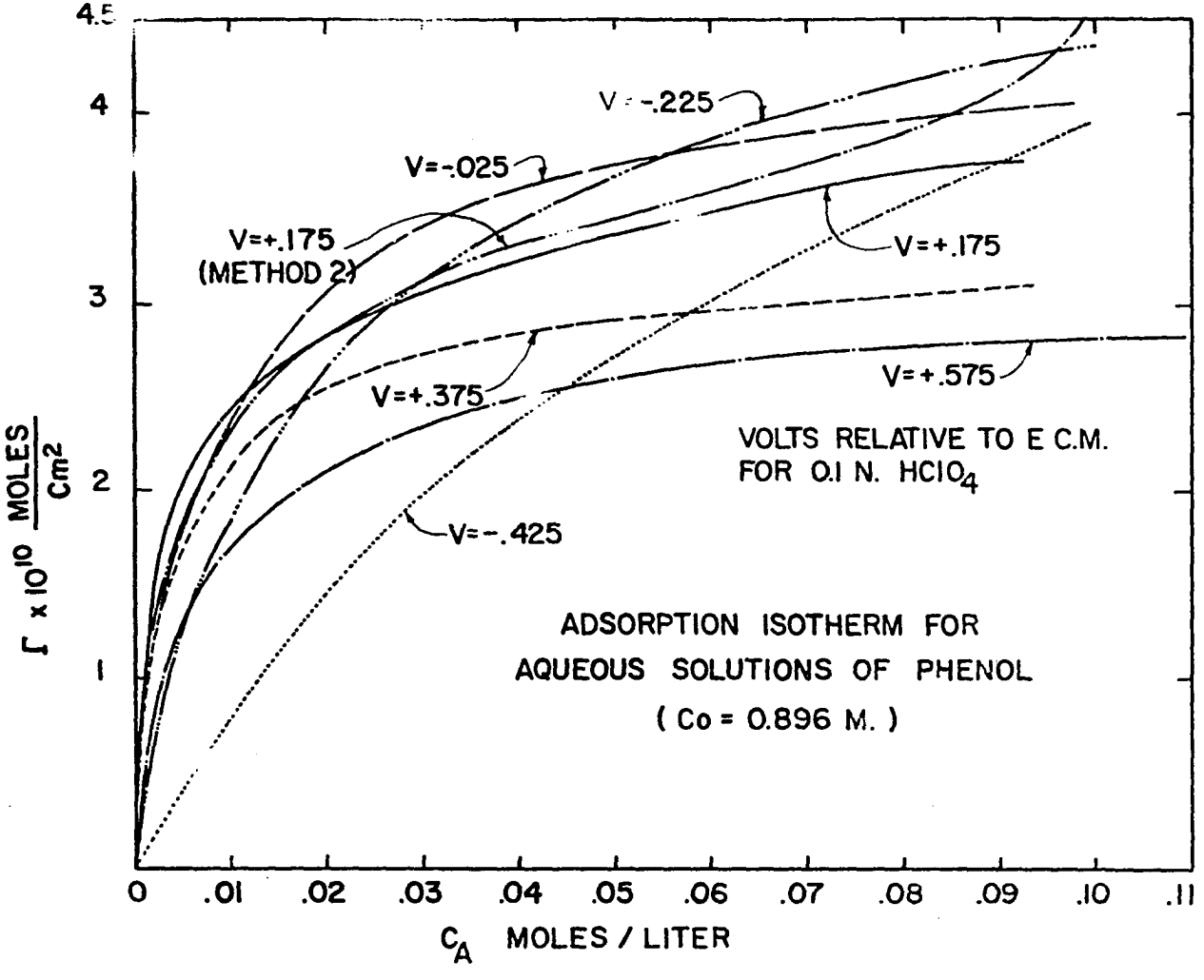

Figure 18. Adsorption isotherms for phenol

for π and C in Equation 40 at any point of the graph where $\Delta\pi = 0$; this procedure yielded a value of 2.53×10^{-10} moles/cm^2 for Γ_m.

In order to find an expression for the surface excess, Γ, Equation 40 must be differentiated, and this gives

$$\Gamma = \frac{d\pi}{d\ RT\ \ln C} = \Gamma_m a\left(\frac{C}{1 + ac}\right) + \frac{C}{RT}\frac{d\ \Delta\pi}{dC} \qquad (41)$$

Thus, graphical differentiation of the correction term $\Delta\pi$ after C is all that is needed to evaluate Γ, and this was done at the high values of π where this deviation became appreciable. This procedure yielded values of Γ which are also shown in Figure 18, designated by "Method 2". Comparison of the two isotherms for V = +0.175 shows that they are in good agreement except at high values of C, where the isotherm calculated using Equation 41 deviates sharply from the Method 1 calculation. Since the correction term $\Delta\pi$ becomes quite large at high values of C, Equation 41 becomes subject to a large error due to graphical differentiation uncertainties, and thus Γ is known with much less certainty at high concentrations. Method 2 is probably superior to Method 1 at low concentrations, however, since the correction used in Method 1 becomes appreciable in this region.

Examination of the isotherms represented in Figures 17 and 18 reveals some interesting qualitative features of adsorption. The n-amyl alcohol isotherms all tend to approach

the same maximum value of Γ for moderate polarizations of the electrode. This would indicate that a monolayer of adsorbed molecules is formed at the interface, and Γ_{max} is approximately 5.8×10^{-10} moles/cm^2. The high positive polarization of +0.493 volts relative to the e.c.m. for C = 0 prevents the formation of a complete monolayer. Assuming that the adsorption is strictly monomolecular, one can calculate a molecular area from

$$S = \frac{1}{\Gamma_{max}} \qquad (42)$$

For n-amyl alcohol, S is calculated to be 31 $\mathring{A}^2$/molecule which agrees with the value of 32 $\mathring{A}^2$/molecule obtained by Hansen *et al.* (24).

The adsorption isotherms for phenol show a remarkable dependence on electrode polarization. Unlike the behavior of n-amyl alcohol, the curves do not converge to a common maximum value of Γ. At positive electrode polarizations, Γ does approach a maximum value at the higher concentrations studied, but this maximum value decreases as the polarization is made more positive. We attribute this to the incomplete formation of a monolayer at high positive polarizations with the molecules laying flat on the mercury surface. Blomgren *et al.* (14) calculate a value of $\Gamma_{max} = 3.5 \times 10^{-10}$ moles/cm^2 from Fisher-Taylor-Hirschfelder models for phenol with this orientation. Figure 18 shows that this value is not attained

at high positive polarizations, but is exceeded by polarizations more negative than V = +0.200 volts. We attribute this to a gradual reorientation of the phenol molecules at the interface, with more molecules abandoning the planar orientation in favor of a vertical position as the surface charge density becomes less positive. This occurrence is rather unfortunate if one is interested in devising a model of adsorption based on fractional surface coverage, Γ/Γ_{max}, since Γ_{max} is not constant but will vary as a function of the relative numbers of molecules oriented planar and vertical to the surface. Thus, the method of Hansen et al. (23, 24) is inapplicable to such a system.

Dependence of ψ on Γ and V

It was observed previously that for the system mercury-aqueous n-amyl alcohol solutions, the function ψ was independent of π at fixed V, and hence was a function of V only (see Figure 14). For the system mercury-aqueous phenol solutions, however, ψ was found to be dependent not only on V, but on π (or Γ) as well. Examining this dependence carefully, it was found that to a first approximation, plots of $S\psi/RT$ vs. Γ^2 followed linear trends as shown in Figure 19. Thus, a general equation of the form

$$\frac{S\psi}{RT} = F_1(V) + F_2(V)\Gamma^2 \qquad (43)$$

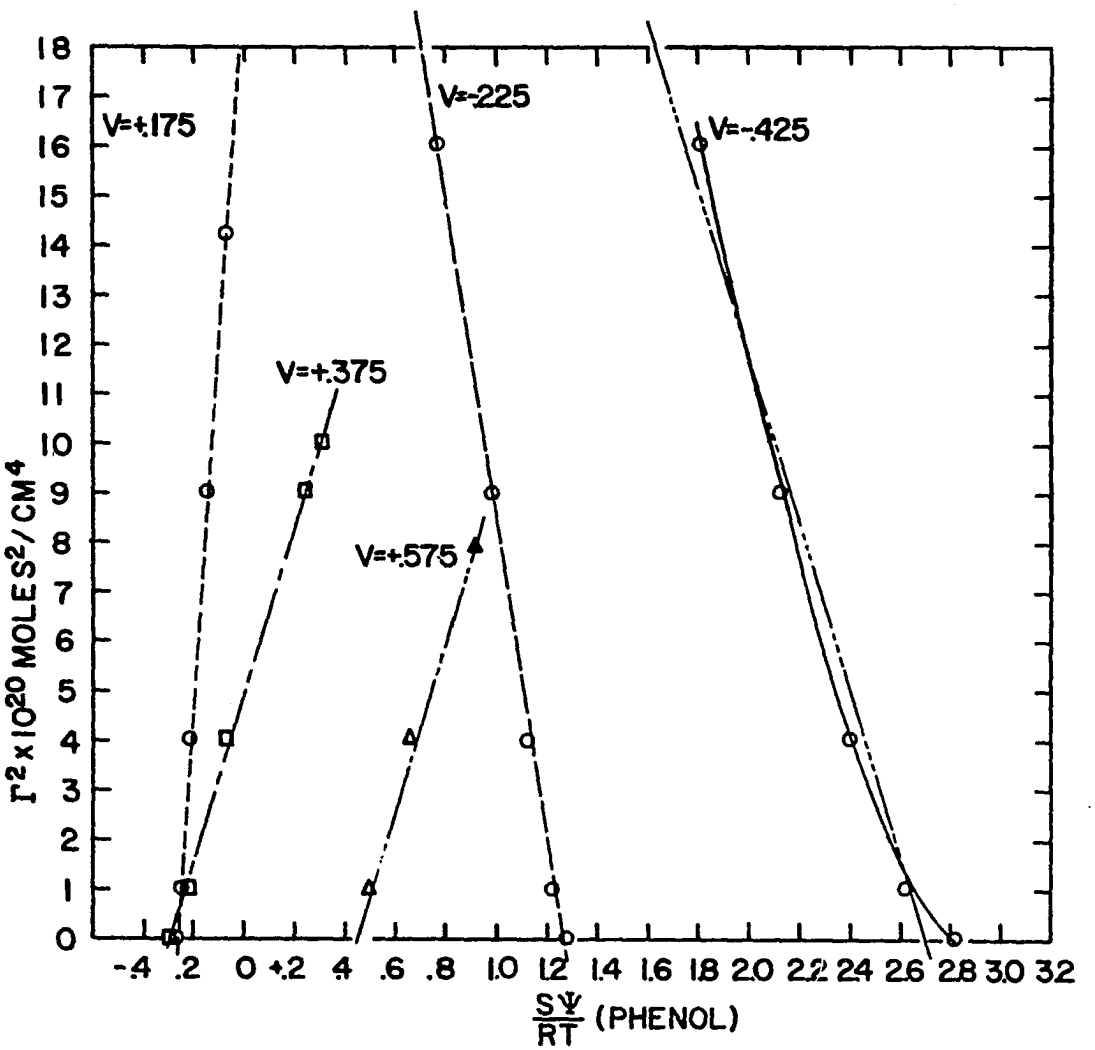

Figure 19. Γ^2 vs. $S\Psi/RT$ for phenol

should describe the function $S\psi/RT$ quite adequately. The values of $S\psi/RT$ at $\Gamma^2 = 0$ allow $F_1(V)$ to be determined as a function of V; the parabolic curve describing $F_1(V)$ vs. V could be approximated analytically by:

$$F_1(V) = 6.57\ V^2 - 3.02\ V \qquad (44)$$

where V is expressed in volts relative to the e.c.m. for 0.10 normal perchloric acid. Similarly, $F_2(V)$ could be determined from the slopes of the lines drawn in Figure 19. Plotting the values of these slopes versus V generated a reasonably straight line which could be described analytically by:

$$F_2(V) = 0.128 \times 10^{20}\ V \ . \qquad (45)$$

Substitution of these values into Equation 43 leads to the empirical relationship

$$\frac{S\psi}{RT} = 6.57\ V^2 - 3.02\ V + 0.128 \times 10^{20}\ V\Gamma^2 \qquad (46)$$

where V is in volts relative to the e.c.m. for 0.10 normal perchloric acid and Γ is the surface excess in moles per square centimeter. We now consider the implications of these results.

From the definition of ψ given by Equation 30, we have

$$\left[\frac{\partial(\frac{S\psi}{RT})}{\partial V}\right]_\pi = \frac{1}{RT}\left(\frac{\partial\mu}{\partial V}\right)_\pi = \frac{Q_W - Q}{RT\Gamma} \ . \qquad (47)$$

But it is also true that

$$\left[\frac{\partial(\frac{S\psi}{RT})}{\partial V}\right]_{\pi} = \left[\frac{\partial(\frac{S\psi}{RT})}{\partial V}\right]_{\Gamma} + \left[\frac{\partial(\frac{S\psi}{RT})}{\partial \Gamma}\right]_{V}(\frac{\partial \Gamma}{\partial V})_{\pi} \quad . \qquad (48)$$

From Equation 25, it follows that

$$d\mu = \frac{1}{\Gamma} d\pi + (\frac{Q_w - Q}{\Gamma}) dV \quad , \qquad (49)$$

and so, by cross differentiation,

$$\left[\frac{\partial(\frac{1}{\Gamma})}{\partial V}\right]_{\pi} = \left[\frac{\partial(\frac{Q_w - Q}{\Gamma})}{\partial \pi}\right]_{V} = RT\left[\frac{\partial^2(\frac{S\psi}{RT})}{\partial \pi \partial V}\right] . \qquad (50)$$

Therefore

$$(\frac{\partial \Gamma}{\partial V})_{\pi} = -\Gamma^2\left[\frac{\partial(\frac{Q_w - Q}{\Gamma})}{\partial \pi}\right]_{V} = -\Gamma^2 RT\left[\frac{\partial^2(\frac{S\psi}{RT})}{\partial \pi \partial V}\right] . \qquad (51)$$

Combining Equations 43, 47, and 51 leads to the expression

$$\frac{Q_w - Q}{RT\Gamma} = F_1'(V) + F_2'(V)\Gamma^2 - 2\Gamma^3 RT\, F_2(V)\left[\frac{\partial^2(\frac{S\psi}{RT})}{\partial \pi \partial V}\right] . \qquad (52)$$

For the mercury-aqueous phenol system, evaluation of each of the terms on the right hand side of Equation 52 indicated that the third term could be neglected without introducing any appreciable error. This third term was evaluated by first determining $\left[\partial(S\psi/RT)/\partial\pi\right]_V$ from the plots of Figure 15, and then plotting this quantity as a function of V and finding the

slope of the resulting curve. This procedure led to an average value of 0.12 cm/dyne-volt for $\left[\partial^2(\frac{S\phi}{RT})/\partial\pi\partial V\right]$. For the concentrations and polarizations studied, the third term in Equation 52 never exceeded a value of 0.2 volt^{-1}, while typical values for the first two terms would be 8.3 and 2.1 volt^{-1}, respectively. Hence, to a good approximation, Equation 52 can be written as

$$\frac{Q_w - Q}{RT\Gamma} = F_1'(V) + F_2'(V)\Gamma^2 \quad , \tag{53}$$

and for the mercury-aqueous n-amyl alcohol system, $F_2'(V) = 0$.

We now suggest a model to account for the observed dependence of $(Q_w - Q)/RT\Gamma$ on Γ^2 in the mercury-aqueous phenol system.

The expression for ϕ which was given in Equation 30 could also be written as

$$\begin{aligned} \frac{S\phi}{RT} &= \frac{1}{RT}\int_0^V \frac{Q_w - Q}{\Gamma}\,dV = \frac{S}{RT}\int_0^V (Q_w - Q_{org})\,dV \\ &= \frac{S}{RT}\int_0^V \left[C_w V - C_{org}(V - V_o)\right]dV \end{aligned} \tag{54}$$

if the Frumkin model given by Equation 7 is assumed to be valid. In Equation 54, C_w and C_{org} are the capacities corresponding to a fractional surface coverage of zero and one, respectively, and are assumed to be independent of V. Figure

10 indicates the magnitude of this assumption, and the validity of Equation 54 is limited to the extent that C_w and C_{org} are actually functions of V. V_o in Equation 54 represents the potential drop across a double layer completely covered with organic material. If reorientation of adsorbate does occur, this will be reflected in V_o, since molecules oriented with their dipoles perpendicular to the surface will generate a greater potential drop across the interface than those dipoles lying parallel to the surface.

Differentiation of Equation 54 leads to

$$\frac{d(\frac{S\psi}{RT})}{dV} = \frac{1}{RT}\left[\frac{Q_w - Q}{\Gamma}\right] = \frac{S}{RT}\left[C_w V - C_{org}(V - V_o)\right] \quad (55)$$

and only the term in V_o will reflect any change in orientation of the adsorbed material. The following treatment will attempt to justify the observed dependence of this potential on the square of the surface coverage.

Consider a molecule which can have Z possible orientations at the surface. The potential drop across the double layer will depend on the number of molecules in each orientation as well as the total number of molecules on the surface. Thus

$$\Gamma \bar{V}_o = 4\pi \sum_{K=0}^{Z} \mu_K \sigma_K \quad (56)$$

where $\bar{V}_o$ is the average potential drop exerted by each dipole,

μ_K is the normal component of the dipole moment of a molecule having orientation K, Γ is the surface excess for the system of interest, and σ_K is the density of dipoles of orientation K. If one assumes that a molecule will be oriented in a unique way depending only on how many nearest neighbors it is in contact with, then $X_K = \sigma_K/N_o\Gamma$, the fraction of molecules with orientation K, also expresses the probability of a molecule coming in contact with K nearest neighbors. We now show why this is so, and then examine the consequences of this statement.

If θ represents the fraction of sites on the surface which are occupied, it also represents the probability that any given site is occupied, and $(1 - \theta)$ is the probability that any given site is empty. We now ask what the probability is of molecule X, adsorbed at some site on the surface, having exactly two nearest neighbors. Assuming a co-ordination number of six, the probability of X having two nearest neighbors at specific sites A and B is given by $P = \theta^2(1 - \theta)^4$. The probability that the two nearest neighbors are located at any two of the six available sites is given by $P = \frac{\theta^2(1 - \theta)^4\, 6!}{4!\, 2!}$. In general, if the co-ordination number is Z, the probability that X has exactly K nearest neighbors at any K of the Z available sites is

$$X_K = \frac{Z!}{K!(Z - K)!}\, \theta^K(1 - \theta)^{Z-K}. \qquad (57)$$

Now σ_K is equal to the number of molecules adsorbed per square centimeter of surface with exactly K nearest neighbors, or expressed mathematically

$$\sigma_K = N_o \Gamma \frac{Z!}{K!(Z - K)!} \theta^K (1 - \theta)^{Z-K} \tag{58}$$

Therefore

$$\Gamma \bar{V}_o = 4\pi N_o \Gamma \sum_{K=0}^{Z} \frac{Z!}{K!(Z - K)!} \mu_K \theta^K (1 - \theta)^{Z-K} \tag{59}$$

Remember that the binomial expansion for $[\theta + (1 - \theta)]^Z$ is given by

$$[\theta + (1 - \theta)]^Z = 1 = \sum_{K=0}^{Z} \frac{Z!}{K!(Z - K)!} \theta^K (1 - \theta)^K \tag{60}$$

It is reasonable to suppose that it takes at least two nearest neighbors acting on a third to cause any change in orientation of that molecule. We will further suppose that in the case of phenol, there are only two possible orientations of the dipole. Concisely expressed, we let

$$\begin{aligned} \mu_K &= \mu_o \quad \text{when} \quad K = 0 \text{ or } 1 \\ \mu_K &= \mu' \quad \text{when} \quad K = 2, 3, \cdots, Z. \end{aligned} \tag{61}$$

Equation 59 then becomes

$$\Gamma \bar{V}_o = 4\pi N_o \Gamma \left[\mu_o \sum_{K=0}^{1} \frac{Z!}{K!(Z - K)!} \theta^K (1 - \theta)^K + \mu' \sum_{K=2}^{Z} \frac{Z!}{K!(Z - K)!} \theta^K (1 - \theta)^{Z-K} \right]$$

$$= 4\pi N_o \Gamma \left[\mu_o \sum_{K=0}^{1} (\cdots) + \mu_o \sum_{K=2}^{Z} (\cdots) + \mu' \sum_{K=2}^{Z} (\cdots) - \mu_o \sum_{K=2}^{Z} (\cdots) \right] \quad (62)$$

$$= 4\pi N_o \Gamma \left[\mu_o + (\mu' - \mu_o) \sum_{K=2}^{Z} \frac{Z!}{K!(Z-K)!} \theta^K (1-\theta)^{Z-K} \right]$$

Equation 62 follows from Equation 60. To the degree that θ can be adequately represented by Γ/Γ_{max}, Equation 62 becomes

$$\bar{V}_o = 4\pi N_o \left[\mu_o + (\mu_1 - \mu_o) \frac{1}{(\Gamma_{max})^Z} \sum_{K=2}^{Z} \frac{Z!}{K!(Z-K)!} \Gamma^K (\Gamma_{max} - \Gamma)^{Z-K} \right] \quad (63)$$

If terms higher than second order in Γ in Equation 63 are neglected, the expression simplifies to the form

$$\bar{V}_o = \alpha + \beta\Gamma^2 \quad (64)$$

If this value for $\bar{V}_o$ is now substituted in Equation 55, we find

$$\frac{d(\frac{S\pi}{RT})}{dV} = \frac{1}{RT}\left[\frac{Q_w - Q}{\Gamma}\right] = \frac{S}{RT}\left[C_w V - C_{org}(V - \alpha - \beta\Gamma^2) \right] \quad (65)$$

Thus, by equating coefficients of terms in Equations 53 and 65, the parameters α and β can be evaluated as

$$\alpha = -3.02 \frac{RT}{SC_{org}} \qquad (66)$$

$$\beta = 0.128 \times 10^{20} \frac{RT}{SC_{org}} \qquad (67)$$

For phenol, reasonable values for S and C_{org} would be of the order of 40×10^{-16} cm^2/molecule and 10 microfarads per square centimeter, respectively. Substitution of these values into Equations 66 and 67 leads to values for the parameters of $\alpha = -0.314$ volts and $\beta = 0.0133 \times 10^{20}$ volt-cm^4/$mole^2$.

Reorientation of phenol as evidenced by capacity measurements

A further verification of the reorientation of the phenol molecules can be found in the capacity results shown in Figure 10. It will be noted that in the neighborhood of V = +0.200 volts, the curves begin crossing one another, that is, the capacity in this region is approximately one microfarad greater for C = 0.100 M. than for C = 0.060 M. Such pseudocapacitance is normally associated with a desorption process occurring at the interface. The large desorption peaks observed for n-amyl alcohol are notable examples, but smaller pseudocapacitive behavior much like that observed here for phenol has been attributed to polymolecular desorption by Melik-Gaikazyan (33). Phenol has been shown to form polymolecular layers, but only when the bulk concentration was at least 50% of the saturation concentration (45); we observe the

pseudocapacitive behavior at concentrations less than 15% of the saturation concentration. Thus, we attribute this pseudocapacitance to a reorientation of the phenol at the interface, and a sample calculation will show that this is a reasonably well-founded conclusion. Making use of the Frumkin model of adsorption which we have shown represents the adsorption process reasonably well, we rewrite Equation 7 as

$$Q = Q_w(1-\theta) + Q_{org}\theta = Q_w(1-\theta) + C_{org}(V-V_o)\theta \qquad (68)$$

and substituting for V_o from Equation 64 and differentiating leads to

$$C = \left(\frac{\partial Q}{\partial V}\right)_\mu = C_w(1-\theta) + C_{org}\theta + S\left[-Q_w + C_{org}(V - \alpha - 3\beta\Gamma^2)\right]\left(\frac{\partial \Gamma}{\partial V}\right)_\mu \quad . \qquad (69)$$

Now the entire pseudo-capacitance will be reflected in the term involving $(\partial\Gamma/\partial V)_\mu$ in Equation 69, and we now have enough information at hand to make a first order evaluation of this term. Figure 22 shows a plot of surface excess versus polarizing potential for several concentrations of phenol. Graphical differentiation of these curves will lead to evaluation of $(\partial\Gamma/\partial V)_\mu$ at any potential and concentration of interest. At a potential of V = +0.200 volts, this quantity was found to be equal to -2.82 microfarads per square centimeter for 0.09 molar phenol, and -2.28 microfarads per square centimeter for

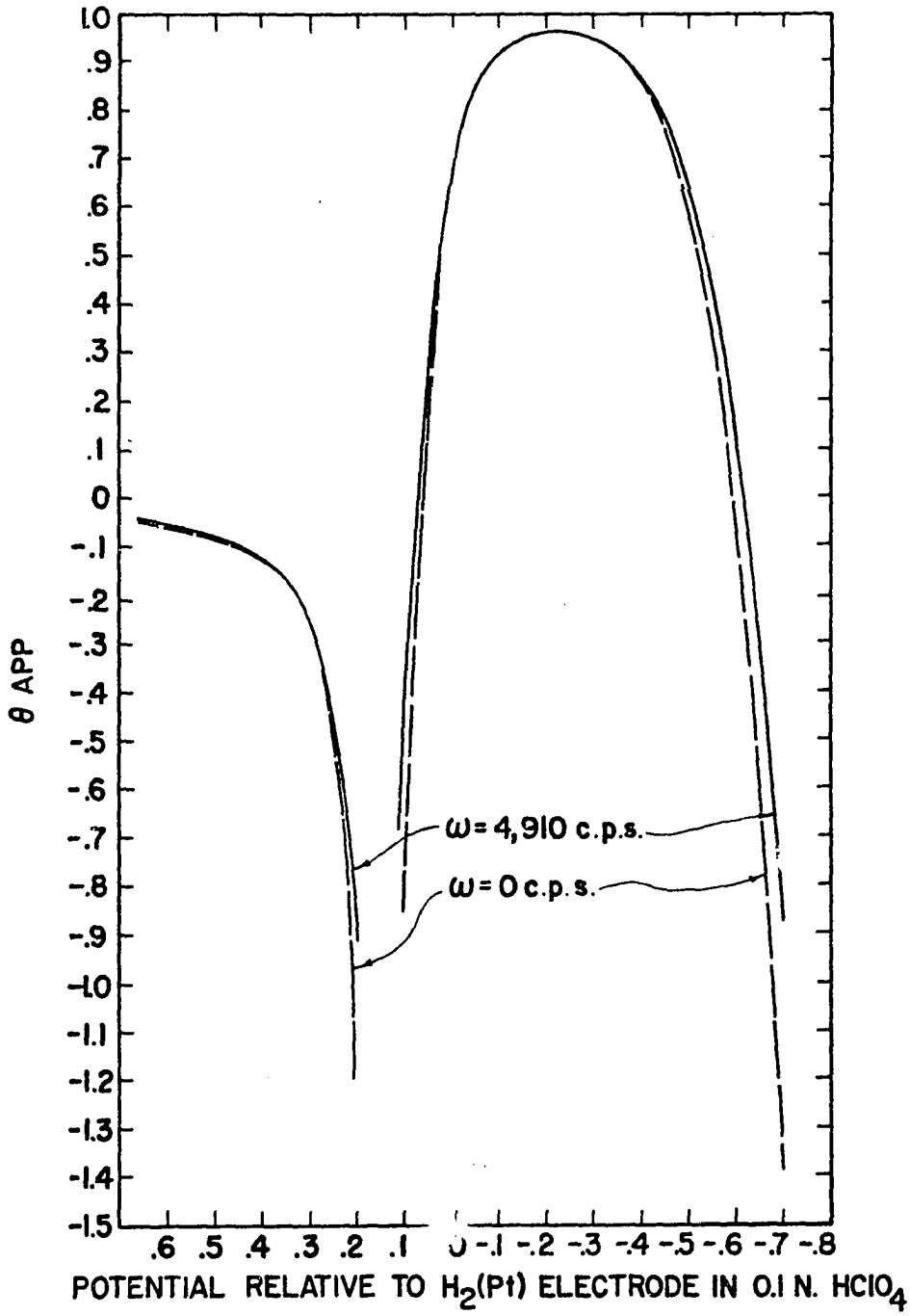

Figure 20. θ_{app} vs. V

0.06 molar phenol. Substitution of these values into Equation 69, and using the same values for the other terms in the equation as were used previously in connection with Equations 66 and 67, one finds that the pseudo-capacitive term is approximately 0.6 microfarads per square centimeter greater for 0.09 molar phenol than for 0.06 molar phenol. This value, determined under the premise that reorientation was responsible for any pseudocapacitance observed, is in excellent agreement with the experimental difference in capacities observed for these concentrations at this potential.

Apparent adsorption from differential capacitance

Hansen et al. (23, 24) found that an apparent fractional coverage defined by

$$\theta_{app} = \frac{C_w - C}{C_w - C_{org}} \qquad (70)$$

gave reasonable values of the surface coverage in the region of maximum adsorption, i.e., between the desorption peaks of the capacitance curves. As stated previously, however, they make no effort to extrapolate their experimental capacities to zero frequency, but rather recorded all of their data at the arbitrary frequency of 1000 cycles per second. We have already shown that it is essential that the zero frequency capacity be used when determining charge density and interfacial tension by numerical integration of capacitance; our

purpose now is to determine whether or not this is also necessary when using Equation 70.

Table 22 lists the values of the apparent surface coverage calculated on the basis of Equation 70 for n-amyl alcohol at a concentration of C/Co = 0.139. Values of C and C_w used in this calculation were experimental; C_{org} was taken from Hansen et al. (24) as being 5.38 microfarads per square centimeter. Apparent fractional coverages were calculated for capacities measured at 4910 and zero cycles per second. Figure 20 shows plots for these frequencies based on the data of Table 22. It can be seen that in the neighborhood of the electrocapillary maximum, reasonable values for surface coverage are obtained for both frequencies examined, and these coverages are in excellent agreement with one another. Since Equation 70 was shown by Hansen et al. to yield apparent surface coverages which coincide with actual coverages only in the neighborhood of the maximum of the θ_{app} vs. V curve, it matters little that the curves for different frequencies differ greatly outside of this region.

Kinetics of Adsorption

Frumkin and Melik-Gaikazyan (32) have derived equations that allow one to distinguish between diffusion control and activation control of adsorption from solution. These equations are based on the frequency dependence of the differential

Table 22. Dependence of apparent adsorption on polarizing potential, V, and A.C. frequency, ω, for C/Co = 0.139 n-amyl alcohol. Electrode potential in volts relative to hydrogen electrode; frequency in cycles per second

V	θ_{app} ω = 4,910	θ_{app} ω = 0	V	θ_{app} ω = 4,910	θ_{app} ω = 0
- .700	-0.880	-1.384	0.000	+0.678	+0.664
- .600	+0.113	-0.064	+ .100	-0.449	-0.835
- .500	+0.657	+0.615	+ .200	-0.868	-1.064
- .400	+0.863	+0.852	+ .300	-0.277	-0.270
- .300	+0.941	+0.937	+ .400	-0.128	-0.122
- .200	+0.952	+0.949	+ .500	-0.074	-0.079
- .100	+0.912	+0.913	+ .600	-0.052	-0.136

capacitance at the desorption peaks, and are, for diffusion control:

$$C_i = \frac{C_{i(\omega=0)}\left[\left(\frac{\partial\Gamma}{\partial C}\right)_V\sqrt{\frac{2\omega}{D}} + 2\right]}{\left[\left(\frac{\partial\Gamma}{\partial C}\right)_V\sqrt{\frac{2\omega}{D}} + 1\right]^2 + 1} \qquad (71)$$

where C_i is the differential capacity at frequency ω, and D is the diffusion coefficient of the organic molecule. For activation control, they find that

$$C_i = C_{i(\omega=0)} \frac{A^2}{\omega^2 + A^2} \qquad (72)$$

where A is a constant at a given concentration of organic material and polarization of the electrode. For C/Co = 0.139 n-amyl alcohol, Figure 8 shows the cathodic desorption peak occurring at a potential of +0.150 volts relative to the hydrogen electrode. Figure 9 shows the anodic desorption peak for 0.010 molar phenol to be located at a polarization of -0.600 volts relative to the hydrogen electrode. Hence, the data for these respective solutions and potentials appearing in Tables 5 and 8 were used in conjunction with Equations 71 and 72 to determine the controlling step in the kinetic process of adsorption for each of these substances.

If the process were activation controlled, then by Equation 72, a plot of ω^2 vs. $C_{i(\omega=0)}/C_i$ should follow a straight line with a slope of $1/A^2$ and an intercept of 1. Plotting the frequency dependence for n-amyl alcohol and phenol in this way, using the data at concentrations and potentials cited previously, showed that neither of these substances appear to be adsorbed via an activation controlled mechanism, since the data followed a parabolic curve rather than a straight line. The phenol data, showing a less pronounced frequency dependence, would follow a more linear trend than the n-amyl alcohol data, but in either case the deviation from linearity would be quite large.

The diffusion control mechanism as described by Equation 71 was found to be compatible with the experimental data for both the phenol and n-amyl alcohol systems if the diffusion coefficient, D, was treated as an adjustable parameter. Graphical differentiation of the adsorption isotherms in Figures 17 and 18 for n-amyl alcohol and phenol, respectively, yield values for $(\partial\Gamma/\partial C)_V$ of 5.5×10^{-6} cm for C/Co = 0.139 n-amyl alcohol at a polarization of +0.150 volts relative to the hydrogen electrode, and for 0.010 molar phenol at a potential of -0.600, a value of 7.3×10^{-6} cm. Substitution of these values in Equation 71, and using $D = 5 \times 10^{-6}$ cm^2/sec for n-amyl alcohol and $D = 68 \times 10^{-6}$ cm^2/sec for phenol, brought the capacities calculated from Equation 71 in good agreement with those observed experimentally. The results of these calculations are tabulated in Table 23.

The diffusion coefficient for molecules of this size is thought to be approximately 8×10^{-6} cm^2/sec (34). This is of the same order of magnitude as that value used for n-amyl alcohol in the above calculation, but is nearly a factor of ten smaller than the value which gave the best fit for the phenol data. Hence, it appears that we can make no firm conclusion concerning the kinetic mechanism controlling the adsorption of phenol, as neither Equation 71 or 72 were descriptive of our data. As pointed out earlier, the frequency dependence observed for 0.10 normal perchloric acid is appre-

Table 23. Comparison of experimental capacities and diffusion controlled capacities calculated from Equation 71 for n-amyl alcohol and phenol. Frequency, ω, in cycles per second; capacities in microfarads per square centimeter

ω	n-amyl alcohol		Phenol	
	$C_{i\ exp}$	$C_{i\ theory}$	$C_{i\ exp}$	$C_{i\ theory}$
9,050	40.72	40.70	20.11	20.40
4,910	45.73	45.30	21.27	21.30
500	56.85	56.60	23.03	23.00
100	59.43	59.90	23.50	23.45

ciable in comparison to the dependence observed for phenol, and hence the data are not really accurate enough for one to base a choice of controlling mechanism on the frequency dependence observed. However, assuming that the system is unstirred during the adsorption process, the adsorption rate cannot exceed the rate calculated for a diffusion-limited process. Yet in the mercury-aqueous phenol system, this rate appears to be exceeded; the adsorption kinetics are represented by diffusion-limited theory only if a diffusion coefficient high by a factor of ten is supposed. This implies that some stirring mechanism must exist in the neighborhood of the interface, and also strongly suggests that there is no energy barrier to the phenol adsorption.

N-Butylacetamide

Studies of adsorption from solution which have made use of the differential impedance bridge have been concerned solely with the adsorption of substances which possess a dielectric constant which is much smaller than that of the solvent, water. Hence, the presence of these substances at the interface is characterized by a lowering of the differential capacity, and at the potentials at which desorption occurs, large pseudo-capacitive peaks are observed. Figures 8 and 9 are typical examples of this behavior. It would be very interesting to observe what effect the adsorption of a high dielectric material at the interface would have on the differential capacitance.

Very few substances possess a dielectric constant which is greater than that of water--78.5 at 25° C (46). Several amides have been observed to have constants exceeding one hundred, however (46, 47), and the adsorption properties of these materials at the mercury-solution interface have not been thoroughly investigated. Damaskin and Povarov (48) have examined the capacitance of the electrical double layer using N-methylformamide as a solvent, and observed capacity curves much like those of water; that is, a characteristic hump appears in the central portion of the curve which is thought to be connected with a change in orientation of the solvent dipoles. These workers also studied the effect of mixing

water with N-methylformamide in varying mole percents, and found that small amounts of water have very little effect on the shape of the capacitance curve in N-methylformamide, but the N-methylformamide is so strongly adsorbed on mercury that even minute amounts of it in water will cause the hump due to the reorientation of the water dipoles to disappear.

The choice of N-butylacetamide as an adsorbent was prompted by two factors: its high dielectric constant of approximately one hundred (46), and the relatively long hydrocarbon chain which should enhance the material's surface activity. The electrocapillary data represented in Figure 6, and the capacitance curve shown in Figure 21, indicate that this material is strongly adsorbed at negative polarizations of the mercury surface, and the dielectric constant of the material in the interphase is less than that of water. This latter point is evidenced by the low values of capacity observed in the region of maximum adsorption indicated by the electrocapillary curve. Thus, the material has a much smaller dielectric constant at the surface than in the bulk phase, supporting the theory (47) that the high bulk dielectric constant is due to the ability of all mono N-substituted amides to form extended hydrogen-bonded "polymers" having a very large dipole moment by virtue of the presence in each molecule of only two sites able to participate in hydrogen bond formation, and because these sites are disposed <u>trans</u> to one

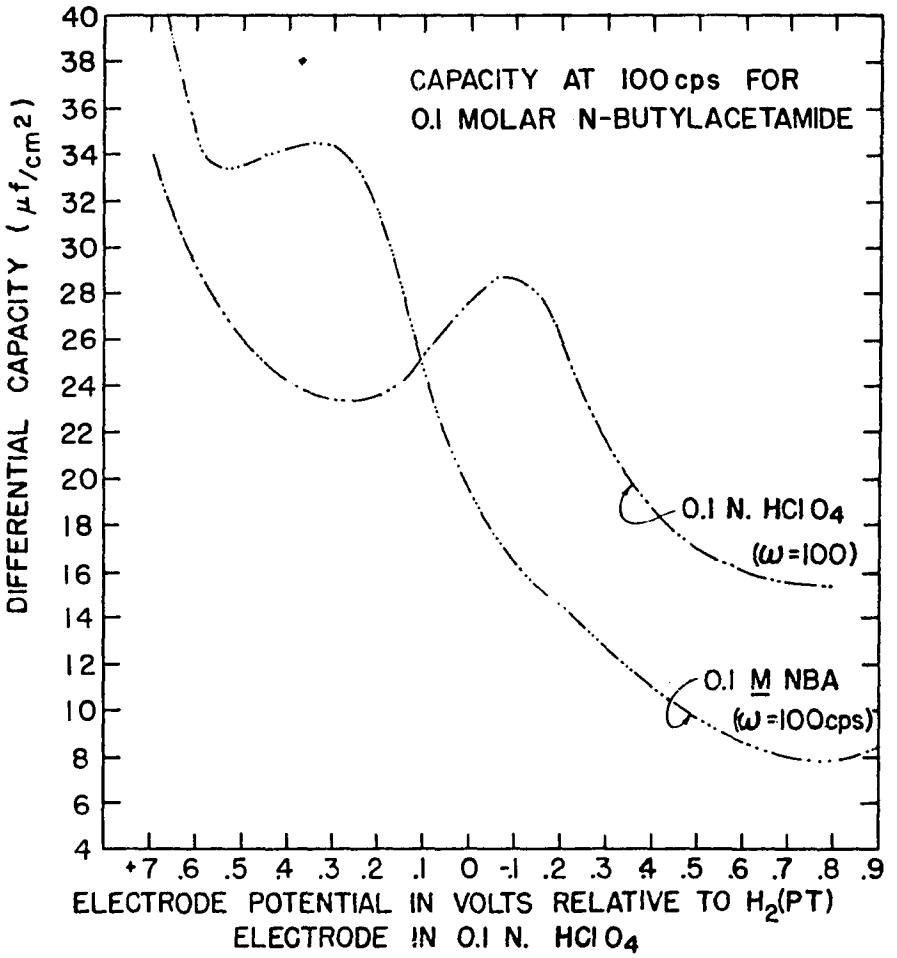

Figure 21. Capacitance curves for N-butylacetamide

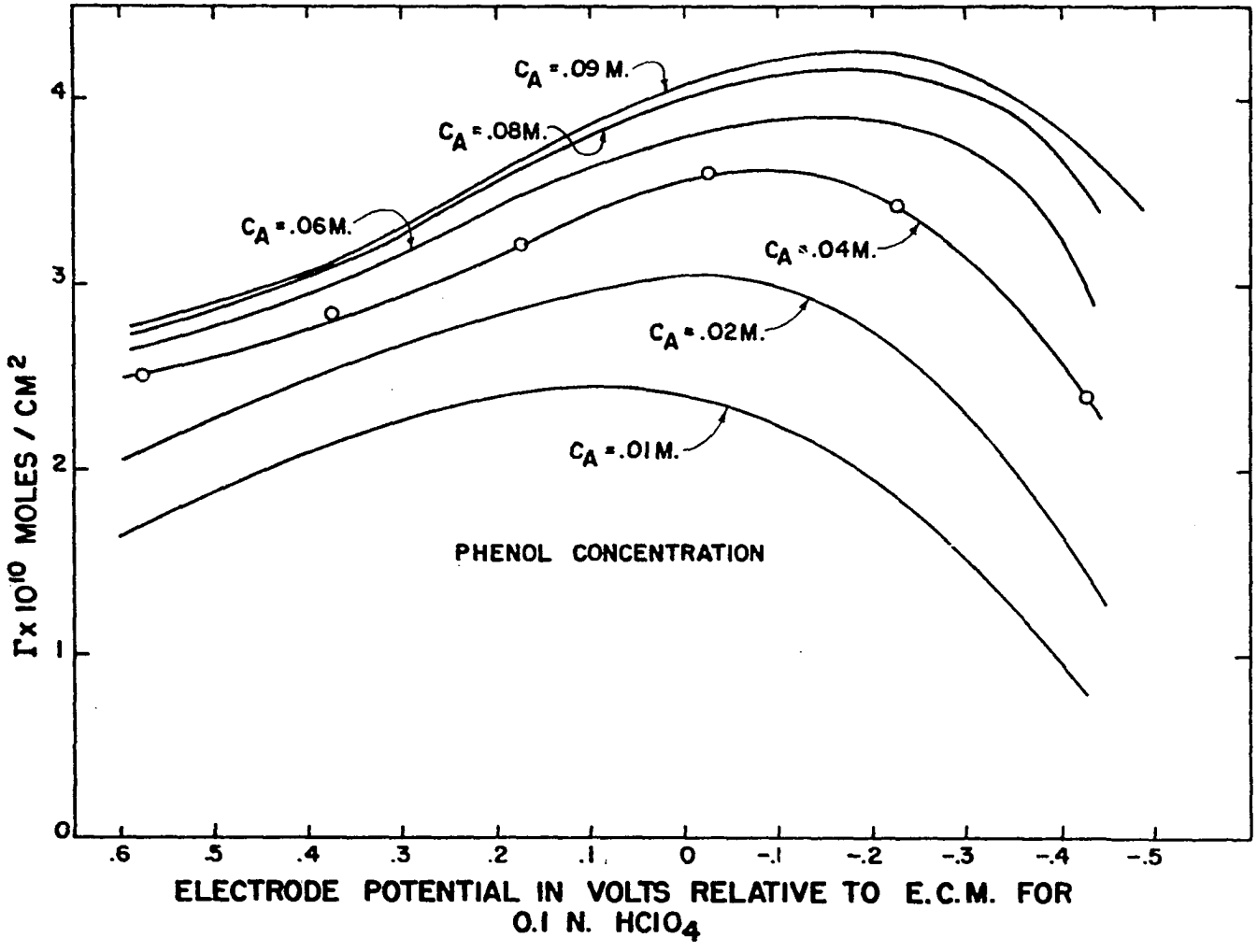

Figure 22. Surface excess vs. potential

another (49). Orientation of the molecules at the mercury-solution interface is probably such that this anomalously high dipole moment is considerably reduced, thus giving rise to a lower dielectric constant than that observed in the bulk phase.

SUMMARY

The effects of surface active components on electrocapillary properties of the mercury--0.1 N. aqueous perchloric acid solution interface were investigated. Two complementary experimental quantities--interfacial tension and zero-frequency differential capacitance--were measured as functions of polarization of the mercury surface and concentration of the organic species in solution. Surface active components investigated were phenol and n-amyl alcohol, with preliminary measurements also being made with N-butylacetamide.

A theory based on the linear dependence of surface charge density on fractional surface coverage of the adsorbed surface active component was developed, and the resulting equations applied to the experimental data. Results show that this model works very well for the n-amyl alcohol system, but must be modified somewhat in the case of phenol to account for the change in potential drop across a monolayer of pure adsorbent as the surface coverage is increased. An argument is presented to account for this in terms of reorientation of the adsorbed component as a function of the square of the coverage. With this modification, quantitative agreement between the theory and experiment is well within experimental error.

The compatability of the capacitance and interfacial tension measurements was checked by doubly integrating the

capacitance results with respect to potential, and then comparing these calculated interfacial tensions with those obtained experimentally. Agreement was within experimental error, but emphasized the importance of using the equilibrium value of the capacitance--that is, the value obtained at zero frequency--to obtain correct results. In the case of n-amyl alcohol, however, adsorption could be inferred from capacities measured at other frequencies if the range of potentials was confined to those within the desorption peaks. Such an inference cannot be made for the phenol system due to the change in orientation of the adsorbed molecules with increased coverage, thus prohibiting the assignment of any one value for Γ_{max}.

Adsorption kinetics for phenol and n-amyl alcohol were inferred from the frequency dependence of capacitance at the desorption peaks. Following Frumkin's analysis of such dependence, one concludes that in either case the kinetics are probably diffusion controlled.

Preliminary studies with N-butylacetamide show this substance to be strongly adsorbed at negative polarizations of the mercury electrode, and further show that the dielectric constant of the material is less than that of water when adsorbed at the mercury surface, whereas in bulk solution the converse is true. This confirms the importance of directed hydrogen bonding in explaining why the bulk dielectric constant should be so high for this material.

SUGGESTED MODIFICATIONS AND EXTENSIONS

The frequency dependence of capacitance observed for the mercury-0.10 normal aqueous perchloric acid solution has been shown by Grantham (44) to be due to improper electrode design rather than to any dielectric relaxation phenomena or other fundamental process occurring in solution. The hydrophobic Desicote used to coat the inner surface of the dropping mercury electrode was supposed to eliminate any frequency dependence caused by solution creeping between the mercury and the glass walls of the capillary, but evidently this procedure was not one-hundred per cent effective. A more satisfactory electrode might be fabricated from one of the commercially available fluorocarbons such as Teflon (polytetrafluorethylene) or Kel-F (polymonochlorotrifluorethylene) which possesses the desired hydrophobic properties. Such an electrode would eliminate worries about variation of hydrophobic properties with time, and should also be more durable than the fragile glass capillaries which were easily (and too often) broken.

A more sensitive capillary electrometer could be made by merely decreasing the diameter of the capillary at the position of the null point. This would necessitate other modifications, however. A more powerful microscope would have to be used to observe the position of the meniscus in the capillary; Conway et al. (20) reported that use of a binocular Bausch and

Lomb "zoom" stereomicroscope greatly improved their viewing of the capillary. To avoid the hazard of high positive pressures in the pressure regulating system above the capillary, it is suggested that the mercury reservoir above the capillary be extended in height in proportion to the decrease in the capillary diameter at the null position.

N-butylacetamide, although not possessing a dielectric constant higher than that of water at the mercury-solution interface, does have some unique electrocapillary properties which deserve closer scrutiny. The ability of this material to remain adsorbed at high cathodic polarizations of the mercury surface is probably due to some specific interaction between the substance and mercury. It is unlikely that this interaction occurs between the hydrocarbon chain and the mercury, for this property would than be common to all hydrocarbon adsorbates. It would be interesting to learn of the orientation of this molecule at the surface from adsorption isotherms, and also find out if this orientation changes as a function of coverage.

If a reorientation of phenol occurs at the interface as described in the Discussion section of this thesis, then the same thing should occur for other polar aromatic compounds at the mercury-solution interface. Thus the electrocapillary properties of compounds such as aniline, benzoic acid, etc., should shed further light on this theory.

BIBLIOGRAPHY

1. Grahame, D. C., Chem. Rev., 41, 443 (1947).

2. Parsons, R., "Equilibrium Properties of Electrified Interphases" in Bockris, J. O'M. and Conway, B. E., editors, Modern Aspects of Electrochemistry, Vol. 1, pp. 103-179, Butterworth, London, 1954.

3. Parsons, R., Advances in Electrochem. and Electrochem. Eng., 1, 1 (1961).

4. Damaskin, B. B., Russian Chemical Reviews (Uspekhi Khimii), 30, 78 (1961).

5. Watts-Tobin, R. J., Phil. Mag., 6, 133 (1961).

6. Mott, N. F. and Watts-Tobin, R. J., Electrochim. Acta, 4, 79 (1961).

7. Mott, N. F., Parsons, R., and Watts-Tobin, R. J., Phil. Mag., 7, 483 (1962).

8. Lippmann, G., Ann. d. Chim. et d. Phys., 5, 494 (1875).

9. Lippmann, G., Ann. d. Chim. et d. Phys., 12, 265 (1877).

10. Lippmann, G., Pogg. Ann., 149, 547 (1878).

11. Butler, J. A. V., Electrical Phenomena at Interfaces, Methuen and Co. Ltd., London (1951).

12. Minturn, R. E., The Inference of Adsorption from Differential Capacity Studies. Unpublished Ph.D. Thesis, Library, Iowa State University of Science and Technology, Ames, Iowa (1955).

13. Hickson, D. A., A Study of Adsorption Processes Occurring at an Ideally Polarizable Electrode-Solution Interphase. Unpublished Ph.D. Thesis, Library, Iowa State University of Science and Technology, Ames, Iowa (1958).

14. Blomgren, E., Bockris, J. O'M., and Jesch, C., J. Phys. Chem., 65, 2000 (1961).

15. Frumkin, A. N., Kaganovich, R. I., and Bit-Popova, E. S., Proc. Acad. Sci. USSR, Phys. Chem. (Doklady Akad. Nauk. SSSR), 141, 899 (1961).

16. Gerovich, M. A., Zhurnal Fiz. Khim., 28, 19 (1954).

17. Gerovich, M. A., Zhurnal Fiz. Khim., 32, 109 (1958).

18. Gerovich, M. A., Doklady Akad. Nauk. SSSR, 96, 3 (1954).

19. Gerovich, M. A., Doklady Akad. Nauk. SSSR, 105, 6 and 1278 (1955).

20. Conway, B. E. and Barradas, R. G., Electrochim. Acta, 5, 319 and 349 (1961).

21. Kruger, F., Z. Physik. Chem., 45, 1 (1903).

22. Kortüm, G. and Bockris, J. O'M., Textbook of Electrochemistry. Elsevier Publishing Co., Amsterdam (1951).

23. Hansen, R. S., Minturn, R. E., and Hickson, D. A., J. Phys. Chem., 60, 1185 (1956).

24. Hansen, R. S., Minturn, R. E., and Hickson, D. A., J. Phys. Chem., 61, 953 (1957).

25. Frumkin, A. N., Z. Physik, 35, 792 (1926).

26. Breiter, M. and Delahay, P., J. Am. Chem. Soc., 81, 2938 (1959).

27. Parsons, R., Trans. Far. Soc., 55, 999 (1959).

28. Schapink, F. W., Oudeman, M., Leu, K. W., and Helle, J. N., Trans. Far. Soc., 56, 415 (1960).

29. Frumkin, A., Ergebn. Exakt. Naturwiss., 7, 235 (1928).

30. Parsons, R., Proc. Roy. Soc., Series A, 261, 79 (1961).

31. Devanathan, M. A. V., Proc. Roy. Soc., Series A, 264, 133 (1961).

32. Frumkin, A. N., and Melik-Gaikazyan, V. I., Doklady Akad. Nauk. SSSR, 77, 855 (1951). (Original not available; privately translated from the Russian and distributed by the Department of Chemistry, Amherst College, Amherst, Massachusetts.)

33. Melik-Gaikazyan, V. I., Zhur. Fiz. Khim. 26, 1184 (1952). (Original available; privately translated from the Russian by E. Jarvesoo and edited by D. C. Grahame, Dept. of Chemistry, Amherst College, Amherst, Massachusetts.)

34. Lorenz, W. and Möckel, F., Z. Elektrochem., 60, 507 (1956).

35. Lange, N. A., Handbook of Chemistry, 8th ed., Handbook Publishers, Inc., Sandusky, Ohio (1952).

36. Furman, N. H., ed., Scott's Standard Methods of Chemical Analysis, 5th ed., Vol. 2, D. Van Nostrand Co., Inc., New York (1939).

37. Adam, N. K., The Physics and Chemistry of Surfaces, 2nd ed., Oxford University Press, London (1938).

38. Smolders, C. A., Rec. trav. chim., 80, 635, 650, and 699 (1961).

39. Gouy, G., Ann. Physique, Series 9, 6, 5 (1916).

40. Craxford, S. R., Electrocapillary Phenomena. Unpublished Ph.D. Thesis, Bodleian Library, Oxford University, Oxford, England (1936).

41. Hansen, L. A. and Williams, J. W., J. Phys. Chem., 39, 439 (1935).

42. Koenig, F. O., Z. Physik. Chem., Series A, 54, 454 (1931).

43. Thomson, G. W., "Determination of Vapor Pressure" in Weissberger, A., editor, Technique of Organic Chemistry, 3rd ed., Vol. 1, Part 1, pp. 401-522. Interscience Publishers, Inc., New York (1959).

44. Grantham, D. H., Relaxation Phenomena in the Electrical Double Layer. Unpublished Ph.D. Thesis. Library, Iowa State University of Science and Technology, Ames, Iowa (1962).

45. Frumkin, A., Gorodetzkaja, A., and Tschugunoff, P., Acta physicochim. URSS, 1, 12 (1934).

46. Vaughn, J. H. and Sears, P. G., J. Phys. Chem., 62, 183 (1958).

47. Leader, G. R. and Gormley, J. G., J. Am. Chem. Soc., 73, 5731 (1951).

48. Damaskin, B. B. and Povarov, Yu. M., Proc. Acad. Sci. USSR, Phys. Chem. (Doklady Akad. Nauk. SSSR), 140, 690 (1961).

49. Mizushima, S., J. Am. Chem. Soc., 72, 3490 (1950).

ACKNOWLEDGEMENTS

The author gratefully acknowledges the patient understanding and support of Professor R. S. Hansen during the course of this research. He suggested the problem and was always ready with a helpful idea when progress seemed to lag.

Special thanks must also go to James Murphy as well as to Wayne Jones and his co-workers in the Glass Shop for fabricating the cells and other glassware; to David Barshatky, who assisted in recording the capacitance data; and to Tom McGee, who programmed and ran the capacitance integrations on the Cyclone Computer. Dan Grantham's helpful suggestions, as well as the invaluable experimental groundwork he performed with the differential impedance bridge, were of great benefit to the author.